Lappeenranta University of Technology

Faculty of Technology

Master's Degree Program in Chemical and Process Engineering

Yegor Chechurin

FAST PYROLYSIS IN CIRCULATING FLUIDIZED BED: FEASIBILITY STUDY

Examiners: Professor Ilkka Turunen

Senior Process Engineer Riku Hyvärinen

ACKNOWLEDGEMENTS

First of all I would like to thank my supervisors Ilkka Turunen and Riku Hyvärinen for giving me the opportunity to do this master's thesis and for their guidance throughout the time I was working on it. Dear Ilkka and Riku due to your advices I have learnt a lot about process design and have become much more confident about my process design skills, thank you very much for this!

The biggest gratitude goes to my parents and all my family. Without their love and support it would be impossible for me to complete this master's thesis. Also I would like to thank all my friends for the inspiration they give me.

Very special thanks go to Yury Avramenko for sharing his knowledge and experience with me. His advices were always making my brain generate right ideas. Other special thanks are for my friend Behnam Zakri who took the trouble to guide me through the Apros software.

Finally I would like to thank two amazing guys from Moscow who I met in Jyväskylä. Alejandro and Oksana you gave me the inspiration during my finalizing of this master's thesis. Thank you so much for the time we spent together in Jyväskylä, I will never forget it.

ABSTRACT

Lappeenranta University of Technology

Faculty of Technology

Master's Degree Program in Chemical and Process Engineering

Yegor Chechurin

FAST PYROLYSIS IN CIRCULATING FLUIDIZED BED: FEASIBILITY STUDY

Master's Thesis

2013

124 pages, 9 figures, 24 tables, 4 appendices

Examiners: Professor, PhD, Ilkka Turunen

Senior Process Engineer, MSc, Riku Hyvärinen

Keywords: biomass, fast pyrolysis, circulating fluidized bed, mass balance, heat balance, equipment sizing, investment cost, operating cost, internal rate of return, profitability estimation.

Today the limitedness of fossil fuel resources is clearly realized. For this reason there is a strong focus throughout the world on shifting from fossil fuel based energy system to biofuel based energy system. In this respect Finland with its proven excellent forestry capabilities has a great potential to accomplish this goal.

It is regarded that one of the most efficient ways of wood biomass utilization is to use it as a feedstock for fast pyrolysis process. By means of this process solid biomass is converted into liquid fuel called bio-oil which can be burnt at power plants, used for hydrogen generation through a catalytic steam reforming process and as a source of valuable chemical compounds. Nowadays different configurations of this process have found their applications in several pilot plants worldwide. However the circulating fluidized bed configuration is regarded as the one with the highest potential to be commercialized.

In the current Master's Thesis a feasibility study of circulating fluidized bed fast pyrolysis process utilizing Scots pine logs as a raw material was conducted. The production capacity of the process is 100 000 tonne/year of bio-oil. The feasibility study is divided into two phases: a process design phase and economic feasibility analysis phase. The process design phase consists of mass and heat balance calculations, equipment sizing, estimation of pressure drops in the pipelines and development of plant layout. This phase resulted in creation of process flow diagrams, equipment list and Microsoft Excel spreadsheet that calculates the process mass and heat balances depending on the bio-oil production capacity which can be set by a user. These documents are presented in the current report as appendices. In the economic feasibility analysis phase there were at first calculated investment and operating costs of the process. Then using these costs there was calculated the price of bio-oil which is required to reach the values of internal rate of return of 5%, 10%, 20%, 30%, 40%, and 50%.

TABLE OF CONTENTS

LIST OF ABBREVIATIONS

ESP *electrostatic precipitator*

HHV *higher heating value*

LHV *lower heating value*

db *dry basis*

wb *wet basis*

daf *dry ash free basis*

PROJECT GOALS

The goal of the current Master's Thesis project is to conduct feasibility study of fast pyrolysis process taking place in circulating fluidized bed installation. The feasibility study consists of two phases. The first phase includes process design aimed at bio-oil production capacity of 100 000 tonne/year and layout of the plant utilizing the process. During the second phase investment cost calculation and profitability analysis of the designed process are carried out.

1 INTRODUCTION

Today energy issues receive significant attention all over the world. Such problems as limitedness of fossil fuels, rapidly expanding world population and greenhouse effect give rise to a research on alternative renewable environmentally neutral energy sources and to development of technologies utilizing these sources [1, 2, 3].

Biomass is viewed as a major world renewable carbon-neutral energy source [1]. Combustion of fuels derived from biomass is believed to be less polluting than that of fossil fuels. For these reasons conversion of biomass into fuels is gaining significant popularity worldwide [2].

Technologies of biomass to energy and fuels conversion can be divided into three major groups: biochemical technologies, thermochemical technologies and chemical technologies. Biochemical methods of biomass conversion are anaerobic digestion and bioethanol production. Thermochemical techniques group is the largest one and it includes such technologies as direct combustion, gasification, pyrolysis and liquefaction. Production of biodiesel from biomass is carried out through a chemical route [2, 4, 5, 6].

Anaerobic digestion is a treatment of biomass by bacteria in absence of oxygen which is usually applied for wet organic wastes. It leads to formation of biogas which mainly consists of methane and carbon dioxide [2, 7]. Biogas can be upgraded to natural gas quality and can be used for liquefaction into methanol and chemical feedstocks [7]. Drawbacks associated with anaerobic digestion are large

area and long residence time of the digesters and also substantial emissions of strong greenhouse gases produced while biogas burning [2].

Conversion to bioethanol is carried out either by direct fermentation of sugar or by first conversion of starch obtained from corn to sugar with its subsequent fermentation. Disadvantage of biomass to bioethanol conversion is low energy efficiency of the production process and competing with food industry, as well as intensive waste material generation [2].

Biomass is directly burned to produce heat and electricity [2, 4, 8]. If to compare coal and biomass combustion characteristics, biomass is similar to low-rank coals, but deposits produced after biomass combustion are harder to remove. Direct combustion of biomass is associated with substantial pollution. For this reason biomass should be converted to gaseous or liquid fuels [4].

Gasification is a partial oxidation of biomass at high temperatures (600-1300 ^{0}C) leading to formation of gaseous fuel, char and ash. The produced gas typically contains hydrogen, carbon monoxide, methane and small amount of other hydrocarbons, carbon dioxide, water, and nitrogen. Composition of the produced gas is highly dependent on the process conditions and type and moisture content of the feed biomass [2, 4, 5, 9]. The produced gas can be either burnt for heat and electricity production or used for synthesis of liquid transportation fuels, hydrogen, methanol, or chemicals [9].

Pyrolysis is a thermal decomposition conducted in oxygen-free conditions. Pyrolysis of biomass leads to formation of biochar and vapour consisting of condensable and non-condensable gases. Quenching of vapour after its separation from char yields a liquid product which is known as bio-oil. Also a gaseous by-product that is referred to as non-condensable gas is obtained after quenching [2, 10, 11, 12].

Pyrolysis process can be operated at several modes depending on what ratio of bio-oil, non-condensable gas and biochar is desired to be obtained. Temperature, heating rate and vapour residence time impact on the distribution between the yields of pyrolysis products. Low temperature and low heating rate pyrolysis

yields mostly biochar. Low temperature, high heating rate and short vapour residence time pyrolysis is suitable for bio-oil yield maximization. High temperature, low heating rate and long vapour residence time pyrolysis is the best one for non-condensable gas production [13].

Pyrolysis methods are divided into two groups according to the heating rates used: slow pyrolysis (0.1 – 1 ^{0}C/s) [14, 15, 16] and fast pyrolysis (100 – 10^{5} ^{0}C/s) [3, 10, 12, 13, 17, 18].

Therefore according to the pyrolysis characteristics stated above main product of slow pyrolysis is either biochar, if a low temperature is used, or non-condensable gas, when a high temperature is used, and main product of fast pyrolysis is bio-oil, if a proper temperature is selected.

Hydrothermal liquefaction is a process where water acts as a reaction medium and high temperature (250 – 350 ^{0}C) and pressure (5 – 25 MPa) are utilized. Because of the water being a reaction medium the necessity for feed drying is eliminated. After the temperature and pressure are returned to normal conditions self-separation of bio-oil from water occurs [6, 14]. Bio-oil produced by hydrothermal liquefaction has a relatively high heating value. By-products of hydrothermal liquefaction are biochar, water soluble substances and gas. Addition of various alkaline catalysts can increase bio-oil yield and improve its quality [6].

Conversion of biomass to biodiesel is performed through a transesterification process in which vegetable oils such as rapeseed oil, soybean oil and palm oil react with methanol or ethanol in the presence of alkaline catalyst. The process also yields a co-product which is glycerol and is contaminated with alkali. The major problem about biodiesel usage as a fuel is that it has 10-25% higher nitrogen oxide emissions than conventional fuels. Similar to bioethanol production biodiesel manufacturing competes with food industry and generates too much waste materials [2].

Summary of biomass valorization techniques is presented below in the table 1.

Table 1: Summary of biomass processing technologies.

Valorization technique	**Process principles**	**Resulting products**
Anaerobic digestion	Treatment by bacteria in absence of oxygen	Biogas which mainly consists of methane and carbon dioxide
Bioethanol production	Direct fermentation of sugar or first conversion of starch obtained from corn to sugar with its subsequent fermentation	Bioethanol
Combustion	Direct burning	Heat
Gasification	Oxidation of at high temperatures (600-1300 ^{0}C)	Gaseous fuel, char, ash
Pyrolysis	Thermal decomposition conducted in oxygen-free conditions	Bio-oil, biochar, non-condensable gas
Hydrothermal liquefaction	Water acts as a reaction medium at high temperature (250 – 350 ^{0}C) and pressure (5 – 25 MPa)	Bio-oil, biochar, non-condensable gas
Biodiesel production	Transesterification reaction of vegetable oils with methanol or ethanol in the presence of alkaline catalyst	Biodiesel

2 FAST PYROLYSIS PROCESS REVIEW

2.1 Raw materials

Biomass is a broad term which is used to denote both phytomass or plant biomass and zoomass or animal biomass. Plant biomass consists mainly of cellulose, hemicellulose and lignin. For this reason it is sometimes referred to as

lignocellulosic biomass. Plant biomass also contains small amount of water, lipids, proteins, simple sugars, starches and ash (inorganic compounds) [4, 13].

Any form of biomass is regarded as a suitable feedstock for fast pyrolysis process. This is confirmed by the fact that approximately 100 different types of biomass were tested as a fast pyrolysis feed at a laboratory scale [10, 12].

In order to investigate the influence of type of biomass, its composition and process conditions on yield and characteristics of fast pyrolysis products tables 2, 3, 4 and 5 were prepared.

Table 2: Examples of wood biomass fast pyrolysis

Type of wood	Process conditions	Bio-oil yield, wt%	Bio-oil HHV, MJ/kg	Notes	Reference
Beech sawdust	BFB reactor (stainless steel) + 2 consecutive cyclones (operated at 400 ^{0}C) + scrubber (Isopar^{TM} V quenching agent, room temperature) + ESP, feed particle size 1.2-1.8 mm and moisture content 10.6 wt%, 0.6-0.7 mm silica sand as a bed material, pyrolysis temperature 500 ^{0}C, vapour residence time 0.9 s	59.9	-	Feed composition, wt% (db): ash content 0.6, nitrogen content 0.11 Non-condensable gas yield 13.3 wt%; composition of non-condensable gas (N_2 free), vol%: CO 43.1, CO_2 44.2, CH_4 7.5, H_2 3.1, C_2H_4+C_2H_6 2.1	[19]
Yellow poplar wood (Liriodendron tulipifera) (debarked)	BFB reactor + cyclone + 2 consecutive condensers (operated at 0 ^{0}C) + ESP, feed particle size 0.5 mm and moisture content 8%, ~ 0.5 mm silica sand as a bed material, N_2 as a fluidizing gas, pyrolysis temperature 500 ^{0}C, 1.2 s vapour residence time	68.5 (wb)	17.2	Feed composition, %: holocellulose (cellulose+hemicellulose) 78.3, lignin 21.3, ash content 0.58 (db) Bio-oil viscosity 31 cSt, pH 2.4; bio-oil composition, wt%: water content 21.6, nitrogen content 0.3 (wb), oxygen content 52.2 (wb) Biochar yield 10 wt% (wb), HHV 28.7 MJ/kg; biochar composition: trace of nitrogen, carbon content 80 wt%	[20]
Japanese red pine (debarked)	Internally CFB reactor (6 mm thick stainless steel) + scrubber + 2 consecutive condensers (operated at 3	35.7 (wb)	23.9	Feed ash content 0.3 wt% Bio-oil yield was calculated by subtracting water from bio-oil; bio-oil	[21]

	^{0}C, filled with methanol which was then removed from bio-oil by evaporation), feed particle size ~ 2 mm and moisture content 9.8 wt%, 0.16 mm silica sand as a bed material, N_2 as a fluidizing gas, pyrolysis temperature 500 ^{0}C, ~ 1 s vapour residence time			composition, wt%: water content 24.7, nitrogen content 1 (db), sulphur content <0.1 (db), oxygen content 37.4 (db) Non-condensable gas yield 22.2 wt% (wb)	
Type of wood	**Process conditions**	**Bio-oil yield, wt%**	**Bio-oil HHV, MJ/kg**	**Notes**	**Reference**
Japanese larch sawdust	BFB (SUS 306 stainless steel) + cyclone (kept at 400 ^{0}C) + hot filter (kept at 400 ^{0}C) + 2 consecutive condensers (operated at -25 ^{0}C) + ESP, feed particle size 0.7 mm (smaller decrease in bio-oil yield, bigger only a tiny decrease) and moisture content <1wt%, 40 µm Emery (NANKO ABRASIVES, Japan) as a bed material, produced non-condensable gas as a fluidizing gas, pyrolysis temperature 450 ^{0}C	64	22.2 (db)	Feed composition, wt%: cellulose 58.6, hemicellulose 13, lignin 20.1, ash 0.2, no sulphur was detected Bio-oil pH 2.1; bio-oil composition, wt%: water content 28, nitrogen content 1.8 (db), oxygen content 34.2 (db), no ash detected Non-condensable gas yield ~ 21 wt%; non-condensable gas composition, wt%: CO_2 51.5, CO 41, C_1-C_4 7.5	[22]
Radiata pine sawdust	BFB reactor (SUS 304 stainless steel) + cyclone (kept at 400 ^{0}C) + hot filter (kept at 400 ^{0}C) + series of quenching columns (minimum temperature -30 ^{0}C), feed particle size 1-2	67	23	Feed composition, wt%: cellulose 44.8, hemicellulose 34.1, lignin 27.5, ash 0.19, nitrogen 0.1 Bio-oil pH 2.5; bio-oil composition, wt%: water	[23]

	mm and moisture content 7.61 wt%, sand as a bed material, produced non-condensable gas as a fluidizing gas, pyrolysis temperature 474 ^{0}C			content 27, nitrogen content 0.07, oxygen content 39.2, ash content 0.01 Non-condensable gas yield 23.2 wt% Biochar yield 9.7 wt%; biochar from cyclone carbon content 73.5 wt%, biochar from hot filter carbon content 40 wt%, no nitrogen and sulphur was detected in both biochars from cyclone and from hot filter; HHV of biochar from cyclone 26 MJ/kg	
Oak (debarked)	BFB reactor + cyclone + 2 consecutive condensers (operated at 0 ^{0}C) + ESP, feed particle size <0.5 mm and moisture content ~ 5%, N_2 as a fluidizing gas, pyrolysis temperature 500 ^{0}C, ~ 2 s vapour residence time	65.7 (db)	17	Feed composition (wt% db): holocellulose 80, lignin 24.7, extractives 2.8, ash 0.8 Bio-oil viscosity 34.6 cSt (at 40 ^{0}C), bio-oil pH 2.4; bio-oil composition, wt%: water content 20.2, nitrogen was not detected, oxygen content 51.3 Non-condensable gas yield 20.2 wt% (db) Biochar yield 14.1 wt% (db), HHV 30.2 MJ/kg; biochar carbon content 85.9 wt% (db), only a trace of nitrogen detected in biochar	[24]

Type of wood	Process conditions	Bio-oil yield, wt%	Bio-oil HHV, MJ/kg	Notes	Reference
Eucalyptus (debarked)	BFB reactor + cyclone + 2 consecutive condensers (operated at 0 ^{0}C) + ESP, feed particle size <0.5 mm and moisture content ~ 5%, N_2 as a fluidizing gas, pyrolysis temperature 500 ^{0}C, ~ 2 s vapour residence time	59.2 (db)	15.5	Feed composition (wt% db): holocellulose 81.4, lignin 25.6, extractives 1.5, ash 0.4 Bio-oil viscosity 19.4 cSt (at 40 ^{0}C), bio-oil pH 1.7; bio-oil composition, wt%: water content 26.4, nitrogen was not detected, oxygen content 54.6 Non-condensable gas yield 25.9 wt% (db) Biochar yield 14.9 wt% (db), HHV 32.2 MJ/kg; biochar carbon content 90 wt% (db), only a trace of nitrogen detected in biochar	[24]
Pitch pine (debarked)	BFB reactor + cyclone + 2 consecutive condensers (operated at 0 ^{0}C) + ESP, feed particle size <0.5 mm and moisture content ~ 5%, N_2 as a fluidizing gas, pyrolysis temperature 500 ^{0}C, ~ 2 s vapour residence time	61.6 (db)	18.3	Feed composition (wt% db): holocellulose 76.1, lignin 28.4, extractives 6.9, ash 0.5 Bio-oil viscosity 10.3 cSt (at 40 ^{0}C), bio-oil pH 2.5; bio-oil composition, wt%: water content 23.6, nitrogen was not detected, oxygen content 49.1 Non-condensable gas yield 21.9 wt% (db) Biochar yield 16.5 wt% (db), HHV 31.5 MJ/kg; biochar carbon content 88.7 wt% (db), only a trace of nitrogen detected in	[24]

				biochar	
Type of wood	**Process conditions**	**Bio-oil yield, wt%**	**Bio-oil HHV, MJ/kg**	**Notes**	**Reference**
Japanese cedar (debarked)	BFB reactor + cyclone + 2 consecutive condensers (operated at 0 ^{0}C) + ESP, feed particle size <0.5 mm and moisture content ~ 5%, N_2 as a fluidizing gas, pyrolysis temperature 500 ^{0}C, ~ 2 s vapour residence time	62.6 (db)	18.9	Feed composition (wt% db): holocellulose 73.3, lignin 35.1, extractives 3.6, ash 0.4 Bio-oil viscosity 45.9 cSt (at 40 ^{0}C), bio-oil pH 2.4; bio-oil composition, wt%: water content 20.5, nitrogen was not detected, oxygen content 43 Non-condensable gas yield 23.5 wt% (db) Biochar yield 13.9 wt% (db), HHV 31.2 MJ/kg; biochar carbon content 87.8 wt% (db), only a trace of nitrogen detected in biochar	[24]
Radiata pine sawdust	BFB (SUS 306 stainless steel) + cyclone (kept at 400 ^{0}C) + hot filter (kept at 400 ^{0}C) + 2 condensers + ESP, feed particle size 0.7 mm (smaller and bigger particles result in decrease in bio-oil yield) and moisture content <1 wt%, 40 μm Emery (NANKO Abrasives, Japan) as a bed material, N_2 as a fluidizing gas, pyrolysis temperature 400 ^{0}C	51	22	Feed composition, wt%: cellulose 44.8, hemicellulose 34.1, lignin 27.5, ash 0.2, nitrogen 0.1 Bio-oil pH 2.3; bio-oil composition, wt%: water content 28.8, nitrogen content 1.7, oxygen content 36.7, no ash detected Non-condensable gas yield ~ 21 wt%; non-condensable gas composition (wt%): CO_2	[25]

				52.1, CO 40, CH_4 4, C_2-C_4 3.9 Biochar yield ~ 28 wt%, HHV 29.9 MJ/kg; biochar carbon content 82.8 wt%, no nitrogen detected in biochar	

Table 3: Examples of herbaceous and agricultural biomass.

Type of biomass	**Process conditions**	**Bio-oil yield, wt%**	**Bio-oil HHV, MJ/kg**	**Notes**	**Reference**
Wheat straw	BFB reactor + 2 consecutive cyclones (kept at 400 ^{0}C) + scrubber (Isopar^{TM} V quenching agent, room temperature) + ESP, feed particle size 0.8-2 mm and moisture content 9.9 wt%, 600-710 µm silica sand as a bed material, pyrolysis temperature 500 ^{0}C, vapour residence time 1.1 s	40.5	-	Feed ash content 6.8 wt% (db), feed nitrogen content 0.72 wt% (db) Bio-oil in two phase form (oil and aqueous phase) Non-condensable gas yield 17.1 wt%; nitrogen free composition of non-condensable gas, vol%:CO_2 52.7, CO 35.8, CH_4 6.5, H_2 2.8, C_2H_4+C_2H_6 2.2	[19]
Cassava rhizome	BFB reactor (SUS 304 stainless steel) + 2 consecutive cyclones + water cooled condenser + ESP + 2 consecutive dry ice/acetone condensers, feed particle size 250-425 µm and moisture content 1.8 wt%, 250-	69.1 (db)	24.8	Feed ash content 3.6 wt% (db) Bio-oil viscosity 18 cSt (at 40 ^{0}C), pH 3.3, density 1.1 kg/L; bio-oil composition, wt%: water content 16.8, nitrogen content 0.4 (db), oxygen content 22.1 (db), ash content	[26]

	425 µm silica sand as a bed material, N_2 as a fluidizing gas, 475 ^{0}C			0.2 Non-condensable gas yield ~ 4 wt% (db) Biochar yield ~ 26.9 wt% (db), HHV 25.49 MJ/kg (db); biochar composition, wt% (db): carbon content 66.76, nitrogen content 1.05	
Cassava rhizome	BFB reactor (SUS 304 stainless steel) + 2 consecutive cyclones + hot filter + water cooled condenser + ESP + 2 consecutive dry ice/acetone condensers, feed particle size 250-425 µm (smaller and bigger particles result in decrease in bio-oil yield) and moisture content 1.8 wt%, 250-425 µm silica sand as a bed material, N_2 as a fluidizing gas, pyrolysis temperature 472 ^{0}C	63.2 (db)	22.1	Feed ash content 3.6 wt% (db) Bio-oil viscosity 5.1 cSt (at 40 ^{0}C), pH 3.1, density 1.1 kg/L; bio-oil composition, wt%: water content 18, nitrogen content 0.5 (db), oxygen content 27.8 (db), ash content <0.01 Non-condensable gas yield ~ 12 wt% (db) Biochar yield ~ 24.8 wt% (db), HHV 25.49 MJ/kg (db); biochar composition, wt% (db): carbon content 66.76, nitrogen content 1.05	[26]
Type of biomass	**Process conditions**	**Bio-oil yield, wt%**	**Bio-oil HHV, MJ/kg**	**Notes**	**Reference**
Cassava stalk	BFB reactor (SUS 304 stainless steel) + 2 consecutive cyclones + water cooled condenser + ESP + 2 consecutive dry ice/acetone condensers, feed	61.4 (db)	24.3	Feed ash content 5.2 wt% (db) Bio-oil viscosity 15.6 cSt (at 40 ^{0}C), pH 3.4, density 1.1 kg/L; bio-oil composition, wt%: water content 19,	[26]

	particle size 250-425 µm and moisture content 2.4 wt%, 250-425 µm silica sand as a bed material, N_2 as a fluidizing gas, pyrolysis temperature 469 ^{0}C			nitrogen content 1.2 (db), oxygen content 21.7 (db), ash content 0.2 Non-condensable gas yield ~ 14 wt% (db) Biochar yield ~ 24.6 wt% (db), HHV 24.66 MJ/kg (db); biochar composition, wt% (db): carbon content 64.16, nitrogen content 1.37	
Cassava stalk	BFB reactor (SUS 304 stainless steel) + 2 consecutive cyclones + hot filter + water cooled condenser + ESP + 2 consecutive dry ice/acetone condensers, feed particle size 250-425 µm and moisture content 2.4 wt%, 250-425 µm silica sand as a bed material, N_2 as a fluidizing gas, pyrolysis temperature 475 ^{0}C	54.1 (db)	22.2	Feed ash content 5.2 wt% (db) Bio-oil viscosity 6.4 cSt (at 40 ^{0}C), pH 3.7, density 1.1 kg/L; bio-oil composition, wt%: water content 32.4, nitrogen content 0.7 (db), oxygen content 15 (db), ash content <0.01 Non-condensable gas yield ~ 24 wt% (db) Biochar yield ~ 21.9 wt% (db), HHV 24.66 MJ/kg (db); biochar composition, wt% (db): carbon content 64.16, nitrogen content 1.37	[26]
Sweet sorghum	BFB reactor + cyclone (kept at 450 ^{0}C) + 2 consecutive ice cooled condensers, feed particle size 0.5 mm and moisture content 5.83 wt% (db), highly spherical Ottawa sand as a bed material, N_2 as	63 (db)	-	Feed ash content 3.1 wt% (db) Non-condensable gases yield, wt% (daf): CO_2 9.7, CO 2.4, CH_4 0.2 Biochar yield 21.4 wt% (db)	[27]

	a fluidizing gas, pyrolysis temperature 450 ^{0}C, vapour residence time 0.5 s				
Sweet sorghum bagasse	BFB reactor + cyclone (kept at 510 ^{0}C) + 2 consecutive ice cooled condensers, feed particle size 0.5 mm and moisture content 10.05 wt% (db), highly spherical Ottawa sand as a bed material, N_2 as a fluidizing gas, pyrolysis temperature 510 ^{0}C, vapour residence time 0.5 s	69.4 (db)	-	Feed ash content 9.2 wt% (db) Non-condensable gases yield, wt% (daf): CO_2 7.8, CO 3, CH_4 0.4, C_2 0.4 Biochar yield 13.4 wt% (db)	[27]
Type of biomass	**Process conditions**	**Bio-oil yield, wt%**	**Bio-oil HHV, MJ/kg**	**Notes**	**Reference**
Corncob	BFB reactor (316 stainless steel) + hot filter (kept at 400 ^{0}C) + condenser, feed particle size 1-2 mm and moisture content 8.6 wt%, 0.1-0.2 mm silica sand as a bed material, CO as a fluidizing gas, pyrolysis temperature 550 ^{0}C	49.6	23.7	Feed composition, wt% (db): cellulose 41.78, hemicellulose 31.84, lignin 12.44 Bio-oil water content ~ 22 wt% Non-condensable gases yield, wt%: CO_2 ~ 15, CO ~ 6, CH_4 ~ 1	[28]
Corncob	BFB reactor (316 stainless steel) + hot filter (kept at 400 ^{0}C) + condenser, feed particle size 1-2 mm and moisture content 8.6 wt%, 0.1-0.2 mm silica	57.1	17.8	Feed composition, wt% (db): cellulose 41.78, hemicellulose 31.84, lignin 12.44 Bio-oil water content ~ 20 wt% Non-condensable gases	[28]

	sand as a bed material, N_2 as a fluidizing gas, pyrolysis temperature 550 ^{0}C			yield, wt%: CO_2 ~ 8, CO ~ 6, CH_4 ~ 1	
Corncob	BFB reactor (316 stainless steel) + hot filter (kept at 400 ^{0}C) + condenser, feed particle size 1-2 mm and moisture content 8.6 wt%, 0.1-0.2 mm silica sand as a bed material, CO_2 as a fluidizing gas, pyrolysis temperature 550 ^{0}C	55.3	20.2	Feed composition, wt% (db): cellulose 41.78, hemicellulose 31.84, lignin 12.44 Bio-oil water content ~ 20 wt% Non-condensable gases yield, wt%: CO_2 ~ 7, CO ~ 6, CH_4 ~ 1	[28]
Type of biomass	**Process conditions**	**Bio-oil yield, wt%**	**Bio-oil HHV, MJ/kg**	**Notes**	**Reference**
Corncob	BFB reactor (316 stainless steel) + hot filter (kept at 400 ^{0}C) + condenser, feed particle size 1-2 mm and moisture content 8.6 wt%, 0.1-0.2 mm silica sand as a bed material, CH_4 as a fluidizing gas, pyrolysis temperature 550 ^{0}C	58.7	17.2	Feed composition, wt% (db): cellulose 41.78, hemicellulose 31.84, lignin 12.44 Bio-oil water content ~ 22 wt% Non-condensable gases yield, wt%: CO_2 ~ 6, CO ~ 4, H_2 ~ 1 CH_4 ~ 0.2	[28]
Corncob	BFB reactor (316 stainless steel) + hot filter (kept at 400 ^{0}C) + condenser, feed particle size 1-2 mm and moisture content 8.6 wt%, 0.1-0.2 mm silica	56.4	24.4	Feed composition, wt% (db): cellulose 41.78, hemicellulose 31.84, lignin 12.44 Bio-oil water content ~ 28 wt% Non-condensable gases	[28]

	sand as a bed material, H_2 as a fluidizing gas, pyrolysis temperature 550 ^{0}C			yield, wt%: CO_2 ~ 9, CO ~ 4, CH_4 ~ 1	
Rice husk	BFB reactor, feed particle size 0.45-1 mm, pyrolysis temperature 520 ^{0}C, vapour residence time <1s	46.36	13.36	Feed composition, %: cellulose 37.15, hemicellulose 23.87, lignin 12.84, extractives 18.59, ash 7.55 Bio-oil viscosity 82.43 cSt (at 40 ^{0}C), pH 3.36, density 1.21 kg/L; bio-oil composition, wt%: water content 33.8, no nitrogen detected, oxygen content 57.37 Yield of non-condensable gas ~ 25 wt%	[29]
Maize stalk	BFB reactor + 2 consecutive cyclones + condenser, feed particle size 0.1-0.5 mm and moisture content 7.67 wt%, 0.45 mm sand as a bed material, N_2 as a fluidizing gas, pyrolysis temperature 500 ^{0}C	66	19.6	Feed ash content 8.33 wt% Bio-oil viscosity 129 cSt (at 20 ^{0}C), pH 3.2, density 1.22 kg/L; bio-oil composition, wt%: water content 22.5, nitrogen content 0.6, sulphur content 0.3, oxygen content 47.5 Non-condensable gas yield 15.9 wt%; non-condensable gas composition, wt%: N_2 85, CO_2 5.78, CO 2.37, CH_4 0.78, C_2H_4 0.62, H_2 0.03	[30]

Type of biomass	Process conditions	Bio-oil yield, wt%	Bio-oil HHV, MJ/kg	Notes	Reference
Coffee grounds	BFB reactor (SUS 316 stainless steel) + cyclone + condenser + ESP, feed particle size 0.2-0.3 mm and moisture content 1.31 wt% (wb), sand as a bed material, N_2 as a fluidizing gas, pyrolysis temperature 550 ^{0}C, vapour residence time 1.07 s	54.85 (wb)	20.38	Bio-oil viscosity 87.7 cP (at 20 ^{0}C), pH 3.1, density 1.15; bio-oil composition, wt%: water content 31.11, nitrogen content 3.06 (daf), no sulphur was detected, oxygen content 35.26 (daf), ash content 0.17 Non-condensable gas yield ~ 16 wt%; non-condensable gas was almost totally composed of CO_2 and CO with the ratio of 2:1 between the former and the latter one	[31]

Table 4: Examples of sewage sludge fast pyrolysis.

Type of sewage sludge	**Process conditions**	**Bio-oil yield, wt%**	**Bio-oil HHV, MJ/kg**	**Notes**	**Reference**
Dehydrated anaerobically digested sewage sludge	Internally CFB reactor (6 mm thick stainless steel) + scrubber + 2 consecutive condensers (operated at 3 ^{0}C, filled with methanol which was then removed from bio-oil by evaporation), feed moisture content 11.5 wt%, feed pulverized to ~ 2 mm, 0.16 mm silica sand as a bed material, N_2 as a fluidizing gas, pyrolysis temperature 500 ^{0}C, ~ 1s vapour residence time	28 (wb)	27	Feed ash content 30 wt% Bio-oil yield was calculated by subtracting water from bio-oil; bio-oil composition, wt%: water content 32.1, nitrogen content 12.3 (db), sulphur content (db), bio-oil oxygen content 19.2 (db), Non-condensable gas yield 7.2 wt% (wb), non-condensable gas contained relatively high amount of CH_4 and C_2 (~ 20 vol%)	[21]
Dehydrated sewage sludge	BFB reactor (SUS 306 stainless steel) + cyclone (kept at 400 ^{0}C) + hot filter (kept at 400 ^{0}C) + 2 consecutive condensers (operated at -25 ^{0}C) + ESP, feed particle size 0.7 mm (smaller and bigger particles result in decrease in bio-oil yield) and moisture content 5.1%, 40 µm Emery [Al_2O_3, (NANKO ABRASIVES, Japan)] as a bed material, produced non-condensable gas as a fluidizing gas, pyrolysis temperature 450	50.4 (wb)	-	Feed ash content 26.9%, feed chlorine content 881 ppm (daf) Bio-oil contained large amount of nitrogen compounds, no ash was detected in bio-oil, bringing pyrolysis vapour into contact with fixed catalyst bed of CaO reduced Cl content in bio-oil from 498 ppm (without using of catalyst) to 73 ppm Non-condensable gas yield 10.5 wt% (wb)	[32]

	^{0}C				
Dehydrated anaerobically digested sewage sludge 1	BFB reactor + cyclone + hot filter + 2 condensers, feed particle size 250-500 µm and moisture content 5.3 wt% (wb), 150-250 µm sand as a bed material, N_2 as a fluidizing gas, pyrolysis temperature 550 ^{0}C	45 (daf)	30.6 (db)	Feed ash content 52 wt% (wb) Bio-oil water content 44.5 wt% (db), bio-oil viscosity 7.92 cSt (db), density 0.972 kg/L (db) Non-condensable gas yield ~ 35 wt% (daf); non-condensable gas composition (N_2 fb), vol%: CO_2 ~ 40, H_2 ~ 25, CO ~ 15, CH_4 ~ 10, H_2S ~ 2, C_2 ~ 2	[33]
Type of sewage sludge	**Process conditions**	**Bio-oil yield, wt%**	**Bio-oil HHV, MJ/kg**	**Notes**	**Reference**
Dehydrated anaerobically digested sewage sludge 2	BFB reactor + cyclone + hot filter + 2 condensers + ESP, feed particle size 250-500 µm and moisture content 7.1 wt% (wb), 150-250 µm sand as a bed material, N_2 as a fluidizing gas, pyrolysis temperature 550 ^{0}C	50 (daf)	31.2 (db)	Feed ash content 41 wt% (wb) Bio-oil water content 46.6 wt% (db), bio-oil viscosity 16.91 cSt (db), density 0.975 kg/L (db) Non-condensable gas yield ~ 30 wt% (daf); non-condensable gas composition (N_2 free), vol%: CO_2 ~ 60, CO ~ 15, H_2 ~ 10, CH_4 ~ 5, H_2S ~ 2, C_2 ~ 1	[33]

Table 5: Examples of microalgae fast pyrolysis.

Type of microal-gae	**Process conditions**	**Bio-oil yield, wt%**	**Bio-oil HHV, MJ/kg**	**Notes**	**Reference**
Remnants of solvent extraction of microal-gae (Chlorel-la vulgaris) for lipid recovery	FB reactor (316 stainless steel) + 2 cyclones + 2 condensers (operated at 20 ^{0}C) + ESP + condenser (operated at 1 ^{0}C), feed moisture content 4.39 wt%, 0.55 mm silica particles as a bed material, pyrolysis temperature 500 ^{0}C	53 (47 oil phase and 6 aque-ous pha-se)	24.57 (oil phase)	Feed ash content 8.34 wt% Bio-oil in two phase form (oil and aqueous phase), the largest amount of bio-oil collected from ESP Oil phase composition, wt%: water content 15.89, nitrogen content 12.8, oxygen content 27.46 Aqueous phase composition, wt%: water content 90.02, nitrogen content 1.78 Biochar yield ~ 31 wt%, HHV 23.04 MJ/kg; biochar composition, wt%: carbon content 61.96, nitrogen content 9.43 Non-condensable gas yield ~ 10 wt%, HHV 5.1 MJ/kg; non-condensable gas composition, vol%: CO_2 71.7, CO 14.7, CH_4 6.6, C_2-C_3 ~ 5	[34]
Microal-gae (Chllorel-la protothe-coides)	BFB reactor + cyclone + series of condensers, feed particle size <0.18 mm and moisture content 5.39%, N_2 as a fluidizing gas, pyrolysis temperature 500 ^{0}C, vapour residence time 2-3 s	17.5 (oil phase, db)	30 (oil phase)	Feed ash content 6.36% Bio-oil in 2 phase form (oil and aqueous phase); bio-oil composition, wt%: nitrogen content 9.74, oxygen content 19.43 Non-condensable gas yield ~ 27.5 wt% Biochar yield ~ 55 wt%	[35]
Microal-gae	BFB reactor + cyclone + series of condensers,	23.7 (oil	29 (oil phase)	Feed ash content 13.26% Bio-oil in 2 phase form (oil and	[35]

(Micro-cystis aerugi-nosa)	feed particle size <0.18 mm and moisture content 4.4%, N_2 as a fluidizing gas, pyrolysis temperature 500 ^{0}C, vapour residence time 2-3 s	phase, db)		aqueous phase); bio-oil composition, wt%: nitrogen content 9.83, oxygen content 20.95 Non-condensable gas yield ~ 56 wt% Biochar yield ~ 20.3 wt%	

According to the tables presented above lignocellulosic biomass appears to be better feedstock for fast pyrolysis process than sewage sludge or microalgae, because it gives higher yields of bio-oil, which is homogeneous and contains much less nitrogen, sulphur and other elements and substances which are associated with environmentally harmful emissions. Among all the types of lignocellulosic biomass wood biomass is superior to herbaceous and agricultural biomass, as it generally contains much less ash and gives higher yields of bio-oil with higher heating values.

Bark pyrolysis yields much less bio-oil than pyrolysis of stem wood. Also bio-oil produced from bark is of inferior quality in comparison to the bio-oil produced from stem wood: it is highly susceptible to phase separation because of bark elevated concentration of extractives and waxy materials. High inorganic species bark content is another bark drawback in terms of bio-oil production, as if sufficient retention of the inorganic species in biochar is not achieved, these species will end up in bio-oil significantly speeding up its aging [36]. Therefore it has to be noted that only debarked wood is a really attractive feedstock for bio-oil production.

Presumably because of the advantages of wood biomass in terms of the bio-oil production and may be also because of the existing very well arranged handling infrastructures, wood biomass is used as a raw material in some commercial scale fast pyrolysis installations. In Canada commercial scale bubbling fluidized bed fast pyrolysis plants with capacity of 30 tonne/day and 200 tonne/day utilize wood waste as a feedstock [2]. In Finland Metso, UPM, Fortum and VTT have constructed an up to 7 tonne/day bio-oil production pilot unit integrated with a conventional fluidized bed boiler. The unit has already produced more than 100 tonne of bio-oil from sawdust and forest residues. Around 40 tonne of that bio-oil has been combusted in Fortum's 1.5 MW district heating plant [37].

2.2 Products

2.2.1 Bio-oil

Bio-oil can be regarded as a microemulsion of organic macromolecules stabilized in an aqueous solution of smaller organic molecules. The following types of organic compounds are mostly found in bio-oil: hydroxyaldehydes, hydroxyketones, sugars and dehydrosugars, carboxylic acids, phenolic compounds, furans, nitrogen compounds and multifunctional compounds [3, 10, 12, 17].

Bio-oil is a viscous (on average around 0.01-0.1 Pa·s at 40 ^{0}C), odorous, dark brown, free flowing, dense (around 1200 kg/m^3) liquid with pH 2-4. It is corrosive, immiscible with petroleum fuels, and susceptible to ageing during storage, which results in an increase in its viscosity and water content, and may lead to a phase separation and deposition of solids. The fact that bio-oil is thermally unstable gives rise to a necessity to store it at a room or lower temperatures, as elevated temperatures accelerate its ageing [3, 10, 11, 12, 17]. Addition of methanol and ethanol into bio-oil is regarded to be a method of improving bio-oil stability during its storage and also of reducing its viscosity [2, 10, 17]. A few examples of this phenomenon are described below.

It was observed that addition of 10 wt% of methanol and 10 wt% of ethanol to bio-oil sample obtained from fast pyrolysis of mixture, comprised from poultry litter and pine wood with ratio of 1:1 between each other, decreased the sample viscosity 6.4 and 5.12 times, respectively, and decreased the rate of viscosity increase of the bio-oil sample while is storage for six months under room temperature 11.5 and 14.3 times, respectively [38]. Methanol addition has also been noticed to improve combustion of poor quality bio-oils [39].

The following effect of 10 wt% of methanol addition to bio-oil produced from pyrolysis of hydbrid poplar has been observed: after 96 hours of exposure of the methanol containing sample to 90 ^{0}C it was still a single phase liquid, while the pure bio-oil sample formed a waxy precipitate floating on its surface only after 8 hours of exposure to 90 ^{0}C [40].

Bio-oil can be used as a fuel, for hydrogen generation through a catalytic steam reforming process [41] and as a source of valuable chemical compounds [2, 10, 11, 12, 17]. Higher heating value of bio-oil is considerably lower than that of petroleum fuels [3, 17, 11, 12]. This is associated with the presence of water in bio-oil and with the fact that almost all constituents of bio-oil are oxygenated [2, 3, 12, 17]. The latter is also believed to be the reason of such bio-oil drawbacks as immiscibility with petroleum fuels, corrosiveness and instability [3, 17].

High bio-oil water content (20-30 wt% on average, see tables II, III, IV, V) results from raw biomass moisture and from the dehydration reactions taking place during the pyrolysis process [3, 17, 18]. Much bio-oil water is attached to polar compounds by hydrogen bonds while some of the bio-oil water is in the form of aldehyde hydrates [3].

2.2.2 Biochar

Biochar can be used for carbon sequestration [2, 42] and soil amendment [2, 42, 43]. Biochar can be used instead of coke derived from fossil fuels in some metallurgical processes which will result in carbon neutral emissions of those processes [2]. Activated carbon with BET surface area of 788 m^2/g, average pore size of 2.2 nm and mineral content of 10 wt% was produced from biochar obtained during pyrolysis of chicken litter at 360 ^0C [44].

2.2.3 Non-condensable gas

Using of non-condensable gas as a fluidizing gas in fluidized bed fast pyrolysis installations is beneficial for bio-oil production. There was observed an increase in bio-oil yield by 7.8 wt% when fluidizing gas was switched from nitrogen to produced non-condensable gas, char yield remained almost the same and non-condensable gas yield declined by 6.7 wt% [32]. Bio-oil yield increase of 9 wt% was observed for the identical reason, char yield and non-condensable gas yield exhibit the same pattern in this case – the former one stayed almost the same while the latter one decreased by ~ 5 wt%, change in non-condensable gas composition was negligible [22]. In another case when fluidizing gas was switched from nitrogen to the produced non-condensable gas there was around 10

wt% rise in the bio-oil yield and a decline in the non-condensable gas yield of approximately the same level, while biochar yield remained the same [45].

N_2, CO_2, CO, CH_4 and H_2 have been evaluated as fluidizing gases for bubbling fluidized bed fast pyrolysis. The results of the evaluation revealed that using of CO_2 and CO as a fluidizing gas leads to formation of bio-oil with smaller amount of methoxy-containing compounds in comparison to other tested gases. Methoxy-containing compounds are believed to have a potential of causing polymerization reactions in bio-oil and thus contribute to its instability [28].

Therefore using of CO_2 and CO as fluidizing gases allows to produce more stable bio-oil. This is another reason in favour of using non-condensable gas as a fluidizing gas in fluidized bed fast pyrolysis installations, as CO_2 and CO are major components of non-condensable gas.

2.2.4 Products summary

The table 6 presented below summarizes characteristics and possible applications of fast pyrolysis products.

Table 6: Fast pyrolysis products overview.

Product	Composition	Characteristics	Applications
Bio-oil	Hydroxyaldehydes, hydroxyketones, sugars and dehydrosugars, carboxylic acids, phenolic compounds, furans, nitrogen compounds and multifunctional compounds	Viscous, corrosive, unstable, HHV 15-25 MJ/kg	Fuel, precursor for hydrogen generation, feedstock for synthesis of various chemicals
Biochar	Carbon content up to 80%, accumulates almost all ash	HHV 25-30 MJ/kg	Fuel, fertilizer, carbon sequester, precursor for activated carbon production
Non-condensable gas	CO_2 (major component can be up	Heating value is very dependent on the type	Fuel in case CO_2 content is low enough,

	to 70%), CO (on average ~ 40%), CH_4 (on average ~ 5%), C2 (on average ~ 2%), H_2 (on average a trace)	of biomass, usually low	increases bio-oil yield and stability when used as a fluidizing gas in fluidized bed installations

Based on the applications of fast pyrolysis products presented in the table 2.5 one should note that non-condensable gas and biochar can be used as fuels and therefore can be utilized within the process of fast pyrolysis to satisfy its internal heat and energy needs [1, 10, 12].

2.2.5 World bio-oil production rate

No direct data about the world bio-oil production rate were found. However based on the available data about the rate of raw biomass consumption by existing today in the world industrial scale fast pyrolysis installations it is possible to estimate an annual bio-oil production rate in the world.

In Netherlands there were built 4 rotating cone fast pyrolysis units with a maximum throughput of biomass of 2 tonne/hour [10]. On the presumption that they operate on the continuous basis 24 hours per day and have totally 1 month of shutdowns per year, their maximum rate of biomass consumption is $2 \cdot 24 \cdot 11 \cdot 4 =$ 2112 tonne/year.

In Canada there were built 4 bubbling fluidized bed fast pyrolysis units with a maximum throughput of biomass of 8 tonne/hour [10]. Using exactly the same assumptions as for the rotating cone units, their maximum rate of biomass consumption is 4 times higher and therefore is 8448 tonne/year.

In Canada there were also built 8 circulating fluidized bed fast pyrolysis units with a maximum throughput of biomass of 4 tonne/hour [10]. Using the same assumptions as for the previous two estimations again, the maximum rate of biomass consumption by these circulating fluidized bed units is equal to the one in the previous case and is 8448 tonne/year.

Therefore total maximum annual worldwide biomass consumption by the industrial scale fast pyrolysis installations is 2112 + 8448 + 8448 =

19008 tonne/year. Assuming the lower limit of the bio-oil yield of these installations is 40 wt% and the higher limit of the bio-oil yield of these installations is 70 wt%, the maximum worldwide rate of the industrial scale bio-oil production lies in the range of 7603.2 tonne/year to 13305.6 tonne/year.

2.3 Process description

2.3.1 Process overview

Block diagram of fast pyrolysis bio-oil production process from wood biomass is shown in the figure 1.

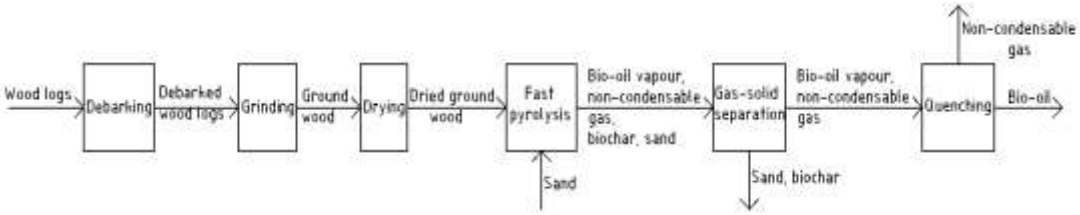

Figure 1: Block diagram of fast pyrolysis bio-oil production process.

At first raw biomass undergoes preprocessing which consists of debarking, grinding of the debarked wood to less than 2 mm particles and subsequent drying to less than 10 % moisture content. After the preprocessing stage the actual fast pyrolysis takes place: ground and dried biomass particles are pyrolysed into bio-oil vapour, non-condensable gas and biochar. Then bio-oil vapour and non-condensable gas are separated from biochar and in case of fluidized bed installations also from bed material. At the final stage of the fast pyrolysis process the mixture of bio-oil vapour and non-condensable gas is quenched. This leads to condensation of bio-oil and thus it gets separated from the non-condensable gas.

2.3.2 Preprocessing

Grinding of feed biomass to less than 2 mm particles and drying of those particles to less than 10 % moisture content are necessary for providing of required rate of

heat transfer during the pyrolysis process and for achieving low bio-oil water content in order to increase its heating value [10, 11, 12, 18].

One can assume that by grinding the feed biomass to particles of a very small size and by subsequent drying of them to a very low moisture content it is possible to maximize the bio-oil yield and its quality. However results of some research studies have demonstrated the opposite.

It was observed that decrease of the size of feed particle to less than 0.7 mm led to a decrease of bio-oil yield and to an increase of non-condensable gas [22]. This phenomenon is attributed to the fact that reducing feed particle size beyond a certain level causes their overheating which results in an undesirable cracking of pyrolysis vapour into non-condensable gas [22, 25, 32].

Even though pyrolysis of biomass with the lowest moisture content will result in production of bio-oil with the lowest water content, nevertheless some minimal amount of moisture in the feed biomass is necessary for efficient heat transfer and biomass decomposition [18].

2.3.3 Fast pyrolysis

Pyrolysis is an endothermic process which requires continuous, intensive heat transfer to the reacting matter. Fast pyrolysis is conducted at the heating rates ranging from 100 to 10^5 ^{0}C/s. Biomass pyrolysis results in formation of biochar and of product vapour consisting of condensable and non-condensable gas [2, 10, 11, 12]. Almost regardless of the type of the feedstock biomass the highest yields of bio-oil are obtained at the reaction temperature of approximately 475-525 ^{0}C if the vapour residence time is short (around 0.2-0.6 s) [3, 10, 18, 46].

When biomass particles are heated to temperatures below 300 ^{0}C during their pyrolysis the following processes mainly occur in them: free radical formation, water evaporation and depolymerization. When temperature is in the range of 300 ^{0}C to 400 ^{0}C breaking of glycosidic linkages of polysaccharides is the prevailing reaction. When biomass particles are heated to the temperature above 400 ^{0}C, dehydration, rearrangement and fission of sugar units take place. Finally when the

temperature exceeds 450 ^{0}C a combination of all the processes described for every temperature range occur simultaneously [13].

While pyrolysis of biomass particles takes place their surfaces become covered with char. This char layer prevents efficient heat transfer and therefore it is needed to be removed [2]. For this reason a friction of biomass particles over a surface heated to the necessary temperature in order to provide attrition of the char layer and required rate of heat transfer can significantly intensify the pyrolysis process. From this point of view fluidized bed reactors should be very efficient pyrolysers, in case a bed of erosive granular material is used, as this provides a very high specific surface, resulting in effective heat transfer and ablation of the char layer from the surface of biomass particles.

2.3.4 Gas-solid separation

Cyclone separators appear to be the most feasible option for separation of product vapour from biochar and in case of fluidized bed installations also from bed material. However efficiency of cyclone separators, depending on their design, is limited to particle of 5-10 μm size [47]. Therefore some char fines will always penetrate into the bio-oil contributing to its instability and thus decreasing its efficiency when being utilized as a fuel [3].

Filtration of hot product vapour prior to its condensation allows to get a char free bio-oil, though the yield of bio-oil in case of hot vapour filtration is reduced because of the cracking of the vapour by char accumulating on the filter surface [12]. Also it is impossible to remove the filter cake from the filter [10]. It was observed that after an incorporation of a hot vapour filter into the process the bio-oil yield dropped by 6-7 wt% (db), water content increased by 1.2 wt% in case of cassava rhizome feed and by 13.4 wt% in case of cassava stalk, non-condensable gas yield rose by 8-10 wt% (db) [26]. The increase in water content the authors explain by secondary reactions taking place on the surface of the hot vapour filter.

2.3.5 Quenching

Quenching of product vapour after its separation from biochar and in case of fluidized bed installations also from bed material is conducted either in an earlier condensed bio-oil or in an immiscible hydrocarbon solvent [12]. While being

quenched bio-oil tends to form stable aerosols of sub-micron droplets in non-condensable gases, thus in order to recover those aerosols and therefore to obtain the highest yields of bio-oil, non-condensable gases should be treated with electrostatic precipitators prior to their internal or external reuse [2, 48].

2.3.6 Fast pyrolysis chemical kinetics models

Van de Velden et al. ([49]) proposed a model for biomass fast pyrolysis process which includes three primary parallel reactions and one secondary reaction. The primary parallel reactions are conversion of raw biomass into non-condensable gas, conversion of raw biomass into bio-oil vapour and conversion of raw biomass into biochar. The secondary reaction is cracking of bio-oil vapour into non-condensable gas. Each of the reactions has its own rate constant. The principle of this model is depicted below in the figure 2 where k_1, k_2, k_3 and k_4 represent reaction constants of corresponding reactions.

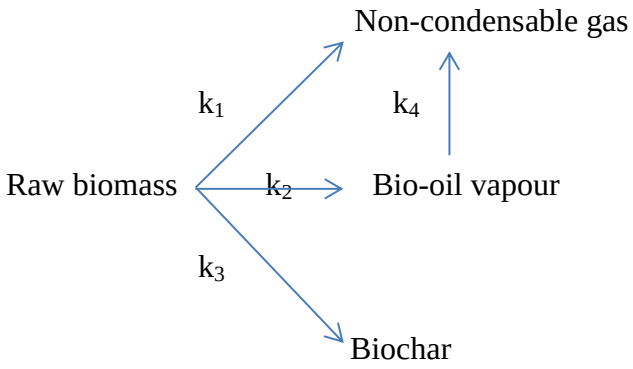

Figure 2: Biomass fast pyrolysis model [49].

Van de Velden et al. ([49]) state that the proposed model has been developed based on certain assumptions, which namely are: 1) the secondary reaction is much slower than the primary ones and it can be suppressed by short residence time of product vapour and by fast separation of product vapour from biochar; 2) small size of biomass particles and high heat transfer rate in the pyrolyser make the internal thermal resistance of the particles negligible which results in their immediate heating to the pyrolysis temperature; 3) reaction rate equations of an

individual biomass particle are of the first order and follow the Arrhenius expression.

Van de Velden et al. ([49]) represent fast pyrolysis reaction rate equations in the following way:

$$k = k_1 + k_2 + k_3 \quad (1)$$

$$\frac{dm_B}{dt} = -km_B \quad (2)$$

$$\frac{dm_G}{dt} = k_1 m_B + k_4 m_O \quad (3)$$

$$\frac{dm_O}{dt} = k_2 m_B - k_4 m_O \quad (4)$$

$$\frac{dm_C}{dt} = k_3 m_B \quad (5)$$

where t time, s

k overall reaction rate constant, s^{-1}

m_B mass of residual biomass divided by mass of initial biomass

m_G mass of formed non-condensable gas divided by mass of initial biomass

m_O mass of formed bio-oil vapour divided by mass of initial biomass

m_C mass of formed biochar divided by mass of initial biomass.

Taking into account that $m_G = 0$, $m_O = 0$ and $m_C = 0$ when t = 0 the solutions for the equations 1 – 5 are:

$$m_B = exp(-kt) \quad (6)$$

$$m_G =$$

$$= \frac{-k[kk_1 exp(-kt) - k_1 k_4 exp(-kt) - k_2 k_4 exp(-kt) - kk_2 exp(-k_4 t) - kk_1 + k_1 k_4 - kk_2 + k_2 k_4]}{k - k_4} \quad (7)$$

$$m_O = \frac{-k_2 exp(-k_4 t)[exp(-t(k-k_4)) - 1]}{k - k_4} \quad (8)$$

$$m_C = \frac{k_3[1-exp(-kt)]}{k} \quad (9)$$

Van de Velden et al. ([49]) claim that the amount of char after the completion of the pyrolysis reaction remains nearly constant and hence a relation between the three primary reaction constants can be written as:

$$k_3 = \frac{m_{C,\infty}}{1-m_{C,\infty}}(k_1 + k_2) \quad (10)$$

where $m_{C,\infty}$ the amount of char after the completion of the pyrolysis reaction.

Van de Velden et al. ([49]) used their model to simulate their own fast pyrolysis experiments conducted in circulating fluidized bed pyrolyser at 510 ^{0}C. In order to perform calculations they used overall rate constant k obtained from thermogravimetric experiments conducted by *Van de Velden et al.* ([50]) who determined that overall rate constant k for spruce wood at 500 ^{0}C is 0.824 s^{-1}. Using of this value may be a source of significant inaccuracy as heating rate in the thermogravimetric experiments performed by *Van de Velden et al.* ([50]) was 1.7 ^{0}C/s, whereas in order to consider a process to be fast pyrolysis heating rate should exceed 100 ^{0}C/s.

To find out rate constants k_1 and k_4 *Van de Velden et al.* ([49]) used preexponential coefficients (A_1 = 14300 s^{-1} and A_4 = 7900 s^{-1} respectively) and activation energies (E_1 = 106.5 KJ/mole and E_4 = 81 KJ/mole respectively) obtained by *Di Blasi et al.* ([51]). However it is not stated under which conditions (feedstock, heating rate, type of pyrolyser) these preexponential coefficients and activation energies were obtained, thus it is unclear whether they can be applied for prediction of distribution of products of pine wood fast pyrolysis process. *Van de Velden et al.* ([49]) calculated rate constants k_2 and k_3 by using the proposed equation 10 validity of which is questionable.

Despite of all the listed above drawbacks the results calculated by means of the proposed by *Van de Velden et al.* ([49]) model are in good agreement (around 1% error) with the results of their own fast pyrolysis experiments conducted in

circulating fluidized bed pyrolyser at 510 ^{0}C with unspecified biomass.

Luo et al. ([52]) proposed a fast pyrolysis model (identical to the model proposed by *Van de Velden et al.* ([49]) presented in figure 1) and obtained a good agreement between the results calculated by the means of their model and experimental data which they got through pyrolysis of wood particles in their sand bed bubbling fluidized bed pyrolyser. Parameters which they used to calculate reaction rate constants are shown below in the table 7.

Table 7: Parameters used for calculation of reaction rate constants by *Luo et al.* ([52]).

Number of reaction in the model scheme	Preexponential coefficient, s^{-1}	Activation energy, kJ/mole
1	$1.08 \cdot 10^7$	121
2	$2 \cdot 10^8$	133
3	$1.3 \cdot 10^8$	140
4	$3.09 \cdot 10^6$	108

Blondeau et al. ([53]) have a special approach to biomass fast pyrolysis modeling. In their model three main biomass components, namely cellulose, hemicellulose and lignin, are pyrolysed separately from each other and no interaction between them is assumed.

Blondeau et al. ([53]) proposed two sets of chemical reactions taking place while pyrolysis of biomass. The first set consists of primary reactions which lead to volatilization of biomass and biochar formation. Corresponding kinetic parameters and enthalpies of formation are provided for these primary reactions. The second set contains secondary reactions of cracking of some of the products emitted to the gas phase during the primary reactions. Only corresponding kinetic parameters are provided for these secondary reactions. Both sets of reactions are presented below in the table 8.

Table 8: Biomass pyrolysis reactions and their parameters [53].

Primary reactions				
Reactant	Products	Preexponential coefficient in reaction rate constant equation, s^{-1}	Activation energy, kJ/mole	Enthalpy of reaction, kJ/kg
CELL	CELLA	$2.8 \cdot 10^{19}$	242.4	447.7
CELLA	0.95 HAA + 0.25 GLYOX + 0.2 CH_3CHO + 0.25 HMFU + 0.2 C_3H_6O + 0.16 CO_2 + 0.23 CO + 0.9 H_2O + 0.1 CH_4 + 0.61 Char	$1.3 \cdot 10^{10}$	150.5	899.6
CELLA	LVG	$3.28 \cdot 10^{14}$	196.5	732.2
CELL	5 H_2O + 6 Char	$8 \cdot 10^{7}$	133.9	-1087.8
HCE	0.4 HCEA1 + 0.6 HCEA2	$2.1 \cdot 10^{16}$	186.7	548.1
HCEA1	0.75 G{H_2} + 0.8 CO_2 + 1.4 CO + 0.5 CH_2O + 0.25 CH_3OH + 0.125 ETOH + 0.125 H_2O + 0.625 CH_4 + 0.25 C_2H_4 + 0.675 Char	$2.6 \cdot 10^{11}$	145.7	447.7
HCEA1	XYL	$8.75 \cdot 10^{15}$	202.4	707.1
HCEA2	0.2 CO_2 + 0.5 CH_4 + 0.25 C_2H_4 + 0.8 G{CO_2} + 0.8 G{COH_2} + 0.7 CH_2O + 0.25 CH_3OH + 0.125 ETOH + 0.125 H_2O + Char	10^{10}	138.1	259.4
LIG-C	0.35 LIG-CC + 0.1 pCOUMARYL + 0.08 PHENOL + 0.41 C_2H_4 + H_2O + 0.495 CH_4 + 0.32 CO + G{COH_2} + 5.735 Char	$4 \cdot 10^{15}$	202.9	602.5

LIG-H	LIG-OH + C_3H_6O	$2 \cdot 10^{13}$	156.9	523
LIG-O	LIG-OH + CO_2	10^9	106.7	510.4
LIG-CC	0.3 pCOUMARYL + 0.2 PHENOL + 0.35 $C_3H_4O_2$ + 0.7 H_2O + 0.65 CH_4 + 0.6 C_2H_4 + G{COH_2} + 0.8 G{CO} + 6.4 Char	$5 \cdot 10^6$	131.8	288.7
LIG-OH	LIG + H_2O + CH_3OH + 0.45 CH_4 + 0.2 C_2H_4 + 1.4 G{CO} + 0.6 G{COH_2} + 0.1 G{H_2} + 4.15 Char	$3 \cdot 10^8$	125.5	100.4
LIG	FE2MACR	$1.5 \cdot 10^9$	143.8	577.4
LIG	H_2O + 0.5 CO + 0.2 CH_2O + 0.4 CH_3OH + 0.2 CH_3CHO + 0.2 C_3H_6O + 0.6 CH_4 + 0.65 C_2H_4 + G{CO} + 0.5 G{COH_2} + 5.5 Char	$7.7 \cdot 10^6$	111.4	-209.2
G{CO_2}	CO_2	10^5	100.4	0
G{CO}	CO	10^{13}	209.2	0
G{COH_2}	CO + H_2	$5 \cdot 10^{11}$	272	0
G{H_2}	H_2	$5 \cdot 10^{11}$	313.8	0

Secondary reactions

Reactant	Products	Preexponential coefficient in reaction rate constant equation, s^{-1}	Activation energy, kJ/mole
HAA	2 CO + 2 H_2	$4.28 \cdot 10^6$	10^8
GLYOX	2 CO + H_2	$4.28 \cdot 10^6$	10^8
C_3H_6O	0.5 CO_2 + 0.5 H_2 + 1.25 C_2H_4	$4.28 \cdot 10^6$	10^8
$C_3H_4O_2$	CO_2 + C_2H_4	$4.28 \cdot 10^6$	10^8
HFMU	CO + 1.5 C_2H_4	$4.28 \cdot 10^6$	10^8
LVG	2.5 CO_2 + 1.5 H_2 + 1.75	$4.28 \cdot 10^6$	10^8

	C_2H_4		
XYL	2 CO_2 + H_2 + 1.5 C_2H_4	$4.28 \cdot 10^6$	10^8
pCOUMARYL	CO_2 + 2.5 C_2H_4 + C	$4.28 \cdot 10^6$	10^8
PHENOL	0.5 CO_2 + 1.5 C_2H_4 + 2.5 C	$4.28 \cdot 10^6$	10^8
FE2MACR	2 CO_2 + 3 C_2H_4 + 3 C	$4.28 \cdot 10^6$	10^8

List of abbreviations

Abbreviation	Name	Atomic composition
CELL	Cellulose	$C_6H_{10}O_5$
CELLA	Activated cellulose	$C_6H_{10}O_5$
HCE	Hemicellulose	$C_5H_8O_4$
HCEA1	Activated hemicellulose 1	$C_5H_8O_4$
HCEA2	Activated hemicellulose 2	$C_5H_8O_4$
LIG	Lignin	$C_{11}H_{12}O_4$
LIG-C	Carbon-rich lignin	$C_{15}H_{14}O_4$
LIG-H	Hydrogen-rich lignin	$C_{22}H_{28}O_9$
LIG-O	Oxygen-rich lignin	$C_{20}H_{22}O_{10}$
LIG-CC	Carbon-rich lignin 2	$C_{15}H_{14}O_4$
LIG-OH	OH-rich lignin	$C_{19}H_{22}O_8$
G{CO_2}	Trapped CO_2	CO_2
G{CO}	Trapped CO	CO
G{COH_2}	Trapped COH_2	COH_2
G{H_2}	Trapped H_2	H_2
HAA	Hydroxyacetaldehyde	$C_2H_4O_2$
GLYOX	Glyoxal	$C_2H_2O_2$
C_3H_6O	Propanal	C_3H_6O
$C_3H_4O_2$	Propanedial	$C_3H_4O_2$
HMFU	5-hydroxymethyl-furfural	$C_6H_6O_3$
LVG	Levoglucosan	$C_6H_{10}O_5$
XYL	Xylose monomer	$C_5H_8O_4$
pCOUMARYL	Paracoumaryl alcohol	$C_9H_{10}O_2$
PHENOL	Phenol	C_6H_6O

FE2MACR	Sinapaldehyde	$C_{11}H_{12}O_4$

Blondeau et al. ([53]) assumed that the proposed reactions follow first order chemical kinetics. Based on this assumption they used their model to simulate rate of biomass mass loss in pyrolysis experiments conducted by *Lu et al.* ([54]) with unspecified hardwood sawdust in an entrained-flow pyrolyser. It turned out that the results calculated by means of the model are in good agreement with the experimental data (around 5% error).

2.4 Commercial processes

2.4.1 Alternatives overview

Even though there has been invented a lot of techniques of fast pyrolysis process, nevertheless nowadays only a few of them are operated on a pilot scale, namely ablative fast pyrolysis and rotating cone fast pyrolysis, while the only type of fast pyrolysis technology that finds its applications on a commercial scale is fast pyrolysis utilizing fluidized bed reactors [2, 10]. Other fast pyrolysis techniques that are either at an early stage of development or do not exhibit promising results, and for these reasons are left out of the scope of the current report, are vacuum fast pyrolysis, entrained flow fast pyrolysis, fixed bed fast pyrolysis, microwave fast pyrolysis and fast pyrolysis integrated with bio-oil upgrading units, such as hydrotreating and catalytic cracking [1, 10, 55].

2.4.2 Ablative fast pyrolysis

Ablative fast pyrolysis process is based on bringing biomass particles into contact with a hot externally heated metal surface. Intensity of contact of biomass particles with the surface should be high enough so that suitable rates of heat transfer and char ablation are achieved. Main advantage of the process is possibility to use large biomass particles and therefore avoid high grinding costs. Disadvantages of this type of pyrolysers are complexity and difficulty of scale-up [2, 10].

2.4.3 Rotating cone fast pyrolysis

Rotating cone pyrolyser is a relatively new type of fast pyrolysis reactors which is based on a principle of transported bed. The bed transport is provided by centrifugal force occurring in a heated rotating cone. An integrated rotating cone fast pyrolysis process flows as follows: biomass particles and sand are fed into the

cone where the former ones are pyrolysed. Product vapour escapes from the top of the cone and is quenched elsewhere. Char and sand drop into a fluid bed surrounding the cone where gas carrier entrains them to a separate fluid bed combustor in which sand is reheated by burning the char. The reheated sand is then transferred back to the cone [1, 10]. The main advantage of the technology utilizing rotating cone pyrolyser is that no carrier gas is used for product vapour transport and therefore its pressure is high. This makes the quenching procedure relatively easy. However the integrated process is admitted to be too complex in operation and difficult for scale-up [1]. Simplified rotating cone reactor and the integrated process are shown below in the figure 3.

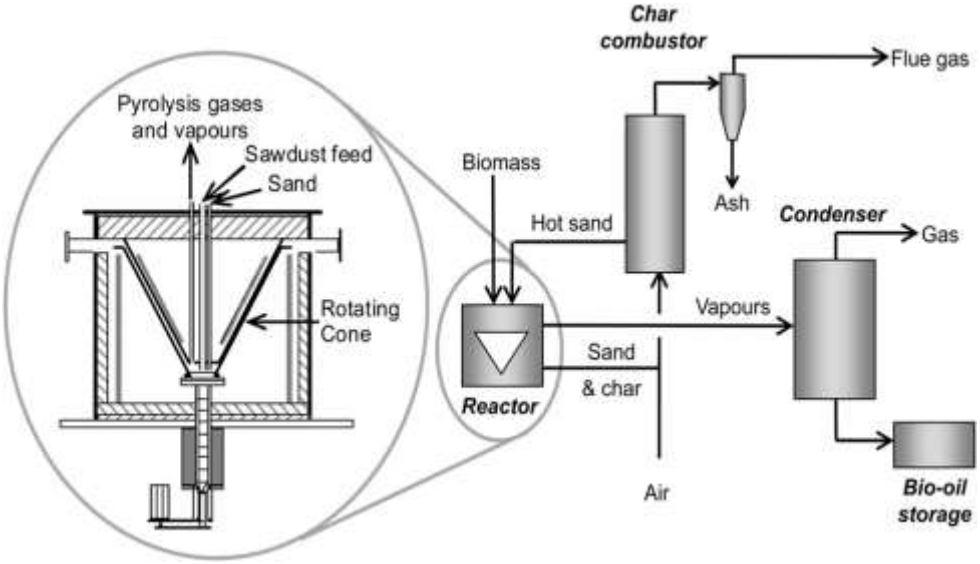

Figure 3: Simplified rotating cone reactor and the integrated rotating cone fast pyrolysis process [10].

2.4.4 Fluidized bed fast pyrolysis

The gist of the fluidized bed fast pyrolysis process is that biomass is fed to a reactor containing fluidized bed of inert (usually sand) hot particles which provide a very good heat transfer and rapidly heat biomass to around 500 ^{0}C leading to its pyrolysis [2].

Two kinds of fluidized beds are used for fast pyrolysis: bubbling fluidized bed and circulating fluidized bed. In bubbling fluidized bed fast pyrolysis reactors heat required for the reaction is provided by indirect heating of bed by burning of the

produced during the pyrolysis process non-condensable gas or char in heat exchange tubes inside the reactor. Biochar and product vapour generated in the reactor are separated from bed material in an internal reactor cyclone. Biochar particles are entrained by carrier gas and product vapour out of the reactor and separated from the gaseous matter in a cyclone separator (or in a series of cyclone separators) [1, 2, 10]. Schematic bubbling fluidized bed fast pyrolysis configuration is presented below in the figure 4.

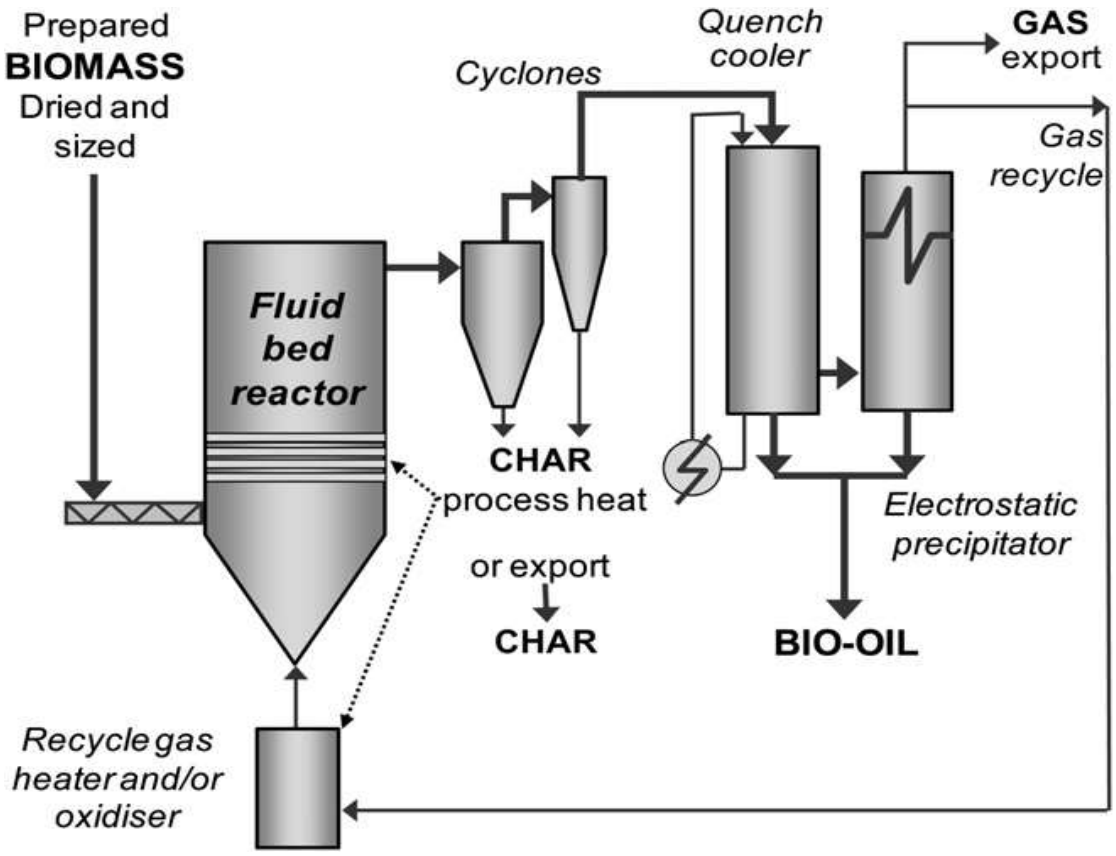

Figure 4: Schematic bubbling fluidized bed fast pyrolysis configuration [10].

In circulating fluidized bed fast pyrolysis reactors bed particles exit the reactor along with the product vapour and biochar. Bed particles and biochar are then separated from product vapour into a cyclone separator (or in a series of cyclone separators) and are transferred to a combustor where bed particles are directly reheated by combustion of biochar. Produced during the pyrolysis process non-condensable gas also can be combusted to reheat the bed particles [1, 2, 10]. Another way to reheat bed particles which is considered to be a more effective alternative is to conduct at first gasification of biochar and then to burn the

resultant syngas to get the necessary heat for restoring bed particle temperature [10]. A typical simplified lay-out of circulating fluidized bed fast pyrolysis installation is depicted below in the figure 5.

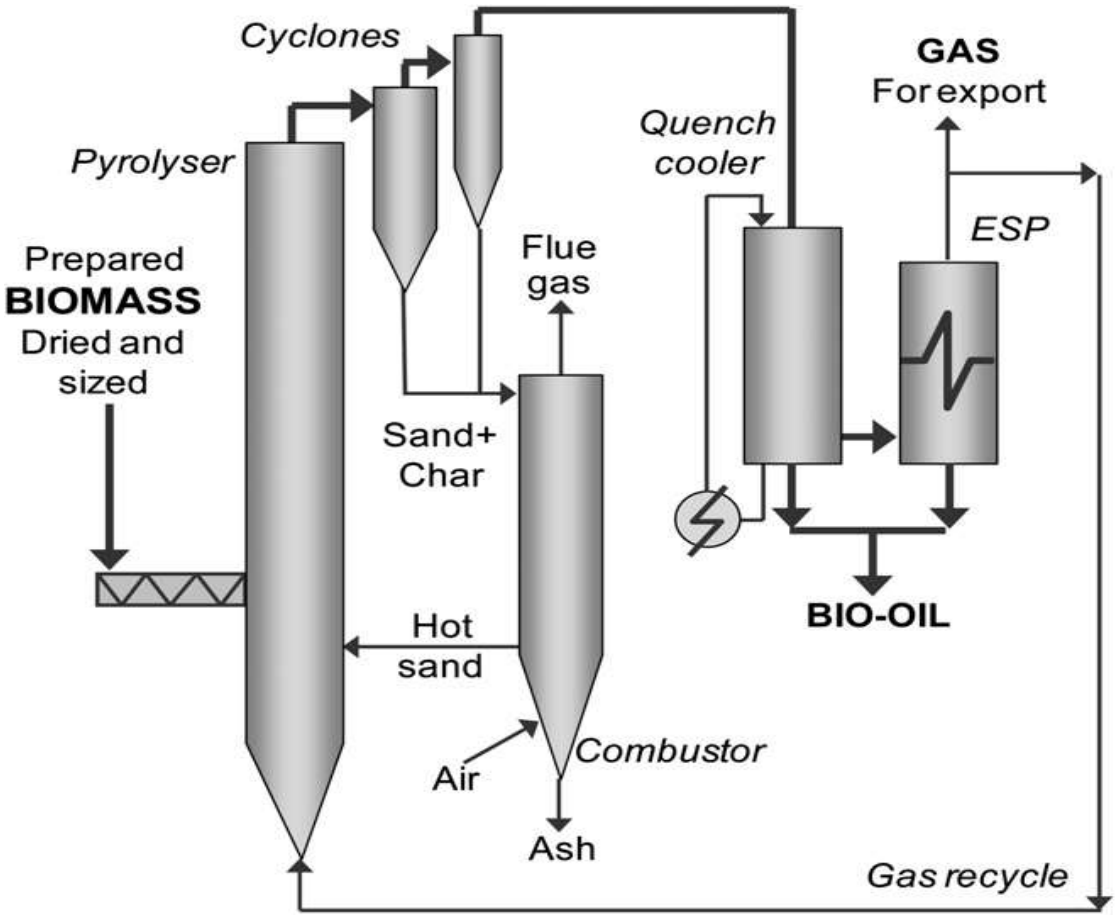

Figure 5: Typical simplified lay-out of circulating fluidized bed fast pyrolysis installation [10].

The bubbling fluidized bed fast pyrolysis reactors are characterized by relatively long vapour and particle residence time (around 5-10 s for vapour and much higher for particles), which ensures complete conversion of feed biomass and thus means a possibility to use large feed biomass particles. In the circulating fluidized bed fast pyrolysis reactors vapour residence time is around 0.5-1 s and particle residence time is around 1s. Such a high ratio between vapour and particle residence time gives rise to the following requirements: finer feed biomass particles (significantly increases the grinding costs) to ensure necessary rates of heat transfer, quick and effective mixing of feed biomass particles with hot bed

material to minimize the amount of unreacted biomass particles, and very quick separation of the exiting the reactor vapour from the hot solids [2]. The latter requirement is caused by the fact that biochar and ash particles present in the exiting the reactor stream act as a catalyst in the vapour cracking reactions and therefore reduce the yield of bio-oil [2, 10, 11, 12].

In comparison to bubbling fluidized bed installations circulating fluidized bed installations are more compact, produce less undesirable by-products because of the shorter vapour residence time and are less sensitive to density differences between heat carrier particles and biomass particles because all the solids are entrained out of the circulating fluidized bed pyrolyser. However circulating fluidized bed technology has a set of disadvantages and these are complexity, need of a bigger amount of fluidizing gas, necessity of fast separation of exiting the reactor vapour from the hot solids, need of finer biomass particles and much less flexibility in terms of produced biochar usage [2].

Circulating fluidized bed fast pyrolysis provides more intensive ablation of biomass particles which implies that it gives the higher bio-oil yield but short solid residence time can give rise to relatively high amount incompletely reacted feed particles and therefore the effect of the intense ablation will be neutralized [2].

Longer solid residence time in bubbling fluidized bed pyrolysers ensures complete conversion of feed biomass particles and therefore allows usage of larger feed biomass particles in comparison to circulating fluidized bed pyrolysers. On the other hand with regard to bubbling fluidized bed pyrolysers very careful selection of mean size and size distribution of feed biomass particles (which significantly increases the screening costs) should be done, as too big feed biomass particles will result in too big biochar particles which will not be effectively entrained out of the pyrolyser and thus will stay in the reaction zone acting as a cracking catalyst and reducing the bio-oil yield [1].

Bubbling fluidized bed fast pyrolysis units are simple in construction and operation [10]. At the same time reliability of circulating fluidized bed technology for high capacity production has been proved by its wide implementation in

petroleum and petrochemical industry [10], namely in Fluid Catalytic Cracking and in Fluid Coking processes [2].

The table 9 below summarizes main advantages and disadvantages of both bubbling fluidized bed and circulating fluidized bed fast pyrolysis technologies.

Table 9: Advantages and disadvantages of bubbling fluidized bed and circulating fluidized bed fast pyrolysis technologies.

Fast pyrolysis technologies	**Advantages**	**Disadvantages**
Bubbling fluidized bed	Lower grinding costs Less fluidizing gas needed All the produced biochar is collected	Higher screening costs Bigger more complicated pyrolyser
Circulating fluidized bed	Lower screening costs Compact simple pyrolyser	Higher grinding costs More fluidizing gas needed All the produced biochar is burnt

2.5 Environmental impacts

If the produced during the fast pyrolysis biochar is not sent to an external consumer, it is burnt at the fast pyrolysis plant in order to provide heat required

for running the process. Along with the heat generation the result of its combustion is production of ash and hot flue gas [10, 12].

According to the results of fast pyrolysis experiments conducted with wood biomass, on average there is only a trace of nitrogen in the biochar produced from wood biomass. Also the content of sulfur in wood biomass is almost zero [56]. Hence it can be assumed that there are virtually no SO_X and NO_X emissions when biochar produced from wood biomass pyrolysis is combusted.

There have been reported only a few studies on biomass ash application as an adsorbent, raw material for ceramics, and as a cement and concrete additive. However the fact that fly ash produced during coal combustion finds its applications as an adsorbent, as a precursor for low grade zeolites, in cement industry and in construction of roadways, together with the fact that biomass ash does not contain toxic metals, give grounds to assume that in the nearest future biomass ash will be also widely used [57].

In [58] there was conducted an evaluation of 19 bio-oil fast pyrolysis samples. The results showed that all the samples were mutagenic, however none of them was found to be ecotoxicological.

In Netherlands in 9 MWth industrial boiler facility there was conducted a comparison between combustion of bio-oil produced from fast pyrolysis of pine wood and combustion of a heavy fuel oil. The results of the test showed that NO_X emissions of bio-oil combustion were 4.1 times lower, particulate emissions of bio-oil combustion were 1.5-2.3 times lower, and that the fouling tendency of the ash from bio-oil was twice lower than that of the heavy fuel oil [59].

Biodegradability of bio-oil is considerably higher than biodegradability of diesel fuels and moreover it can be accelerated by neutralization of bio-oil with basis such as lime [3]. Bio-oil biodegradability is also is confirmed by the results obtained in [58]. This fact gives grounds to assume that in case of accidental leakage of bio-oil during its storage or transportation it will be much easier to deal with the consequences of such a leakage than in the case of the diesel fuel accidental leakage.

3 INTEGRATION OF BIOMASS FLUIDIZED BED COMBUSTION WITH BIOMASS FLUIDIZED BED FAST PYROLYSIS

3.1 Biomass fluidized bed combustion overview

Oxidation of biomass with excess amount of air is called biomass combustion. It is conducted in boilers where the resultant hot flue gas produces steam in heat exchange elements. The produced steam is used for electricity generation [60]. Fluidized bed combustion is the most suitable type of combustion for biomass [4].

In bubbling fluidized bed biomass combustion air is used as both fluidizing and oxidizing gas and sand or limestone is used as a bed material. The bottom part of the bubbling fluidized bed biomass boiler has such a cross-sectional area that superficial velocity of the fluidizing gas is above the minimum fluidization velocity and therefore the bed is kept in a fluidized state. There is an increase in the cross-sectional area of the boiler along its vertical axis so that the superficial velocity of the air is below the minimum fluidization velocity in the upper part of the boiler above the bed. This upper part functions as a disengaging zone and is usually referred to as freeboard. In the freeboard there may be placed an internal cyclone for circulation of fines entrained by upward flowing flue gas back to the bed. Also an overfire air may be injected into the freeboard to insure complete combustion of fines. An external burner fired by a conventional fuel is usually used for bed preheating to the biomass ignition temperature which is around 540 ^{0}C. After the biomass is fed into the bottom section of the boiler the bed temperature rises to its operating range (790-870 ^{0}C). The bed temperature should be kept below the fusion temperature of the ash contained in the biomass under combustion. Temperature of the freeboard zone where the combustion is completed may be up to around 1000 ^{0}C. Complete ash carryover usually takes place in bubbling fluidized bed biomass boilers, so some gas-solid separation devices, such as cyclones or bag filters, are normally placed downstream the boilers [60].

As in the bubbling fluidized bed boilers in circulating fluidized bed boilers air is used as both fluidizing and oxidizing gas and sand or limestone is used as a bed

material. In circulating fluidized bed boilers the air superficial velocity is higher throughout the boiler and due to this substantial amount of solids is entrained by the flue gas out of the boiler. Then solids are separated from the flue gas and circulated back to the boiler [60].

3.2 Integration alternatives

Both bubbling fluidized bed and circulating fluidized bed combustion units have all the necessary preconditions for an integration with fast pyrolysis fluidized bed technology. There can be two options for the integration of each of the combustion methods: the bubbling fluidized bed combustion is integrated with either bubbling fluidized bed or circulating fluidized bed fast pyrolysis technology, and identically the circulating fluidized bed combustion is integrated with either bubbling fluidized bed or circulating fluidized bed fast pyrolysis technology.

1) Integration of bubbling fluidized bed combustion with bubbling fluidized bed fast pyrolysis technology.

The necessary modifications to the bubbling fluidized bed combustion unit are as follows: a bubbling fluidized bed pyrolyser and an external gas-solid separation system attached to the pyrolyser outlet are installed upstream the bubbling fluidized bed boiler. The solid outlet of the pyrolysis gas-liquid separation system is connected to the boiler, while the gas outlet of the pyrolysis gas-solid separation system is connected to the quenching system. This arrangement enables to transport biochar produced in the pyrolyser to the boiler where it is burnt for the heat production and to transport the vapour produced during the pyrolysis process to the quenching system where bio-oil and non-condensable gas are separated from each other.

2) Integration of bubbling fluidized bed combustion with circulating fluidized bed fast pyrolysis technology.

The necessary modifications to the bubbling fluidized bed combustion unit are as follows: a circulating fluidized bed pyrolyser and an external gas-solid separation system attached to the pyrolyser outlet are installed upstream the bubbling

fluidized bed boiler. The solid outlet of the pyrolysis gas-liquid separation system is connected to the boiler, while the gas outlet of the pyrolysis gas-solid separation system is connected to the quenching system. The pyrolyser bed material and biochar produced during the pyrolysis process exit the pyrolysis gas-solid separation system and are transported to the boiler where biochar is burnt for heat production and simultaneously for the pyrolyser bed material reheating. After being reheated the pyrolyser bed material is transported back to the pyrolyser. The vapour produced during the pyrolysis process exits the pyrolysis gas-solid separation system and is transported to the quenching system where bio-oil and non-condensable gas are separated from each other.

3) Integration of circulating fluidized bed combustion with bubbling fluidized bed fast pyrolysis technology.

The necessary modifications to the circulating fluidized bed combustion unit are as follows: a bubbling fluidized bed pyrolyser and an external gas-solid separation system attached to the pyrolyser outlet are installed upstream the circulating fluidized bed boiler. The solid outlet of the pyrolysis gas-liquid separation system is connected to the boiler, while the gas outlet of the pyrolysis gas-solid separation system is connected to the quenching system. This arrangement enables to transport biochar produced in the pyrolyser to the boiler where it is burnt for the heat production and to transport the vapour produced during the pyrolysis process to the quenching system where bio-oil and non-condensable gas are separated from each other.

4) Integration of circulating fluidized bed combustion with circulating fluidized bed fast pyrolysis technology.

The necessary modifications to the circulating fluidized bed combustion unit are as follows: a circulating fluidized bed pyrolyser and an external gas-solid separation system attached to the pyrolyser outlet are installed upstream the circulating fluidized bed boiler. The solid outlet of the pyrolysis gas-liquid separation system is connected to the boiler, while the gas outlet of the pyrolysis gas-solid separation system is connected to the quenching system. The pyrolyser bed material and biochar produced during the pyrolysis process exit the pyrolysis

gas-solid separation system and are transported to the boiler where biochar is burnt for heat production and simultaneously for the pyrolyser bed material reheating. The produced during the biochar combustion flue gas entrains the ash remained after the biochar combustion and the reheated pyrolyser bed material to the external boiler gas-solid separation system where the reheated pyrolyser bed material is separated from the flue gas and ash. The separated reheated pyrolyser bed material is then recycled back to the pyrolyser. The vapour produced during the pyrolysis process exits the pyrolysis gas-solid separation system and is transported to the quenching system where bio-oil and non-condensable gas are separated from each other.

4 COMPARISON OF FLUIDIZED BED FAST PYROLYSIS TECHNOLOGIES DESIGN CONSIDERATIONS

Internal heat transfer elements of the bubbling fluidized bed pyrolyser are difficult to design and scale up. Another design difficulty with regard to bubbling fluidized bed pyrolysers is associated with the importance of providing as much turbulence in the bed zone as possible in order to achieve the highest attrition of biochar particles so that they become sufficiently small and therefore are entrained by vapour and fluidizing gas out of the pyrolyser as effectively as possible [1].

Design of a sweep gas introduction to the top of the bubbling fluidized bed pyrolyser is very important, as not enough narrow feed biomass particle size distribution will result in a considerable amount of biochar particles with such a size that will be small enough to make them float in the top section of the pyrolyser but at the same time will be big enough not to be entrained out of the pyrolyser by the rising product vapour and fluidizing gas [1].

A core aspect of the design of the circulating fluidized bed fast pyrolysis process is design of the bed material circulation system. Another important design consideration concerning circulating fluidized bed pyrolysers is the requirement of quick and effective mixing of feed biomass particles with hot bed material in order to minimize the amount of unreacted biomass particles. This gives rise to a necessity of very careful design of raw biomass feeding.

A crucial aspect of design of both bubbling fluidized bed and circulating fluidized bed fast pyrolysis installations is the temperature at which it is required to keep the product vapour line and external gas-solid separation system in order to prevent premature condensation of product vapour.

A summary of design considerations peculiar to each of the fluidized bed fast pyrolysis technologies is presented in the table 10.

Table 10: design considerations peculiar to each of the fluidized bed fast pyrolysis technologies.

Fast pyrolysis technology	**Design considerations peculiar to the technology**
Bubbling fluidized bed	Internal heat transfer elements Turbulent conditions in the bed zone Sweep gas introduction
Circulating fluidized bed	Bed material circulation system Raw biomass feeding

5 PROCESS DESIGN

5.1 Process description

Schematic process diagram is depicted below in the figure 6. At first Scots pine logs are debarked. After that debarked wood and bark are ground to 2 mm particles. Bark and excess wood are transported to the sand reheater. The residual wood is dried to 10 wt% (wb) moisture content and fed to the pyrolyser. In pyrolyser feed particles come into contact with hot sand and are converted into bio-oil vapour, non-condensable gas and biochar. After leaving the pyrolyser bio-oil vapour and non-condensable gas are separated from sand and biochar in cyclone 1. Sand and biochar are transported to the sand reheater where biochar, bark and excess debarked wood are burnt in order to restore the sand temperature to the necessary value. Reheated sand flows back to the pyrolyser. After being separated bio-oil vapour and non-condensable gas are transported to the quench

column where bio-oil vapour is condensed by drops of cooled bio-oil sprayed from the top of the quench column. Condensed bio-oil is transported to storage while bio-oil which was used for condensation is cooled in the bio-oil cooler and sprayed from the top of the quench column again. The part of non-condensable gas which was produced in the pyrolyser is discharged from the quench column to the environment while the other part of non-condensable gas is used in the pyrolyser as a fluidizing gas.

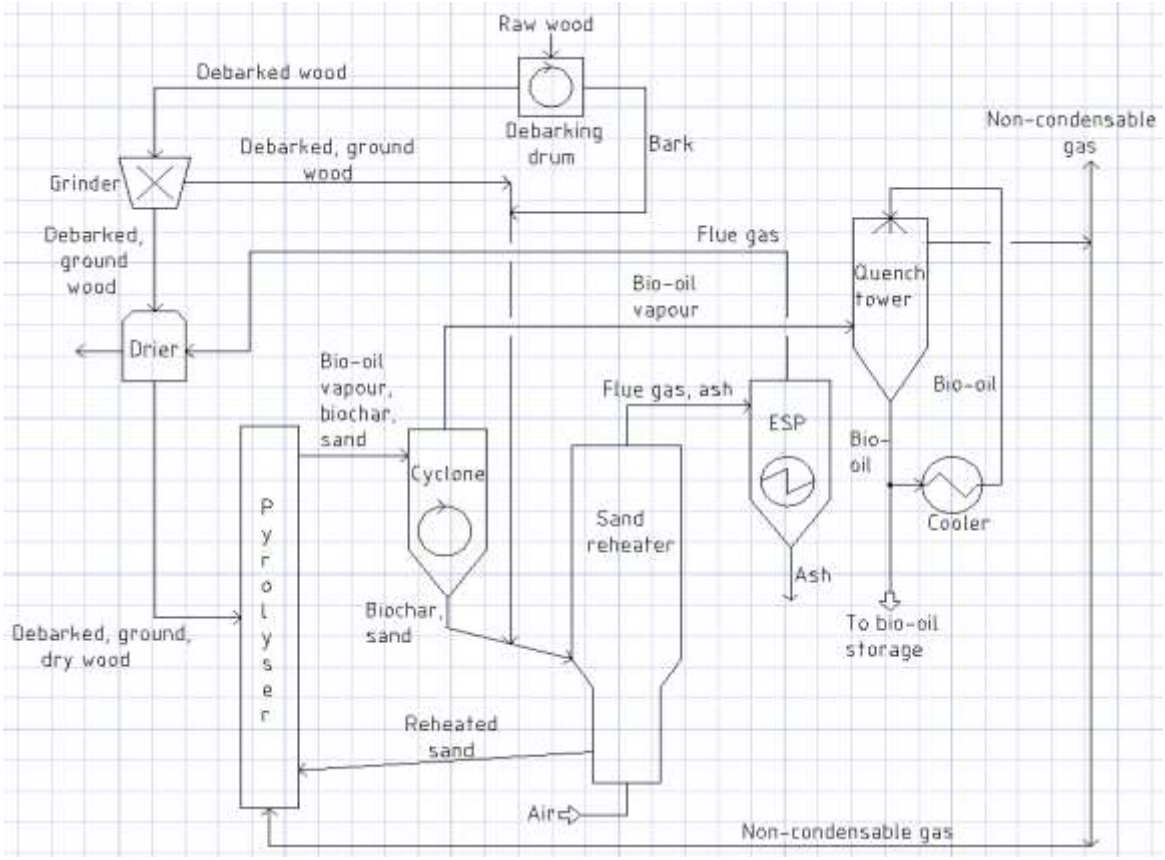

Figure 6: Schematic process diagram.

5.2 Feed selection and characteristics

Scots pine accounts for half of the Finnish forest resources [61]. For this reason Scots pine wood is chosen as a feed for current fast pyrolysis process design study.

Sable et al. ([62]) investigated wood composition of 27-year old Scots pine grown in Latvia and determined that it contained 49% of cellulose, 27.1% lignin, 20.7% of hemicellulose, 2.9% of extractives and 0.3% of ash on dry basis. As there was

found no composition of Scots pine grown in Finland and because of the relatively close geographical position of Latvia to Finland, the data obtained by *Sable et al.* ([62]) will be used to describe the composition of feed material in the current report.

5.3 Pyrolyser material and heat balances

5.3.1 Material balance

It is designed that prior to be fed to the pyrolyser debarked ground Scots pine is dried to the moisture content of 10 wt% on wet basis. Thus when it is fed to the pyrolyser its composition is the following (wb): 44.1 wt% of cellulose, 24.4 wt% of lignin, 18.63 wt% of hemicellulose, 2.6 wt% of extractives, 0.27 wt% of ash and 10 wt% of water.

Blondeau et al. ([63]) proposed mass fractions of fixed carbon in each of the main wood constituents: 0 for cellulose, 0.075 for hemicellulose and 0.3 for lignin. By means of this hypothesis it was calculated that fixed carbon content in Scots pine wood fed to the pyrolyser is 8.7 wt% (wb).

The sum of fixed carbon content and ash content in Scots pine wood fed to the pyrolyser is necessary for determination of mass fraction of feed that will remain in solid form after complete pyrolysis. In our case it is 8.97 wt% (wb).

This value of mass fraction of feed that will remain in solid form after complete pyrolysis was used to simulate the pyrolyser product distribution in the current design study by means of models proposed by *Van de Velden et al.* ([49]) and *Luo et al.* ([52]), but in both cases the mass balance was not converged. However in case of using the model proposed by *Van de Velden et al.* ([49]) quite reasonable value of 2.93 s for the time required for complete pyrolysis of the feed under consideration in the current design study t_{pyr}^{compl} was obtained. This value of t_{pyr}^{compl} is used in the module 5.5 for determining the necessary pyrolyser height. The model proposed by *Blondeau et al.* ([53]) was not used for fast pyrolysis product distribution simulation due to its complexity.

In order to predict pyrolyser product distribution experimental results ([21], [23], [24], [25]) obtained with different types of pine wood were used. Based on these results it is assumed that in the current design study 1 kg of Scots pine wood fed to the pyrolyser is converted into 0.6 kg of bio-oil, 0.25 kg of non-condensable gas and 0.15 kg of biochar.

The desired production capacity is 100 000 tonne of bio-oil per year. Taking into account the assumption about product distribution it was calculated that feed throughput to the pyrolyser that satisfies the production capacity requirement G_F is 5.36 kg/s. Therefore the flow rate of bio-oil vapour produced in the pyrolyser G_{BO} is 3.216 kg/s, the flow rate of non-condensable gas produced in the pyrolyser G_{NG} is 1.34 kg/s, and the flow rate of biochar produced in the pyrolyser is 0.804 kg/s.

5.3.2 Heat balance

The heat balance in pyrolyser is expressed below by the equation 11:

$$G_F Q_P + G_{FG}^{suppl} Q_{FG}^{suppl} + L_P = G_S Q_S \qquad (11)$$

where G_F feed throughput, kg/s

G_{FG}^{suppl} flow rate of the fluidizing gas supplied to the pyrolyser, kg/s

Q_P specific heat required for pyrolysis, kJ/kg

L_P heat losses in pyrolyser, kW

Q_{FG}^{suppl} specific heat required to heat the fluidizing gas supplied to the pyrolyser to the pyrolysis temperature, kJ/kg

G_S sand flow rate, kg/s

Q_S specific heat transferred to sand in sand reheater, kJ/kg.

Specific heat required for pyrolysis is assumed to be comprised of several components which are presented below in the table 11.

Table 11: Components of specific heat required for pyrolysis and their calculations procedures.

Component of specific heat required for pyrolysis	Symbol	Unit	Calculation procedure
Sensible specific heat required to heat the water containing in the feed to 100 ^{0}C	$Q_{W,S}$	kJ/kg	$Q_{W,S} = wc_{pW}(100 - T_F)$
Latent specific heat required to evaporate the water containing in the feed	$Q_{W,L}$	kJ/kg	$Q_{W,L} = wE_W^{100}$
Sensible specific heat required to heat the water vapour to the pyrolysis temperature	$Q_{V,S}$	kJ/kg	$Q_{V,S} = wc_{pV}(T_P - 100)$
Sensible specific heat required to heat the feed to the pyrolysis temperature	$Q_{F,S}$	kJ/kg	$Q_{F,S} = (1 - w)c_{pF}(T_P - T_F)$
Specific heat required for endothermic pyrolysis reactions	Q_E	kJ/kg	$Q_E = (1 - w)Q_R$

Explanation of the symbols used in the table I:

w water mass fraction in feed on wet basis, -

c_{pW} water specific heat capacity at 1 bar (4.2 kJ/kg ^{0}C [64])

c_{pV} water vapour specific heat capacity at 1 bar (2 kJ/kg ^{0}C [64])

T_P pyrolysis temperature (500 ^{0}C)

T_F feed temperature (20 ^{0}C)

E_W^{100} enthalpy of water vaporization at 100 ^{0}C and 1 bar (2256.43 kJ/kg [64])

c_{pF} feed specific heat capacity, kJ/kg ^{0}C

Q_R total sum of enthalpies of pyrolysis reactions, kJ/kg.

Thus after all the components presented in the table 11 are calculated we can find the heat required for pyrolysis by adding all the components together:

$$Q_P = Q_{W,S} + Q_{W,L} + Q_{V,S} + Q_{F,S} + Q_E \quad (12).$$

The formula for calculation of the specific heat required to heat the fluidizing gas supplied to the pyrolyser to the pyrolysis temperature Q_{FG}^{suppl} is given below:

$$Q_{FG}^{suppl} = c_{pFG}^{suppl}(T_P - T_{quench}) \quad (13)$$

where c_{pFG}^{suppl} specific heat capacity of fluidizing gas supplied to the pyrolyser, kJ/kg ^{0}C

T_{quench} temperature of bio-oil and non-condensable gas leaving the quench column, ^{0}C.

In order to calculate $Q_{F,S}$ we need to know specific heat capacity of dry Scots pine wood. Heat capacity of dry wood is virtually species independent and can be calculated as [65]:

$$c_{pF} = 4.1854 \cdot [0.25 + 6 \cdot 10^{-4} \cdot (1.8 \cdot T_{DF} + 32)] \quad (14)$$

where T_{DF} mean temperature of dry feed during its heating to pyrolysis temperature, ^{0}C.

It is assumed that the feed is heated from 20 ^{0}C to 500 ^{0}C, so T_{DF} = 260 ^{0}C. Then the c_p(F) is 2.302 kJ/ kg ^{0}C.

Rath et al. ([66]) performed simultaneous Thermogravimetric-Differential Scanning Calorimetry measurements in which they heated spruce wood particles (0.25 – 1 mm) from 75 to 500 ^{0}C at 10 ^{0}C/min. They determined that the enthalpy

of reaction of bio-oil vapour formation was 1277 kJ/kg. Using this value Q_E was calculated to be 1149.3 kJ/kg.

Calonaci et al. ([67]) proposed that enthalpy of cellulose pyrolysis is 991.7 kJ/kg, enthalpy of hemicellulose pyrolysis is 1962.3 kJ/kg and enthalpy of lignin pyrolysis is 2393.2 kJ/kg. Using the data obtained by *Sable et al.* ([62]) for our calculations Q_E was calculated to be 1386.62 kJ/kg.

In order to ensure that enough heat is supplied for the pyrolysis process the latter value of Q_E was used for calculation of heat required for pyrolysis.

Using the latter value of Q_E for calculation of heat required for pyrolysis (in order to ensure that enough heat is supplied for the pyrolysis process), $G_F Q_P$ was calculated to be 14.6 MW.

G_{FG}^{suppl} and T_{quench} which are required for calculations will be determined later in the course of calculating material and heat balances in the quench column and bio-oil cooler.

Heat losses in pyrolyser are assumed to account for 20% of $(G_F Q_P + G_{FG}^{suppl} Q_{FG}^{suppl})$, then the amount of heat that is had to be supplied to the pyrolyser is $(17.52 + 1.2 \cdot G_{FG}^{suppl} Q_{FG}^{suppl})$ MW.

The amount of heat that must be contained in the sand entering the pyrolyser is equal to the value presented above:

$$G_S Q_S = (17.52 + 1.2 \cdot G_{FG}^{suppl} Q_{FG}^{suppl}) \text{ MW}.$$

5.4 Condensing section material and heat balances in winter

5.4.1 Quench column heat balance equation derivation

Condensing section consists of a quench column where bio-oil is condensed and of a cooler where part of the condensed bio-oil is cooled and then returned back to the quench column where it is used as a condensing agent. This cooled recirculated bio-oil is referred to as “condensing bio-oil” and it is designed that it

enters the quench column at the temperature of 20 ^{0}C. Condensing bio-oil is cooled to this temperature in a cooler. Pyrolysis vapour enters bottom of the quenching column and while it rises to the top of the quench column it comes into contact with droplets of the condensing bio-oil sprayed from the top of the quench column. As a result bio-oil vapour is condensed on the droplets of the condensing bio-oil. It is designed so that the temperature of bio-oil and non-condensable gas leaving the quench column T_{quench} is 40 ^{0}C.

The amount of heat that is needed to be absorbed in the quench column H_{quench} is calculated according to the following formula:

$$H_{quench} = 1.2 \cdot (H_{BO} + H_{NG} + H_{FG}^{suppl}) \quad (15)$$

where H_{BO} heat required to be absorbed from bio-oil vapour, MW

H_{NG} heat required to be absorbed from non-condensable gas produced in the pyrolyser, MW

H_{FG}^{suppl} heat required to be absorbed from fluidizing gas supplied to the pyrolyser, MW.

The coefficient 1.2 in the formula 15 is needed to ensure that sufficient amount of the condensing agent is used and therefore bio-oil condensation is complete.

Mass fraction of water vapour in bio-oil vapour is assumed to be 0.25. Then the heat required to be absorbed from bio-oil vapour in the quench column is calculated as follows:

$$H_{BO} = G_{BO}(0.75\left[c_{pBO}^{V}(T_P - T_{cond}) + E_{BO} + c_{pBO}^{L}(T_{cond} - T_{quench})\right] +$$

$$+0.25\left[c_{pW}^{V}(T_P - 100) + E_W^{100} + c_{pW}^{L}(100 - T_{quench})\right]) \quad (16)$$

where c_{pBO}^{V} specific heat capacity of bio-oil vapour, kJ/kg ^{0}C

c_{pBO}^{L} specific heat capacity of liquid bio-oil, kJ/kg ^{0}C

E_{BO} enthalpy of bio-oil condensation, kJ/kg

T_{cond} temperature of bio-oil condensation, ^{0}C

T_{quench} temperature of bio-oil and non-condensable gas leaving the quench column, ^{0}C

c_{pW}^{V} specific heat capacity of water vapour (2.0268 kJ/kg ^{0}C [64])

c_{pW}^{L} specific heat capacity of liquid water (4.2 kJ/kg ^{0}C [64]).

The heat required to be absorbed in the quench column from non-condensable gas produced in the pyrolyser is determined using the following formula:

$$H_{NG} = G_{NG} c_{pNG} (T_P - T_{quench}) \quad (17)$$

where c_{pNG} specific heat capacity of non-condensable gas produced in the pyrolyser, kJ/kg ^{0}C.

Calculation procedure of the heat required to be absorbed from fluidizing gas supplied to the pyrolyser is presented below:

$$H_{FG}^{suppl} = G_{FG}^{suppl} \cdot c_{pFG}^{suppl} \cdot (T_P - T_{quench}) \quad (18)$$

where $c_{pFG}^{supplied}$ specific heat capacity of fluidizing gas supplied to the pyrolyser, kJ/kg ^{0}C.

Physical properties of bio-oil are modeled by those of phenol. Boiling point of phenol at 1 bar is 181.8 ^{0}C [64]. Based on this c_{pBO}^{V} is taken as specific heat capacity of gaseous phenol at 340.9 ^{0}C which is 1.97 kJ/kg ^{0}C [68] and c_{pBO}^{L} is taken as specific heat capacity of liquid phenol at 110.9^{0}C which is 2.41 kJ/kg ^{0}C [68]. E_{BO} is taken as heat of vaporization of phenol at boiling point which is 503.33 kJ/kg [68]. Therefore H_{BO} is 6.22 MW.

Specific heat capacity of non-condensable gas produced in the pyrolyser is taken as specific heat capacity of carbon monoxide at 1 bar and 327 ^{0}C which is 1.087 kJ/kg ^{0}C [64]. Therefore H_{NG} was calculated to be 0.67 MW.

Specific heat capacity of fluidizing gas supplied to the pyrolyser is also taken as specific heat capacity of carbon monoxide at 1 bar and 327 ^{0}C which is 1.087 kJ/kg ^{0}C [64]. Thus H_{FG}^{suppl} is $0.5 \cdot G_{FG}^{suppl}$ MW.

Therefore the amount of heat that is needed to be absorbed in the quench column H_{quench} is $(8.27 + 0.6 \cdot G_{FG}^{suppl})$ MW.

5.4.2 Determination of the flow rate of the fluidizing gas supplied to the pyrolyser

The same amount of heat as H_{quench} is needed to be absorbed in the cooler in order to restore the condensing bio-oil temperature to 20 ^{0}C. Therefore the heat transfer area of the cooler must be sufficiently large so that not less than H_{quench} is transferred.

Shell and tube heat exchanger with counter-current flow mode is chosen to perform cooler functions. Thus logarithmic mean temperature difference ΔT_{LM} is calculated as follows:

$$\Delta T_{LM} = \frac{(T_1 - t_2) - (T_2 - t_1)}{ln\frac{(T_1 - t_2)}{(T_2 - t_1)}} \quad (19)$$

where T_1 hot fluid temperature at the inlet, ^{0}C

T_2 hot fluid temperature at the outlet, ^{0}C

t_1 cold fluid temperature at the inlet, ^{0}C

t_2 cold fluid temperature at the outlet, ^{0}C.

Cooling water is used for recovering of the used condensing bio-oil to the temperature of 20 ^{0}C from 40 ^{0}C. It is designed so that the cooling water enters the cooler at the temperature of 5 ^{0}C and leaves it at the temperature of 15 ^{0}C. Under these conditions ΔT_{LM} is 19.6 ^{0}C. The overall heat transfer coefficient U in the cooler is taken as 250 W/m^2 ^{0}C [69].

Guidelines concerning outer diameter of tubes, height of tubes, tube arrangement, shell outer diameter and shell wall thickness given in [69] were used in order to calculate approximate heat transfer areas and amounts of heat that can be

transferred through them using the selected values for overall heat transfer coefficient (250 $W/m^2\ ^0C$) and logarithmic mean temperature difference (19.6 ^0C) for various cooler configurations. The results are presented below in the table 12.

Table 12: Various cooler configurations and their corresponding approximate characteristics.

Outer diameter of tubes, mm	Height of tubes, m	Shell outer diameter, m	Shell wall thickness, mm	Approximate number of tubes	Approximate heat transfer area, m^2	Approximate heat transferred, MW
19	4.88	0.976	9.5	1744	508	2.5
19	6.10	1.22	11.1	2732	995	4.9
19	7.32	1.464	11.1	3960	1729	8.5
25	4.88	0.976	9.5	1008	386	1.9
25	6.10	1.22	11.1	1578	756	3.7
25	7.32	1.464	11.1	2288	1314	6.4
32	4.88	0.976	9.5	616	302	1.5
32	6.10	1.22	11.1	964	590	2.9
32	7.32	1.464	11.1	1396	1027	5

According to the table 12 the most economical way to provide heat transfer area required to absorb H_{quench} from the used condensing bio-oil is to use in parallel two heat exchangers with tubes of 32 mm outer diameter and 7.32 m height. It means that the used condensing bio-oil stream is split into two equal parts and then each part is cooled separately. The highest amount of heat that can be transferred using this configuration is 10 MW. This value was assigned to H_{quench} and the maximum value of the flow rate of the fluidizing gas supplied to the pyrolyser that can be allowed was found to be 2.9 kg/s.

In order to ensure fulfillment of all the stated above requirements the flow rate of the fluidizing gas supplied to the pyrolyser G_{FG}^{suppl} is designed to comprise 80% of its maximum value and thus is 2.3 kg/s. Therefore the amount of heat that is needed to be absorbed at first in the quench column and then in the two parallel coolers H_{quench} is 9.65 MW.

5.4.3 Material balances

The flow rate of the condensing bio-oil G_{BO}^{Cond} that is required to absorb H_{quench} was calculated according to the following formula:

$$G_{BO}^{Cond} = \frac{H_{quench}}{c_{pBO\_Cond} \cdot (T_{quench} - 20)} \quad (20)$$

where c_{pBO_Cond} specific heat capacity of condensing bio-oil, kJ/kg ^{0}C.

Specific heat capacity of the condensing cooled bio-oil is taken as the specific heat capacity of liquid phenol at 50 ^{0}C which is 2.25 kJ/kg ^{0}C [68]. Using the value of the flow rate of the fluidizing gas supplied to the pyrolyser G_{FG}^{suppl} determined in the previous module, it was calculated that the amount of heat that is needed to be absorbed at first in the quench column and then in the two parallel coolers H_{quench} is 9.65 MW. Thus the flow rate of the condensing bio-oil G_{BO}^{Cond} is 214.45 kg/s.

Specific heat capacity of cooling water used for recovering of the used condensing bio-oil to the temperature of 20 ^{0}C from 40 ^{0}C is taken as 4.2 kJ/kg ^{0}C [64]. Then the required amount of cooling water G_{W}^{Cool} (it enters the cooler at the temperature of 5 ^{0}C and leaves it at the temperature of 15 ^{0}C) was calculated to be 229.8 kg/s.

5.5 Condensing section material and heat balances in summer

During the summer period it is designed that the temperature of bio-oil and non-condensable gas leaving the quench column T_{quench} is 50 ^{0}C and that condensing bio-oil enters the quench column at the temperature of 30 ^{0}C. The cooling water enters the cooler at the temperature of 15 ^{0}C and leaves it at the temperature of 25 ^{0}C.

Under these conditions H_{quench} is 9.5 MW, required heat transfer area in the cooler is 1939 m^2, the flow rate of the condensing bio-oil G_{BO}^{Cond} is 211 kg/s and the required amount of cooling water G_{W}^{Cool} is 226 kg/s. As these values are almost identical to those of the winter case, there is no need to calculate the size of the quench column and bio-oil cooler separately for each period.

5.6 Pyrolyser sizing

5.6.1 Introduction

Pyrolyser is a vertical column to the bottom of which biomass particles and sand are introduced. Below the feed point there is a distributor plate through which fluidizing gas is blown. It entrains the particles and conveys them to the top of the pyrolyser where the exit point is situated. In the current design study diameter and height of the pyrolyser are estimated. The diameter calculations are based on the superficial velocity of fluidizing gas required for particle conveying and on the volumetric flow rate of the fluidizing gas. The height calculations are based on the time required complete pyrolysis t_{pyr}^{compl}.

5.6.2 Fluidizing gas superficial velocity determination

The diameter calculations are based on the superficial velocity of fluidizing gas required for particle conveying and on the volumetric flow rate of the fluidizing gas. At first the required superficial velocity of fluidizing gas was determined.

The value of fluidizing gas superficial velocity should satisfy two requirements: 1) it should be higher than the terminal velocity of particles; 2) it should exceed a minimal safe fluidizing velocity to avoid shutdown in the pyrolyser. At first terminal velocities of sand and biomass particles are calculated. The following formula is used for calculation of particle terminal velocities [70]:

$$u_t = \sqrt{\frac{4}{3}\frac{(\rho_p - \rho_g) g d_p}{(5.31 - 4.88\varphi)\rho_g}} \quad (21)$$

where u_t particle terminal velocity, m/s

ρ_p particle density, kg/m^3

ρ_g fluidizing gas density, kg/m^3

g acceleration of gravity, m/s^2

d_p particle diameter, m

φ partile spericity, -.

The density of gas in the pyrolyser is approximated as a density of CO_2 at 1 atm and 250 ^{0}C, which is 1.012 kg/m^3 [71].

Diameter of feed biomass particles is 2 mm. Sphericity of feed biomass particles is taken as 0.63 (sphericity of broken solids [72]) and density as 510 kg/m^3 [65]. Using these data terminal velocity of feed biomass particles u_t(fb) was calculated to be 2.43 m/s.

Diameter of biochar particles is assumed to be its mass yield fraction (0.15) multiplied by diameter of feed biomass particles, and therefore is 0.3 mm. Sphericity of biochar particles is assumed to be the same as of feed biomass particles. Density of biochar particles is calculated based on the densities and mass fractions of its constituents. Density of lignin is taken as density of feed biomass and density of ash is taken as density of CaO. Calculation of biochar density is presented below in the table 13.

Table 13: Calculation of biochar density.

Biochar component	Mass fraction	Density, kg/m^3
Carbon	0.8	2200 [64]
Lignin	0.182	510
Ash	0.018	3340 [64]
Biochar overall	**1**	**1913**

Based on the presented above assumptions about biochar particles their terminal velocity u_t(c) was calculated to be 1.82 m/s.

The average terminal velocity of biomass in the pyrolyser $u_t^{av}(b)$ was taken as a mean of terminal velocities of feed biomass particles and biochar particles and therefore is equal to 2.125 m/s.

Terminal velocity of sand particles $u_t(s)$ should equal the average terminal velocity of biomass $u_t(s) = u_t^{av}(b)$ so that they are transported by the fluidizing gas at the same pace as biomass and thus the most efficient heat transfer in the pyrolyser is ensured. Hence we need to find such diameter of sand particles d_S that satisfies this requirement. Sphericity of sand particles is taken as 0.66 (sphericity of sharp sand [72]) and density as 2648 kg/m^3 (density of α-quartz [64]).

$$d_S = \frac{3u_t^2(5.31-4.88\varphi)\rho_g}{4(\rho_p-\rho_g)g} = 0.27 \text{ mm}.$$

As the flow rate of sand particles is much more than that of biomass particles, parameters of sand particles are used to estimate the required superficial velocity of fluidizing gas in the pyrolyser U_{FF}. It was found out that minimal safe fluidizing velocity for sodium sulphate particles with density of 1280 – 1440 kg/m^3 and size not exceeding 0.5 mm is 3.1 m/s [72]. Size of the sand particles used in the system under design is 0.3 mm and their density is around two times the density of the sodium sulphate particles. Hence it is a reasonable approximation to assume that the minimal safe fluidizing velocity for the sand particles used in the system under design is two times higher than that for the sodium sulphate particles and therefore is 6.2 m/s. Based on this approximation the superficial velocity of fluidizing gas in the pyrolyser U_{FF} is taken as 7 m/s.

5.6.3 Fluidizing gas volumetric flow rate determination

In order to determine the volumetric flow rate of the fluidizing gas in the pyrolyser the following factor should be taken into account: vertical pneumatic transport of solids can be conducted in either a dilute phase flow regime or in a dense phase flow regime. The former one is preferable to the latter one because in the dilute phase flow transport regime the pressure drop across the pyrolyser height is much smaller and the solids mixing is more intensive. Dilute phase flow is usually characterized by 0.01/1 to 15/1 solids to gas mass ratios, while dense phase flow is usually characterized by 15/1 to 200/1 solids to gas mass ratios [70].

The pyrolyser hydrodynamics is designed so that the operation takes place in the upper region of the dilute phase flow regime – the ratio between the mass of solids and the mass of fluidizing gas is taken as 10 to 1. In our case the mass flow rate of solids is comprised of the mass flow rate of sand and of the mass flow rate of biomass particles. The latter ones undergo pyrolysis as they travel along the pyrolyser height and thus their mass flow rate varies from the mass flow rate of the feed biomass to the mass flow rate of the produced during the pyrolysis biochar. Hence the mass flow rate of biomass particles in the pyrolyser was taken as a mean between the mass flow rate of the feed biomass and the mass flow rate of the produced during the pyrolysis biochar. Therefore the mass flow rate of solids in the pyrolyser G_{solids} was calculated as follows:

$$G_{solids} = \frac{G_F + G_{Ch}}{2} + G_S = (3.1 + G_S) \text{ kg/s.}$$

Then the mass flow rate of the fluidizing gas in the pyrolyser G_{FG} is:

$$G_{FG} = \frac{G_{solids}}{10} = (0.31 + 0.1 \cdot G_S) \text{ kg/s.}$$

The fluidizing gas in the pyrolyser is composed of the gas supplied to the pyrolyser through the pyrolyser distributor plate and of the gas produced during the pyrolysis. The mass flow rate of the gas produced during the pyrolysis varies from zero to the sum of mass flow rates of bio-oil vapour G_{BO} and non-condensable gas produced in the pyrolyser G_{NG}. Thus the mass flow rate of the gas produced during the pyrolysis is taken as a mean between zero and the sum of mass flow rates of bio-oil vapour and non-condensable gas. Taking this into account the mass flow rate of fluidizing gas that is needed to be supplied to the pyrolyser G_{FG}^{supplied} is:

$$G_{FG}^{supplied} = G_{FG} - \frac{G_{BO} + G_{NG}}{2} = (0.1 \cdot G_S - 1.97) \text{ kg/s.}$$

Since mass flow rate of fluidizing gas that is needed to be supplied to the pyrolyser G_{FG}^{supplied} is 2.3 kg/s, the mass flow rate of the fluidizing gas in the pyrolyser G_{FG} and the sand flow rate G_S are:

$$G_{FG} = G_{FG}^{supplied} + \frac{G_{BO} + G_{NG}}{2} = 2.3 + 2.28 = 4.58 \text{ kg/s,}$$

$$G_S = 10 \cdot G_{FG}^{supplied} + 19.7 = 10 \cdot 2.3 + 19.7 = 42.7 \text{ kg/s}.$$

Using the value of the mass flow rate of the fluidizing gas in the pyrolyser G_{FG} and the approximation that the fluidizing gas density is equal to the density of CO_2 at 1 atm and 250 ^{0}C, which is 1.012 kg/m^3 [71], its volumetric flow rate in the pyrolyser V_{FG} was calculated to be 4.53 m^3/s.

5.6.4 Diameter and height calculations

The pyrolyser cross-sectional area A_{pyr} is:

$$A_{pyr} = \frac{V_{FG}}{U_{FF}} = 0.65 \text{ m}^2.$$

Then the pyrolyser diameter D_{pyr} is:

$$D_{pyr} = \sqrt{\frac{4A_{pyr}}{\pi}} = 0.9 \text{ m}.$$

The required height of pyrolyser H_{pyr} is determined as a product of multiplication of the velocity of particles in the pyrolyser u_p^{pyr} by the time required for their complete pyrolysis t_{pyr}^{compl} calculation procedure of which is discussed above in the module 5.3. Velocity of particles in the pyrolyser is defined as follows:

$$u_p^{pyr} = U_{FF} - u_t^{av} \quad (22).$$

Thus the required height of pyrolyser H_{pyr} is:

$$H_{pyr} = t_{pyr}^{compl} \cdot (U_{FF} - u_t^{av}) = 14.3 \text{ m}.$$

5.6.5 Pressure drop calculation

The formula for calculation of the pressure drop across the pyrolyser height ΔP_{pyr} is presented below [70]:

$$\Delta P_{pyr} = \frac{U_{FF}^2 \rho_g}{2} + G_{solids} u_p^{pyr} + \frac{2f\rho_g U_{FF}^2 H_{pyr}}{D_{pyr}} + \frac{0.057 G_{solids} H_{pyr} g}{\sqrt{g D_{pyr}}} + \frac{G_{solids} H_{pyr} g}{u_p} +$$

$$+ \rho_g H_{pyr} g \quad (23)$$

where f gas-wall friction factor, -.

The value of the gas-wall friction factor f depends on the value of the pyrolyser Reynolds number Re_{pyr} which is defined as follows:

$$Re_{pyr} = \frac{D_{pyr} U_{FF} \rho_g}{\mu} \quad (24)$$

where μ viscosity of gas in the pyrolyser, Pa·s.

If Re_{pyr} lies in the range from $3 \cdot 10^3$ to 10^5, then the gas-wall friction factor f is [72]:

$$f = 0.0791 \cdot Re_{pyr}^{-0.25} \quad (25).$$

If Re_{pyr} lies in the range from 10^5 to 10^8, then the gas-wall friction factor f is [72]:

$$f = 0.0008 + 0.0552 \cdot Re_{pyr}^{-0.237} \quad (26).$$

Using the approximation that viscosity of gas in the pyrolyser is equal to viscosity of CO_2 at 250 ^{0}C, which is 24.28 μPa·s [73], the pyrolyser Reynolds number Re_{pyr} was calculated to be $2.6 \cdot 10^5$. This allowed to determine that the pressure drop across the pyrolyser height ΔP_{pyr} is 0.02 bar.

5.7 Cyclone sizing

By means of simulation in Aspen Plus it was determined that in order to achieve 99% separation efficiency two consecutive cyclones are required. Pressure drop in each cyclone is 0.015 bar. Cyclone dimensions (in meters) are depicted in the figure below.

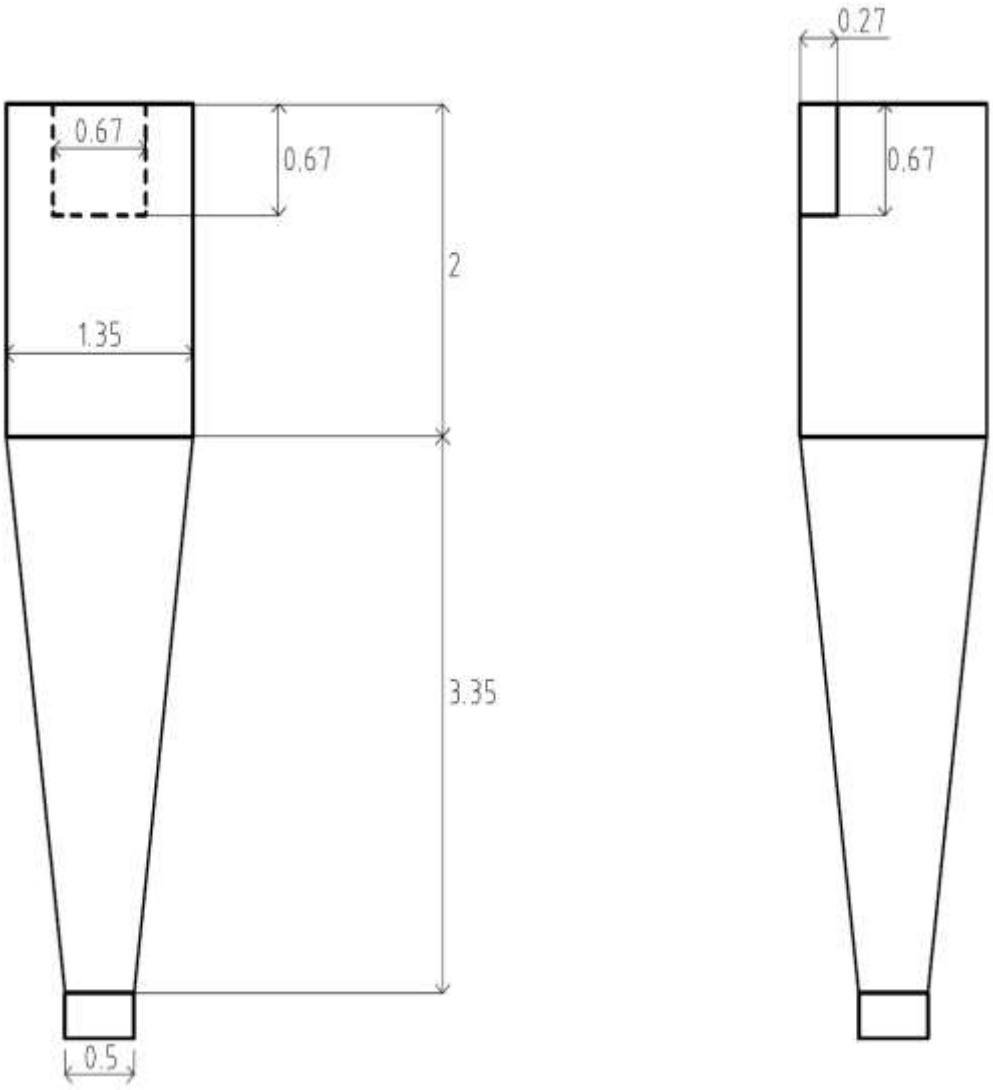

Figure 7: Cyclone dimensions.

5.8 Quench column sizing

Bio-oil vapour and non-condensable gas enter the quench column from its bottom at the temperature of 500 ^{0}C. Condensed bio-oil cooled to the temperature of 20 ^{0}C is sprayed from the top of the column. When bio-oil vapour comes into contact with the liquid drops it condenses. Resulting bio-oil condensate exiting the column from its bottom has the temperature of 40 ^{0}C. The non-condensable gas also cools to 40 ^{0}C and leaves the column from its top.

Densities of bio-oil vapour and non-condensable gas were calculated at 270 ^{0}C and 1 bar. Bio-oil was approximated as phenol. By means of the equation of state

of an ideal gas bio-oil vapour density was calculated to be 2.1 kg/m^3. Non-condensable gas composition based on the data presented in the table 2 in the module 2.1 is assumed to be as follows: CO_2 60 wt%, CO 40 wt%. Using the equation of state of an ideal gas for this gas mixture its density was calculated to be 0.833 kg/m^3. Mass fraction of bio-oil vapour in the gas mixture entering the quench column is 0.47, thus density of gas phase in the quench column is 1.43 kg/m^3.

Density of liquid drops was taken as 1054.5 kg/m^3 [64]. Sphericity of liquid drops was taken as 1. When diameter of liquid drops is 0.5 mm their terminal velocity (according to the formula 21) is 3.35 m/s. It is assumed that 2 m/s is safe velocity for the gas phase from flooding point of view. Volumetric flow rate of gas phase is 4.8 m^3/s. Then if gas velocity is 2 m/s, diameter of the quench column D_{QQ} is 1.75 m.

It is assumed that 5 s is sufficient contact time between bio-oil vapour and liquid drops to get complete condensation of the vapour. Based on this assumption height of the quench column H_{QQ} is 10 m.

Pressure drop in the quench column by means of simulation in Aspen Plus was determined to be $7.5 \cdot 10^{-6}$ bar.

5.9 Bio-oil cooler sizing

Bio-oil cooler is used to cool bio-oil that is sprayed from the top of the quench column for condensation of the bio-oil vapour coming out of the pyrolyser. While calculating the flow rate of the fluidizing gas supplied to the pyrolyser G_{FG}^{suppl} in the module 5.4.2, it was determined that bio-oil cooling requires two shell and tube heat exchangers with shell outer diameter of 1.464 m and tubes of 32 mm outer diameter and 7.32 m height. Approximate number of tubes is 1396. The heat exchangers are used in parallel.

It is designed that bio-oil flows in tubes and water flows in the shell space. By means of simulation in Aspen Plus it was determined that pressure drop in tubes is 0.06 bar and pressure drop in the shell space is 0.2 bar.

5.10 Sand reheater material and heat balances

5.10.1 Introduction

Sand and biochar after being separated from bio-oil vapour and non-condensable gas are transported to the sand reheater where the sand must be reheated to such a temperature so that it provides enough heat for the pyrolysis when it flows back to the pyrolyser.

At first it was verified whether the sand reheating can be achieved by means of biochar combustion only without any external fuel addition. Solving the heat balance for the situation when only biochar is burnt in the sand reheater revealed that it is impossible and therefore addition of some external fuel is needed.

Then it was verified whether the sand reheating can be achieved by burning of biochar and totally dry bark obtained after the debarking step. It was determined that in this case sand temperature is also not restored to the necessary value.

Finally it was calculated what value of raw undebarked Scots pine throughput gives enough bark and excess debarked wood to be burned in the sand reheater at its green moisture content along with biochar so that sand is reheated to the required temperature.

In all heat balance equations it is assumed that heat losses in the sand reheater comprise 20% of all the heat produced in and supplied to the sand reheater. In all combustion reactions the required amount of oxygen was calculated as 1.1 of the stoichiometric amount on the presumption that 10% excess of oxygen is needed in order to ensure complete combustion.

5.10.2 Reheating based on biochar combustion

Biochar composition is assumed to be as follows [21, 23, 24, 25]: 80 wt% of carbon, 18.2 wt% of lignin and 1.2 wt% of ash. Oxidation of carbon and lignin

during the biochar combustion produces heat which is transferred to the resulting flue gas and sand. Part of the heat is lost to the environment. Thus if only biochar combustion is used to obtain the heat necessary to reheat the sand to the required temperature and no other fuels are added, the heat balance of sand reheater is expressed by the following equation:

$$0.8 \cdot [G_{Ch}(cHV_C + lLHV_L) + G_{Ch}^{AF} Q_{Ch}^{AF}] = G_S Q_S + G_G^{Flue} Q_G^{Flue} \quad (27)$$

where G_{Ch} biochar flow rate, kg/s

c carbon mass fraction in biochar, -

HV_C carbon heating value (32.8 MJ/kg [64])

l lignin mass fraction in biochar, -

LHV_L lignin lower heating value, MJ/kg

G_{Ch}^{AF} ash free biochar flow rate, kg/s

Q_{Ch}^{AF} specific heat transferred to ash free biochar, kJ/kg

G_G^{Flue} biochar combustion flue gas flow rate, kg/s

Q_G^{Flue} specific heat transferred to biochar combustion flue gas in sand reheater, kJ/kg.

Temperature of both biochar and sand entering the sand reheater is taken as T_P (500 ^{0}C). It is also assumed that all the products generated in the sand reheater leave it at the same temperature T_{comb} [72]. Based on these assumptions the expressions for Q_{Ch}^{AF}, Q_G^{Flue} and Q_S were written in the following way

$$Q_{Ch}^{AF} = c_{pCh\_AF}(T_P - T_F) \quad (28)$$

$$Q_G^{Flue} = c_{pG\_Flue}(T_{comb} - T_F) \quad (29)$$

$$Q_S = c_{pS}(T_{comb} - T_P) \quad (30)$$

where c_{pCh_AF} specific heat capacity of ash free biochar, kJ/kg ^{0}C

c_{pG_Flue} specific heat capacity of biochar combustion flue gas, kJ/kg ^{0}C

c_{pS} specific heat capacity of sand, kJ/kg ^{0}C.

In order to simulate combustion of lignin it was represented by a pseudo component. One of the lignin monomers appeares to be the most suitable substance for this purpose. There are three lignin monomers, namely *trans-p*-coumaryl ($C_9H_{10}O_2$), *trans*-coniferyl ($C_{10}H_{12}O_3$) and *trans*-sinapyl ($C_{11}H_{14}O_4$) [74, 75]. As atomic composition of *trans*-coniferyl is an average of all three lignin monomers, *trans*-coniferyl was chosen to be the pseudo component for lignin combustion simulation. Combustion reaction of *trans*-coniferyl ($C_{10}H_{12}O_3$) is as follows:

$$C_{10}H_{12}O_3 + 11.5O_2 = 10CO_2 + 6H_2O$$

Combustion reaction of carbon is as follows:

$$C + O_2 = CO_2$$

The necessary flow rate of air required for complete combustion of biochar G_{AIR} is 9.62 kg/s. The composition of flue gas resulting from complete biochar combustion and specific heat capacities of its components are presented below in the table 14.

Table 14: Composition of flue gas resulting from complete biochar combustion and its specific heat capacity.

Gas	Flow rate, kg/s	Mass fraction	Specific heat capacity at 427 ^{0}C and 1 bar, kJ/ kg ^{0}C
N_2	7.27	0.7	1.098 [64]
CO_2	2.718	0.26	1.127 [64]
H_2O	0.088	0.008	2.0867 [64]
O_2	0.223	0.02	1.031 [64]
Ar	0.129	0.012	0.5205 [64]
Flue gas total	**10.428**	**1**	**1.105**

Higher heating value of lignin HHV_L (MJ/kg) was calculated using formula proposed in [74]:

$$HHV_L = 0.335 \cdot C + 1.423 \cdot H - 0.154 \cdot O \quad (31)$$

where C, H and O carbon, hydrogen and oxygen content respectively, wt%.

Carbon content of *trans*-coniferyl ($C_{10}H_{12}O_3$) is 66.67 wt%, oxygen content is 26.66 wt% and hydrogen content is 6.67 wt% which means that HHV_L is 27.72 MJ/kg. Heat of vaporization of the released water Q_{VW} during combustion of 1 kg of lignin was determined to be 1.35 MJ/kg. Thus lower heating value of lignin LHV_L is 26.37 MJ/kg. Carbon heating value HV_C is 32.8 MJ/kg [64]. Therefore the total amount of heat produced during complete combustion of biochar $G_{Ch}(cHV_C + lLHV_L)$ is 24.96 MW.

According to the table 14 the heat that is transferred to the flue gas $G_G \cdot Q_G$ was calculated as follows:

$$G_G^{Flue} Q_G^{Flue} = G_G^{Flue} c_{pG\_Flue}(T_{comb} - T_F) = (11.523 \cdot T_{comb} - 230.46) \text{ kW}.$$

The heat that is transferred to sand $G_S \cdot Q_S$ is:

$$G_S Q_S = G_S c_{pS}(T_{comb} - T_P) = (51.24 \cdot T_{comb} - 25620) \text{ kW}.$$

The ash free biochar flow rate G_{Ch}^{AF} is:

$$G_{Ch}^{AF} = G_{Ch} - G_{Ash} = 0.7895 \text{ kg/s}.$$

Specific heat capacity of ash free biochar c_{pCh_AF} was approximated as a sum of specific heat capacities of graphite (1.2 kJ/kg ^{0}C at 227 ^{0}C and 1 bar [64]) and lignin in accordance with their mass fractions in the ash free biochar (0.815 for graphite and 0.185 for lignin). The lignin heat capacity was taken as the wood heat capacity at 260 ^{0}C (2.302 kJ/kg ^{0}C). Based on these presumptions the amount of heat contained in the ash free biochar can be calculated was calculated as follows:

$$G_{Ch}^{AF} Q_{Ch}^{AF} = G_{Ch}^{AF} c_{pCh\_AF}(T_P - T_F) = 530.544 \text{ kW}.$$

Using the knowledge that G_SQ_S = 18.9 MW the temperature at which flue gas resulting from complete biochar combustion, ash and sand leave the sand reheater T_{comb} was calculated to be 778 ^{0}C.

5.10.3 Determination of the required combustion temperature

It was calculated in the module 5.3.2 that G_SQ_S is equal to $(17.52 + +1.2 \cdot G_{FG}^{suppl} Q_{FG}^{suppl})$ MW. The flow rate of the fluidizing gas supplied to the pyrolyser G_{FG}^{suppl} is 2.3 kg/s. Specific heat of fluidizing gas supplied to the pyrolyser during the pyrolysis process Q_{FG}^{suppl} was calculated in the following way:

$$Q_{FG}^{suppl} = c_{pFG}^{suppl} \cdot (T_P - T_{quench}) = 500 \text{ kW}.$$

Thus the amount of heat that is had to be contained in the sand leaving the sand reheater G_SQ_S is:

$$G_S Q_S = 17.52 + 1.2 \cdot G_{FG}^{suppl} Q_{FG}^{suppl} = 18.9 \text{ MW}.$$

Combustion temperature in the sand reheater at which G_SQ_S = 18.9 MW T_{comb}^{Req} was calculated by means of the formula given below:

$$T_{comb}^{Req} = \frac{Q_S + c_{pS} T_P}{c_{pS}} \quad (32)$$

where c_{pS} is specific heat capacity of sand, kJ/kg ^{0}C.

As it was calculated in the module 5.5.3 G_S is 42.7 kg/s and therefore Q_S is 442.6 kW. Specific heat capacity of sand was taken as a mean value in the range from 700 to 1000 K at 1 bar – 1.2 kJ/kg ^{0}C [64]. Then the required combustion temperature in the sand reheater T_{comb}^{Req} is:

$$T_{comb}^{Req} = \frac{Q_S + c_{pS} T_P}{c_{pS}} = \frac{442.6 + 1.2 \cdot 500}{1.2} = 869 \ ^0\text{C}.$$

As the required combustion temperature is higher than the temperature generated by the biochar combustion, addition of some external fuel is needed.

5.10.4 Reheating based on combustion of biochar and bark

Bark obtained after the debarking step was selected to serve as an additional fuel. At first the case for absolutely dry bark was calculated in order to find whether the heat requirement can be satisfied by means of addition only the bark obtained after the debarking step.

Moisture content of raw scots pine is 79 wt% (db) or 44.134 wt% (wb) [65]. Therefore feed throughput of raw debarked material G_F^{Raw} is 8.635 kg/s. Burk comprises 8.77 wt% of the Scots pine industrially usable stemwood [76]. Thus flow rate of raw undebarked material having 79 wt% (db) or 44.134 wt% (wb) moisture content G_{Undeb}^{Raw} and of raw bark coming out of the debarking unit G_{Bk}^{Raw} are 9.465 kg/s and 0.83 kg/s respectively. Bark ash content is around five times higher than wood ash content [77], therefore it is reasonable to assume that in our case bark ash content is 1.5 wt% (db). Taking into account that raw bark flow rate is 0.83 kg/s and that its moisture content is 79 wt% (db) or 44.134 wt% (wb), dry bark flow rate G_{Bk}^{Dry} is 0.457 kg/s.

Bark composition of coniferous trees can be presented as $C_{0.537}\ H_{0.06}O_{0.403}$ [78]. Therefore bark combustion reaction is as follows:

$$C_{0.537}\ H_{0.06}O_{0.403} + 0.3505O_2 = 0.537CO_2 + 0.03H_2O$$

The required oxygen flow rate is 0.435 kg/s which means that 1.875 kg/s of air is needed. Based on this the composition of the flue gas resulting from complete bark combustion was found:

Table 15: Composition and specific heat capacity of the flue gas resulting from the combustion of absolutely dry bark.

Gas	Flow rate, kg/s	Mass fraction	Specific heat capacity at 427 ^{0}C and 1 bar, kJ/kg ^{0}C
N_2	1.415	0.6	1.098 [64]
CO_2	0.834	0.36	1.127 [64]
H_2O	0.0193	0.008	2.0867 [64]

O_2	0.0435	0.018	1.031 [64]
Ar	0.025	0.014	0.5205 [64]
Flue gas total	**2.337**	**1**	**1.11**

The equation for heat balance in the sand reheater with bark used as an additional fuel is as follows:

$$0.8 \cdot (H_{Ch} + G_{Ch}^{AF} Q_{Ch}^{AF} + H_{Bk}) = G_S Q_S + G_{G1}^{Flue1} Q_{G1}^{Flue1} + G_{G2}^{Flue2} Q_{G2}^{Flue2} \quad (33)$$

where H_{Ch} heat released during biochar combustion, kJ/s

H_{Bk} heat released during bark combustion, kJ/s

G_{G1}^{Flue1} mass flow rate of flue gas resulting from biochar combustion, kg/s

G_{G2}^{Flue2} mass flow rate of flue gas resulting from bark combustion, kg/s

Q_{G1}^{Flue1} specific heat of flue gas resulting from biochar combustion, kJ/kg

Q_{G2}^{Flue2} specific heat of flue gas resulting from bark combustion, kJ/kg.

Specifc heats of flue gas resulting from biochar combustion Q_{G1}^{Flue1} and flue gas resulting from bark combustion Q_{G2}^{Flue2} were calculated as follows:

$$Q_{G1}^{Flue1} = c_{pG1\_Flue1}(T_{comb}^{Req} - 20) \quad (34)$$

$$Q_{G2}^{Flue2} = c_{pG2\_Flue2}(T_{comb}^{Req} - 20) \quad (35).$$

Dry Scots pine bark LHV is 19.53 MJ/kg [79]. Thus heat released during combustion of absolutely dry bark H_{Bk}^{Dry} is:

$$H_{Bk}^{Dry} = G_{Bk}^{Dry} \cdot LHV^{Dry} = 9061.92 \text{ kW}.$$

Heat that is contained in the flue gas resulting from combustion of absolutely dry bark:

$$G_{G2}^{Flue2} c_{pG2\_Flue2}(T_{comb} - T_F) = (2.594 \cdot T_{comb} - 51.9)\ \text{kW}.$$

The combustion temperature in the sand reheater T_{comb} when absolutely dry bark is used as an additional fuel was calculated to be 819 ^{0}C. This value of T_{comb} is lower than T_{comb}^{Req} and therefore the only way to create T_{comb}^{Req} in the sand reheater is to increase undebarked raw Scots pine throughput so that there is more bark available for burning and also there is some excess of debarked wood that also can be burned in the sand reheater.

5.10.5 Reheating based on combustion of biochar, bark and excess debarked wood

The idea is to determine such a flow rate of raw undebarked Scots pine that will allow to create T_{comb}^{Req} in the sand reheater by burning bark and excess debarked wood at their green moisture content thus avoiding spending of energy required for their drying.

The equation for heat balance in the sand reheater with raw bark and excess debarked raw wood used as an additional fuel in order to make the combustion temperature T_{comb} be equal to the T_{comb}^{Req} is as follows:

$$0.8 \cdot (H_{Ch} + G_{Ch}^{AF} Q_{Ch}^{AF} + H_{Bk} + H_{Wood}) = G_S Q_S + G_{G1}^{Flue1} Q_{G1}^{Flue1} + \\ + G_{G3}^{Flue3} Q_{G3}^{Flue3} \quad (36)$$

where H_{Wood} heat released during excess debarked raw wood combustion, kJ/s

G_{G3}^{Flue3} mass flow rate of flue gas resulting from raw bark and excess debarked raw wood combustion, kg/s

Q_{G3}^{Flue3} specific heat of flue gas resulting from raw bark and excess debarked raw wood combustion, kJ/kg.

Dry scots pine debarked stem wood LHV is 19.31 MJ/kg [79]. LHV of bark and excess debarked wood with green moisture content was calculated as follows:

$$LHV = (1 - M) \cdot LHV^{Dry} - M \cdot E_W^{25} \quad (37)$$

where LHV^{Dry} lower heating value of dry material, MJ/kg

E_W^{25} enthalpy of water vaporization at 25 ^{0}C and 1 bar (2441.67 kJ/kg [64])

M moisture mass fraction, -.

It was calculated that the raw bark flow rate G_{Bk}^{Raw} and excess debarked raw wood flow rate G_{Excess}^{Raw} required to generate T_{comb}^{Req} in the sand reheater are 0.982 kg/s and 1.582 kg/s respectively. Thus the necessary throughput of raw undebarked Scots pine G^{Raw} is 11.2 kg/s.

Based on the Scots pine composition [62] combustion reaction of debarked wood is as follows:

$$C_{6.9}H_{10.12}O_{4.22} + 7.32O_2 = 6.9CO_2 + 5.06H_2O$$

The required air flow rate supplied to the sand reheater G_{Air} is 18.04 kg/s. Composition and specific heat capacity of the flue gas leaving the sand reheater is given below in the table 16:

Table 16: Composition and specific heat capacity of the flue gas leaving the sand reheater.

Gas	Flow rate, kg/s	Mass fraction	Specific heat capacity at 427 ^{0}C and 1 bar, kJ/ kg ^{0}C
N_2	13.546	0.636	1.098 [64]
CO_2	5.370	0.252	1.127 [64]
H_2O	1.733	0.081	2.0867 [64]
O_2	0.416	0.02	1.031 [64]
Ar	0.235	0.011	0.5205 [64]

Flue gas total	**21.3**	**1**	**1.178**

5.11 Sand reheater sizing

5.11.1 Introduction

The sand reheater is designed so that it consists of three sections: 1st section is the bottom one, 2nd section is the middle one, and 3d section is the top one. The supplied air is used as both fluidizing gas and as an oxidizing agent for combustion. While biochar, bark, wood and sand rise through the 1t section, biochar, bark and wood are burned by the supplied air. The idea behind the sand reheater configuration is to design the height of the 1st section so, that by the time biochar, bark and wood reach the 2nd section they are completely converted into ash and therefore all the heat resulting from their combustion is released in the 1st section. The diameter of the 2nd section must be designed so that the fluidizing gas velocity becomes lower than the terminal velocity of sand particles but at the same time stays higher than the terminal velocity of the ash particles. This ensures that sand particles fall down to the collection ports while ash particles are transferred higher to the 3d section of the sand reheater.

The same formulas as in the module "Pyrolyser sizing" were used for calculation of particle terminal velocities and pressure drops in the sand reheater sections.

5.11.2 First section

Density of fluidizing gas in the 1st section was calculated to be 0.52 kg/m^3 at 427 ^{0}C and 1 bar. It was taken as a mean between the air and flue gas densities. Data for both air and flue gas were taken from [64]. The same formula as in the module "Pyrolyser sizing" was used for calculation of particle terminal velocities:

$$u_t = \sqrt{\frac{4}{3}\frac{(\rho_p - \rho_g) g d_p}{(5.31 - 4.88\varphi)\rho_g}}$$

Terminal velocity of sand particles in the 1st section u_t^{1st}(s) was calculated to be 2.93 m/s. Density of Scots pine at green moisture content is 660 kgm^3 [65]. Sphericity of wood particles is taken as 0.63 (sphericity of broken solids [72]).

Based on these parameters terminal velocity of wood particles in the 1st section $u_t^{1st}(w)$ was calculated to be 3.84 m/s. Terminal velocity of biochar particles in the 1st section $u_t^{1st}(c)$ was calculated to be 2.54 m/s. Density of ash was taken as 3340 kg/m^3 (density of CaO [64]) and based on this terminal velocity of ash particles in the 1st section $u_t^{1st}(a)$ was calculated to be 0.45 m/s. It is designed that terminal velocity of bark particles is equal to the terminal velocity of sand particles. Density of bark is taken as half of the density of wood at its green moisture content. Size of bark particles d_b in this case was determined to be 2.3 mm. Terminal velocities of particles in the 1st section of the sand reheater are summarized below in the table 17.

Table 17: Terminal velocities of particles in the first section of the sand reheater.

Type of particles	Terminal velocity, m/s
Sand	2.93
Bark	2.93
Wood	3.84
Biochar	2.54
Ash	0.45

Mass gas flow rate in the 1st section of the sand reheater G_G^{1st} is taken as a mean of flue gas flow rate and air flow rate and is 19.67 kg/s. Therefore volumetric gas flow rate in the 1st section of the sand reheater V_G^{1st} is 37.83 m^3/s. As it was determined in the module 5.6 fluidizing velocity for sand particles U_{FF} is 7 m/s. Therefore cross-sectional area A_{SR}^{1st} and diameter D_{SR}^{1st} of the 1st section of the sand reheater are:

$$A_{SR}^{1st} = \frac{V_G^{1st}}{U_{FF}} = 5.4 \text{ m}^2,$$

$$D_{SR}^{1st} = \sqrt{\frac{4 \cdot A_{SR}^{1st}}{3.14}} = 2.6 \text{ m}.$$

It was assumed that time required for complete combustion of biochar particles does not exceed 2 s [80]. Time required for complete combustion of wood and

bark particles was also assumed not to exceed 2 s. Velocity determining the height of the sand reheater 1st section was taken as a mean of those particles which are transferred at highest velocities, namely biochar and ash particles. Therefore height of the 1st section of the sand reheater H_{SR}^{1st} is:

$$H_{SR}^{1st} = 2 \cdot (U_{FF} - \frac{u_t^{1st}(c) + u_t^{1st}(a)}{2}) = 11 \text{ m}.$$

The flow rate of solids in the sand reheater 1st section G_{solids}^{1st} was taken as a sum of sand flow rate and of a mean of biochar, wood, bark and ash flow rates and was calculated to be 44.4 kg/s. The ratio between the mass of solids and fluidizing gas in the sand reheater 1st section is 2.3. This corresponds to dilute phase flow regime [70] and therefore pressure drop in the 1st section of the sand reheater ΔP_{SR}^{1st} was calculated by identical formula as in the module "Pyrolyser sizing":

$$\Delta P_{SR}^{1st} = \frac{U_{FF}^2 \rho_g}{2} + G_{solids}^{1st} u_p^{1st} + \frac{2 f \rho_g U_{FF}^2 H_{SR}^{1st}}{D_{SR}^{1st}} + \frac{0.057 G_{solids}^{1st} H_{SR}^{1st} g}{\sqrt{g D_{SR}^{1st}}} + \frac{G_{solids}^{1st} H_{SR}^{1st} g}{u_p} + \rho_g H_{SR}^{1st} g.$$

Viscosity of fluidizing gas in the 1st section was calculated to be 33.19 μPa·s at 427 ^{0}C and 1 bar. It was taken as a mean between the air and flue gas viscosities. Data for both air and flue gas were taken from [64]. Based on this pressure drop in the sand reheater 1st section ΔP_{SR}^{1st} was calculated to be 0.012 bar.

5.11.3 Second section

2nd section has an inverted conical shape: lower diameter is smaller and equals the 1st section diameter while upper diameter is larger and is equal to the 3d section diameter. Velocity of gas in the 2nd section as it reaches top of the section should become less than terminal velocity of sand particles but higher enough than terminal velocity of ash particles. If this requirement is satisfied ash is entrained to the 3d section while sand particles fall down to the collection ports and flow back to the pyrolyser.

Only flue gas, sand and ash are present in the 2nd section of the sand reheater and their temperature is 869 ^{0}C. Density of flue gas at this temperature and 1 bar was calculated to be 0.331 kg/m^3. It was calculated by means of the equation of state

of an ideal gas. Based on this density using the same formula as earlier terminal velocity of sand particles in the 2nd section $u_t^{2nd}(s)$ was calculated to be 3.675 m/s and that of ash particles $u_t^{2nd}(a)$ was calculated to be 0.56 m/s.

Fluidizing gas velocity at the top of the sand reheater 2nd section $U_{FF}^{2nd\_top}$ was selected to be 2.5 m/s according to the calculated values of sand and ash particle terminal velocities. Volumetric gas flow rate in the 2nd section of the sand reheater V_G^{2nd} is 64.35 m^3/s. Therefore cross-sectional area $A_{SR}^{2nd\_top}$ and diameter $D_{SR}^{2nd\_top}$ of the top of the sand reheater 2nd section are:

$$A_{SR}^{2nd\_top} = \frac{V_G^{2nd}}{U_{FF}^{2nd\_top}} = 25.74 \text{ m}^2,$$

$$D_{SR}^{2nd\_top} = \sqrt{\frac{4 \cdot A_{SR}^{2nd\_top}}{3.14}} = 5.7 \text{ m}.$$

Height of the 2nd section of the sand reheater H_{SR}^{2nd} was designed to be 1.5 m. Pressure drop in the sand reheater 2nd section is neglected.

5.11.4 Third section

Diameter of the sand reheater 3d section D_{SR}^{3d} is equal to the diameter of the top of the sand reheater 2nd section $D_{SR}^{2nd\_top}$ and therefore is 5.7 m. Height of the 3d section of the sand reheater H_{SR}^{3d} was designed to be 3 m. Pressure drop in the sand reheater 3d section is neglected.

5.11.5 Summary

Height of the sand reheater H_{SR} is 15.5 m. Its other basic dimensions are depicted in the figure 8 below.

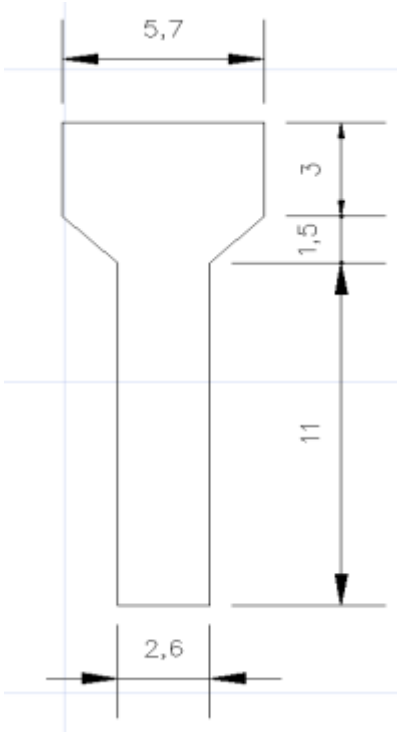

Figure 8: Basic dimensions of sand reheater.

Pressure drop of the sand reheater ΔP_{SR} was calculated to be 0.012 bar.

5.12 Electrostatic precipitator sizing

ESP sizing was carried out by means of simulation in Aspen Plus. ESP with the efficiency of ash removal equal to 99% has 35 plates with height 8.1 m and length 6.3 m. Total width of the ESP is 7.752 m. Power requirement of the ESP is 16.4 kW. Pressure drop in the ESP is 0.0001 bar.

5.13 Drying section material and heat balances

5.13.1 Introduction

The flue gas produced in sand reheater is used to dry the incoming raw biomass to the required moisture content, which is 10 wt% (wb). The temperature of the flue gas is 869 ^{0}C which is too high, as it can cause the incoming raw biomass to pyrolyse in the drying section. For this reason the flue gas is diluted by the

ambient air so that the temperature of the mixture is 200 ^{0}C (the temperature which is supposed to be safe in terms of premature pyrolysis). This gas mixture is then used as a drying agent in the drying section.

Heat capacity of air is taken at 107 ^{0}C and 1bar and is 1.012 kJ/ kg ^{0}C [64]. According to the values of air and flue gas heat capacities the flow rate of air G_{Drying_Air} required to obtain the 200 ^{0}C gas mixture was calculated in the following way:

$$G_{Drying\_Air}^{Summer} = \frac{G_G^{Flue} c_{pG\_Flue}(T_{comb}^{Req} - 200)}{c_{pAir}(200-20)} = \frac{21.3 \cdot 1.178 \cdot (869-200)}{1.012 \cdot (200-20)} = 92.2 \text{ kg/s},$$

$$G_{Drying\_Air}^{Winter} = \frac{G_G^{Flue} c_{pG\_Flue}(T_{comb}^{Req} - 200)}{c_{pAir}(200+20)} = \frac{21.3 \cdot 1.178 \cdot (869-200)}{1.012 \cdot (200+20)} = 75.4 \text{ kg/s}.$$

The flow rate of water that must be removed from the biomass during the drying process G_W^{Rem} was calculated to be 3.275 kg/s.

5.13.2 Summer period

The water content of the ambient air with which the flue gas is mixed is assumed to be 0.01 kg(water)/kg(dry air) which corresponds to relative humidity of 80% at the temperature of 20 ^{0}C. It is also assumed that the drying capacity of the gas mixture comprises 90% percent of the air with the same water content. Using the theoretical adiabatic drying model and Mollier air psychrometric chart [47], it was determined that 62.1 kg/s of gas mixture is needed when the temperature of the gas mixture leaving the dryer is 50 ^{0}C. As in the theoretical adiabatic drying model heat transfer to the material under drying is neglected, the value of the required gas mixture flow rate determined by this model was multiplied by a correction coefficient 1.2 and therefore the required flow rate of the gas mixture in the real dryer is 74.5 kg/s. Thus 39 kg/s of the gas mixture is left during the summer time.

5.13.3 Winter period

The ambient air during the winter period was assumed to have the same water content. Using the same assumptions as while calculating the required gas mixture flow rate for the summer period, required flow rate of the gas mixture in the real

dryer during the winter period was determined to be 77.25 kg/s and therefore 19.45 kg/s of the gas mixture is left during the winter period.

5.14 Dryer sizing

Commercially available belt dryer with the following dimensions [81]: width 4.3 m, length 3.98 m and height 3.1 m was selected for drying purposes.

5.15 Pressure drops in pipelines

5.15.1 Introduction

Stated diameters of pipelines are inner diameters [82]. Roughness of pipeline walls is taken as 150 μm [83]. Pressure drops in the pipelines were determined by means of simulation in Aspen Plus. Valves and fittings were not taken into account while determining the pressure drops.

5.15.2 Pipeline connecting pyrolyser to first cyclone and between cyclones

Cross-sectional area of the cyclone inlet is 0.18 m^2. It was decided to make the cross-sectional area of the pipeline connecting the pyrolyser outlet and the cyclone inlet to be as close as possible. Thus diameter of this pipeline was selected to be 475.4 mm. Length of the pipeline was designed to be 0.5 m. In Aspen Plus pressure drop in this pipeline is 0.001 bar.

Diameter of pipeline connecting the 1^{st} cyclone with the 2^{nd} one is 675.2 mm. Height of the vertical part is 0.5 m and length of the horizontal part is 1.2 m. Pressure drop in this pipeline without taking the bend into account is 0.006 bar. The bend is assumed to give the pressure drop of 0.01 bar. Thus the pressure drop in the pipeline is 0.016 bar.

5.15.3 Pipeline connecting second cyclone to quench column

The diameter is 675.2 mm. The horizontal part is 1 m long. The vertical part is 14.8 m. Pressure drop in the horizontal part is 0.00005 bar. Pressure drop in the

vertical part is 0.0008 bar. Thus pressure drop in the whole pipeline is 0.00085 bar.

5.15.4 Pipeline connecting quench column to pyrolyser

Total length of the pipeline is estimated to be 15 m. The diameter is 190.2 mm. It is assumed that the pipeline has three bends. Pressure drop without taking the bends into account is 0.03 bar. Pressure drop taking the bends into account is 0.15 bar.

5.15.5 Pipeline connecting pump 1 to quench column

Vertical part of the pipeline is 12 m. Diameter is 314.8 mm. Frictional pressure drop in the vertical part is 0.035 bar. Pressure drop associated with the head of the bio-oil in the pipeline was calculated to be 1.4 bar (bio-oil density was taken as 1200 kg/m^3 [3, 10, 11, 12, 17]). Pressure drop in horizontal parts of the pipeline was taken to be 0.1 bar (including bio-oil coolers). Pressure drop in the control valve was estimated using the number of velocity heads lost at the valve [69]. Velocity of bio-oil in the pipeline is 2.31 m/s and thus velocity head is 0.28 m of bio-oil. Number of velocity heads lost was taken as 50 [69] and therefore pressure drop in the control valve was estimated to be 1.65 bar. Therefore pressure drop in the whole pipeline is 3.185 bar.

5.15.6 Pipeline connecting pump 2 to bio-oil coolers

Diameter of the pipeline is 369.4 mm and thus velocity of cooling water in the pipeline is 2.3 m/s. Using the same method as in the module 5.15.5 it was estimated that pressure drop in the control valve is 1.33 bar. Pressure drop in the whole pipeline was estimated to be 2.5 bar.

5.15.7 Pipeline connecting sand reheater to electrostatic precipitator

Total length of the pipeline is estimated to be 17 m. The diameter is 532.6 mm. It is assumed that the pipeline has three bends. Pressure drop without taking the bends into account is 0.11 bar. Pressure drop taking the bends into account is 0.25 bar.

5.15.8 Pipeline connecting electrostatic precipitator to the point where flue gas is mixed with the ambient air

Total length of the pipeline is estimated to be 12 m. The diameter is 532.6 mm. It is assumed that the pipeline has two bends. Pressure drop without taking the bends into account is 0.075 bar. Pressure drop taking the bends into account is 0.15 bar.

5.16 Plant layout

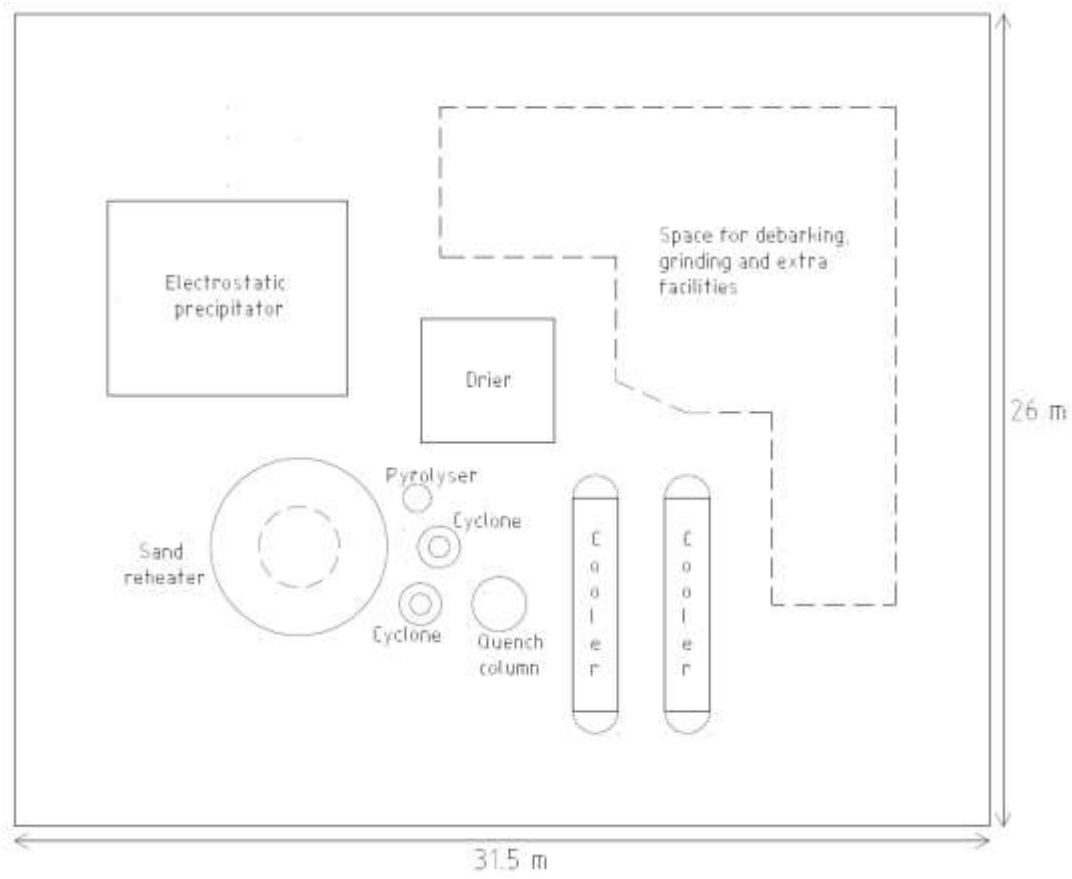

Figure 9: Bio-oil plant layout.

6 ECONOMIC FEASIBILITY ANALYSIS

6.1 Investment cost calculation

Total investment cost is comprised of fixed capital investment and working capital. Fixed capital investment consists of ISBL (inside battery limits) investment, off-site investment, design and engineering costs, and contingency charges. ISBL investment is the cost of the plant itself which includes all the process equipment, piping, instruments, installation labour, civil works, etc. Off-site investment is the cost of the site infrastructure modification necessary for accommodation of potential future expansion. Contingency charges must be added to the project budget to cover inaccuracies of cost estimates and unexpected expenses [69].

Factorial estimates method is used to calculate the ISBL investment. In this method purchased equipment cost C_e is multiplied by the sum of a set of factors in order to be transferred into capital equipment cost C which takes into account not only the cost of the equipment itself but also the cost of buildings and structures, installation labour, piping, materials, instruments, and civil works required for installation and future operation of the equipment. When capital costs of all the equipment items are added together the ISBL investment is obtained.

According to the equipment list presented in the Appendix II we have equipment made from carbon steel, stainless steel 316 and Inconel. Installation factors used for all these materials are given below in the table 18.

Table 18: Installation factors (fluids-solids process type) [69].

Item for which the factor is used	Factor value for carbon steel	Factor value for stainless steel 316	Factor value for inconel
Equipment erection	0.5	0.385	0.294
Piping	0.6	0.6	0.6
Instrumentation	0.3	0.23	0.18

and control			
Electrical work	0.2	0.154	0.12
Civil engineering work	0.3	0.23	0.18
Structures and buildings	0.2	0.154	0.12
Lagging and paint	0.1	0.077	0.06
Overall installation factor	2.2	1.83	1.554

Purchased equipment costs were obtained for the year 2007 in $ [84]. They were at first transferred to costs in $ for May 2013 by means of cost indices which were 613.4 in March 2007 [85] and 692.8 in May 2013 [86]. Then costs in € in May 2013 were calculated using average euro to dollar ratio in May 2013 which was 1.2975 [87]. Off-site cost was taken as 40% of ISBL cost [69]. Engineering cost was taken as 30% of sum of ISBL cost and off-site cost [69]. Contingency charges account for 30% of the fixed capital investment. Breakdown of fixed capital investment for each equipment item is presented below in the table 19.

Table 19: Breakdown of fixed capital investment for each equipment item.

Equipment item	Purchased cost, €	Erection cost, €	Piping cost, €	Instru-mentation cost, €	Electri-cal work cost, €	Civil work cost, €	Structures and buildings cost, €	Lagging and paint cost, €	Off-site cost, €	Engineering cost, €	Contingency charges, €
Debarker	741 850	285 327	445 110	171 196	114 131	171 196	114 131	57 065	840 002	882 003	1 638 005
Dryer	446 690	171 804	268 014	103 082	68 722	103 082	68 722	34 361	505 791	531 080	986 292
Pyrolyser	32 400	12 462	19 440	7 477	4 985	7 477	4 985	2 492	36 687	38 521	71 539
Cyclone 1	27 430	13 715	16 458	8 229	5 486	8 229	5 486	2 743	35 110	36 866	68 465
Cyclone 2	27 430	13 715	16 458	8 229	5 486	8 229	5 486	2 743	35 110	36 866	68 465
Sand reheater	207 970	61 168	124 782	36 701	24 467	36 701	24 467	12 234	211 395	221 965	412 221
Electrostatic precipita-tor	388 600	194 300	233 160	116 580	77 720	116 580	77 720	38 860	497 408	522 278	969 946
Quench tower	56 440	21 708	33 864	13 025	8 683	13 025	8 683	4 342	63 907	67 103	124 620

Equipment item	Purchased cost, €	Erection cost, €	Piping cost, €	Instru-menta-tion cost, €	Electri-cal work cost, €	Civil work cost, €	Structures and buildings cost, €	Lagging and paint cost, €	Off-site cost, €	Engineering cost, €	Contingency charges, €
Cooler 1	445 470	171 335	267 282	102 801	68 534	102 801	68 534	34 267	504 409	529 630	983 598
Cooler 2	445 470	171 335	267 282	102 801	68 534	102 801	68 534	34 267	504 409	529 630	983 598
Pump 1	25 520	9 815	15 312	5 889	3 926	5 889	3 926	1 963	28 896	30 341	56 348
Pump 2	27 960	10 754	16 776	6 452	4 302	6 452	4 302	2 151	31 659	33 242	61 736
Blower 1	52 600	26 300	31 560	15 780	10 520	15 780	10 520	5 260	67 328	70 694	131 290
Blower 2	459 400	229 700	275 640	137 820	91 880	137 820	91 880	45 940	588 032	617 434	1 146 662
Blower 3	1 188 900	594 450	713 340	356 670	237 780	356 670	237 780	118 890	1 521 792	1 597 882	2 967 494
Storage tank 1	466 230	179 319	279 738	6 452	71 728	107 592	71 728	35 864	487 460	511 833	950 547
Storage tank 2	466 230	179 319	279 738	6 452	71 728	107 592	71 728	35 864	487 460	511 833	950 547

Potentially missing items	1 500 000	750 000	900 000	450 000	300 000	450 000	300 000	150 000	1 920 000	2 016 000	3 744 000

Based on the data given in the table 19 total investment cost was calculated. Working capital was taken as was estimated to be as high as 15% of fixed capital investment [69]. Breakdown of the total investment cost is presented below in the table 20.

Table 20: Breakdown of the total investment cost.

Equipment cost, €	7 006 590
Equipment erection cost, €	3 096 525
Piping cost, €	4 203 955
Instrumentation cost, €	1 655 640
Electrical work cost, €	1 238 610
Civil work cost, €	1 857 915
Structures and buildings cost, €	1 238 610
Lagging and paint cost, €	619 305
Off-site cost, €	8 366 860
Engineering cost, €	8 785 200
Contingency charges, €	16 315 375
Working capital, €	8 157 690
Total investment cost, €	**62 542 275**

6.2 Operating cost calculation

6.2.1 Raw material

Average wood energy price in Finland in 2013 is 19 €/MWh. It is assumed that wood energy content is 0.8 MWh/loose m^3 (or 2900 MJ/ loose m^3). By multiplying these two values we get the price 15.2 €/loose m^3. As 1 loose m^3 is equal to 0.38 dry solid m^3, price per 1 dry solid m^3 is 40 €. Density of dry solid wood is taken as 445 kg/m^3 and therefore final price is 0.09 €/kg of raw material which means that annual cost of the raw material is 31 062 060 €/year [88].

6.2.2 Utilities

It is supposed that the bio-oil production site will be located by a lake or a river hence cooling water will be pumped from the water body. Therefore electricity is

only utility price of which should be taken into account. According to the equipment list given in the appendix II total electricity consumption is 9966 kW. However in order to take into account electricity consumption of potentially missing equipment items a factor of 1.5 was used and therefore annual electricity consumption is 14949 kW. Electricity price is taken as 6.44 cents/kWh [89]. Therefore annual expenses for electricity account for 8 317 860 €/year.

6.2.3 Maintenance

Maintenance is referred to both materials and labour and is taken as 5% of ISBL investment [69] which is 750 225 €/year.

6.2.4 Operating labour and associated expenses

It is assumed that there are 20 workers operating the bio-oil production site and that their annual salary is 840 000 €/year. It is also assumed that expenses required for supervision account for 100 000 €/year. Based on these assumptions expenses for fringe benefits, payroll taxes and health insurance are 376 000 €/year [69]. Thus operating labour and associated expenses are 1 316 000 €/year.

6.2.5 Other expenses

Other expenses comprising operating cost are property taxes and insurance, rent of land, and allocated environmental charges [69]. Their values and ways of calculation are presented below in the table 21.

Table 21: Calculation of other expenses comprising operating cost.

Expense item	Cost, €/year	Way of calculation
Property taxes and insurance	418 345	2% of ISBL investment [69]
Rent of land	1 087 690	2% of fixed capital investment [69]
Allocated environmental charges	543 845	1% of fixed capital investment [69]
Total	2 049 880	Sum of all the items

6.2.6 Total operating cost

Total operating cost and its breakdown are given below in the table 22.

Table 22: Total operating cost breakdown.

Expense item	Cost, €/year
Raw material	31 062 060
Utilities	8 317 860
Maintenance	750 225
Operating labour and associated expenses	1 316 000
Other expenses	2 049 880
Total	**43 496 025**

6.3 Profitability estimation

The main aim of the current profitability estimation is to calculate how much should be the bio-oil price in order to reach certain values of IRR (internal rate of return). A set of assumptions was used while calculations: residual value was taken as zero, it was assumed that every year all the produced bio-oil is sold for the same price and therefore cash flow is the same every year. In case of uniform cash flows NPV (net present value) is calculated according to the following formula:

$$NPV = (AI - OC) \cdot \frac{1-(1+i)^{-n}}{i} - IC \qquad (38)$$

where AI annual income, €

OC operating cost, €

IC total investment cost, €

i interest rate

n lifetime, years.

As IRR is such an interest rate when NPV is zero, the equation 38 was equated to zero and bio-oil price was calculated at several values of IRR. Lifetime was set to

be 15 years. Based on the calculated bio-oil price there was determined payback period PP corresponding to each value of IRR using the following formula:

$$PP = \frac{IC}{AI - OC} \quad (39).$$

Results are given below in the table 23. Density of 1200 kg/m^3 [3, 10, 11, 12, 17] was used to convert bio-oil price per kilogram into bio-oil price per liter.

Table 23: Bio-oil price, cash flow and payback period at different values of IRR.

IRR, %	Bio-oil price, €/kg	Bio-oil price, €/liter	Payback period, years
5	0.50	0.60	10.4
10	0.52	0.62	7.6
20	0.57	0.68	4.68
30	0.63	0.75	3.3
40	0.69	0.82	2.5
50	0.75	0.90	2

According to the tables given in the module 2.1 it is reasonable to assume that energy content of bio-oil is 18 MJ/kg. Based on this assumption there was calculated bio-oil price with regard to the thermal energy produced. Results are presented below in the table 24.

Table 24: Bio-oil price with regard to the thermal energy produced.

IRR, %	Energy price, €/MWh
5	99
10	103.4
20	113.75
30	125.3
40	137.35
50	149.7

For comparison 30.5 €/MWh is the price for natural gas in europe in January 2013 [90]. Price for crude oil is around 46 €/MWh [91]. Average wood energy price in Finland in 2013 is 19 €/MWh [88].

CONCLUSIONS

Biomass fast pyrolysis is a process which yields liquid biofuel called bio-oil. Bio-oil can be burnt in thermal power stations and used as a precursor for production of hydrogen and valuable chemical compounds. After an upgrading step bio-oil can be used as a transport fuel. Therefore biomass fast pyrolysis is a process which produces a biofuel that potentially can replace conventional fossil based fuels.

According to the literature survey conducted in the current master's thesis woody biomass is the best type of biomass for fast pyrolysis as bio-oil produced from woody biomass has superior qualities in comparison to bio-oil produced from other types of biomass. For this reason woody biomass was selected to be the raw material in the current master's thesis. Scots pine wood was chosen among the woody biomass as it comprises half of the Finnish forest resources.

There was carried out a comparison of different existing biomass fast pyrolysis concepts and the results revealed that circulating fluidized bed installations have the highest potential to grow into commercial scale plants. Hence there was made a feasibility study for Scots pine wood circulating fluidized bed fast pyrolysis process with a bio-oil production capacity of 100 000 tonne/year. Process design and profitability estimation were performed within the feasibility study.

As a result of a process design there were developed several documents. The first one is "Balance calculator" Excel spreadsheet calculating temperatures and mass flow rates of all the process streams depending on the value of the bio-oil production capacity. The second one is process flow diagram stating temperature, pressure, mass flow rate and pipe diameter of all the process streams and dimensions of the main equipment for bio-oil production capacity of 100 000 tonne/year. Both documents are presented in the current master's thesis as appendixes.

During the profitability estimation it was determined that investment cost for the bio-oil plant of 100 000 tonne/year production capacity is 62 545 275 € and operational cost is 43 496 025 €/year. It was also calculated that in order to achieve 20% internal rate of return bio-oil price per MWh of generated thermal

energy must be 113.75 € which is around 6 times higher than that of wood, 4 times higher than that of natural gas and 2.5 times than that of crude oil.

This means that bio-oil cannot enter the fuel market at the current stage of development of the biomass circulating fluidized bed fast pyrolysis process and therefore subsidies from the government and further improvement of the technology are required in order to enable bio-oil be a competitive product in the fuel market.

REFERENCES

1. Isahak W. N. R. W., A review on bio-oil production from biomass by using pyrolysis method, Renewable and Sustainable Energy Reviews, 16 (2012), pp. 5910 – 5923.

2. Briens C., Piskorz J., Berruti F., Biomass Valorization for Fuel and Chemicals Production – A Review, International Journal of Chemical Reactor Engineering, 6 (2008), Review R2.

3. Qiang L., Wen-Zhi L., Xi-Feng Z., Overview of fuel properties of biomass fast pyrolysis oils, Energy Conversion and Management, 50 (2009), pp. 1376 – 1383.

4. Saidur R., Abdelaziz E. A., Demirbas A., Hossain M. S., Mekhilef S., A review on biomass as a fuel for boilers, Renewable and Sustainable Energy Reviews, 15 (2011), pp. 2262 – 2289.

5. Panwar N. L., Kothari R., Tyagi V. V., Thermo chemical conversion of biomass – Eco friendly energy routes, Renewable and Sustainable Energy Reviews, 16 (2012), pp. 1801 – 1816.

6. Toor S. S., Rosendahl L., Rudolf A., Hydrothermal liquefaction of biomass: A review of subcritical water technologies, Energy, 36 (2011) 5, pp. 2328 – 2342.

7. Liew L. N., Shi J., Li Y., Methane production from solid-state anaerobic digestion of lignocellulosic biomass, Biomass and Bioenergy, 46 (2012), pp. 125 – 132.

8. Tarelho L. A. C., Neves D. S. F., Matos M. A. A., Forest biomass waste combustion in a pilot-scale bubbling fluidized bed combustor, Biomass and Bioenergy, 35 (2011) 4, pp. 1511 – 1523.

9. Balat M., Balat M., Kirtay E., Balat H., Main routes of the thermo-conversion of biomass into fuels and chemicals. Part 2: Gasification systems, Energy Conversion and Management, 50 (2009), pp. 3158 – 3168.

10. Bridgwater A. V., Review of fast pyrolysis of biomass and product upgrading, Biomass and Bioenergy, 38 (2012), pp. 68 – 94.

11. Bridgwater A. V., Fast pyrolysis process for biomass, Renewable and Sustainable Energy Reviews, 4 (2000), pp. 1 – 73.

12. Bridgwater A. V., Renewable fuels and chemicals by thermal processing of biomass, Chemical Engineering Journal, 91 (2003), pp. 87 – 102.

13. Balat M., Balat M., Kirtay E., Balat H., Main routes for the thermo-conversion of biomass into fuels and chemicals. Part 1: Pyrolysis systems, Energy Conversion and Management, 50 (2009), pp. 3147 – 3157.

14. Vardon D. R., Sharma B. K., Blazina G. V., Rajagopalan K., Strathmann T. J., Thermochemical conversion of raw and defatted algal biomass via hydrothermal liquefaction and slow pyrolysis, Bioresource Technology, 109 (2012), pp. 178 – 187.

15. Karaosmanoglu F., Tetik E., Gollu E., Biofuel production using slow pyrolysis of the straw and stalk of the rapeseed plant, Fuel Processing Technology, 59 (1999) 1, pp. 1 – 12.

16. Brossard L. E., Cortez L. A. B., Penedo M., Bezzon G., Olivares E., Total condensable effluents yield in slow pyrolysis of bagasse briquettes, Energy Conversion and Management, 41 (2000) 3, pp. 223 – 233.

17. Qi Z., Jie C., Wang T., Ying X., Review of biomass pyrolysis oil properties and upgrading research, Energy Conversion and Management, 48 (2007), pp. 87 – 92.

18. Akhtar J., Amin N. S., A review on operating parameters for optimum liquid oil yield in biomass pyrolysis, Renewable and Sustainable Energy Reviews, 16 (2012), pp. 5101 – 5109.

19. Jendoubi N., Broust F., Commandre J. M., Mauviel G., Sardin M., Lede J., Inorganics distribution in bio oils and char produced by biomass fast pyrolysis: The key role of aerosols, Journal of Analytical and Applied Pyrolysis, 92 (2011) 1, pp. 59 – 67.

20. Kim K. H., Eom I. Y., Lee S. M., Choi D., Yeo H., Choi I-G., Choi J. W., Investigation of physicochemical properties of biooils produced from yellow poplar wood (Liriodendron tulipifera) at various temperatures and residence times, Journal of Analytical and Applied Pyrolysis, 92 (2011) 1, pp. 2 – 9.

21. Cao J-P., Xiao X-B., Zhang S-Y., Zhao X-Y., Sato K., Ogawa Y., Wei X-Y., Takarada T., Preparation and characterization of bio-oils from internally circulating fluidized bed pyrolyses of municipal, livestock, and wood waste, Bioresource Technology, 102 (2011) 2, pp. 2009 – 2015.

22. Park H. J., Dong J-I., Jeon J-K., Park Y-K., Yoo K-S., Kim S-S., Kim J., Kim S., Effects of the operating parameters on the production of bio-oil in the fast pyrolysis of Japanese larch, Chemical Engineering Journal, 143 (2008) 1-3, pp. 124 – 132.

23. Kang B-S., Lee K. H., Park H. J., park Y-K., Kim J-S., Fast pyrolysis of radiata pine in a bench scale plant with a fluidized bed: Influence of char separation system and reaction conditions on the production of bio-oil, Journal of Analytical and Applied Pyrolysis, 76 (2006) 1-2, pp. 32 – 37.

24. Kim K. H., Kim T-S., Lee S-M., Choi D., Yeo H., Choi I-G., Choi J. W., Comparison of physicochemical features of biooils and biochars produced from various woody biomasses by fast pyrolysis, Renewable Energy, 50 (2013), pp. 188 – 195.

25. Park H. J., Park Y-K., Kim J. S., Influence of reaction conditions and the char separation system on the production of bio-oil from radiate pine sawdust by fast pyrolysis, Fuel Processing Technology, 89 (2008) 8, pp. 797 – 802.

26. Pattiya A., Suttibak S., Production of bio-oil via fast pyrolysis of agricultural residues from cassava plantations in a fluidised-bed reactor with a hot vapour filtration unit, Journal of Analytical and Applied Pyrolysis, 95 (2012), 227 – 235.

27. Piskorz J., Majerski P., Radlein D., Scott D. S., Bridgwater A. V., Fast pyrolysis of sweet sorghum and sweet sorghum bagasse, Journal of Analytical and Applied Pyrolysis, 46 (1998) 1, pp. 15 – 29.

28. Zhang H., Xiao R., Wang D., He G., Shao S., Zhang J., Zhong Z., Biomass fast pyrolysis in a fluidized fast reactor under N_2, CO_2, CO, CH_4 and H_2 atmospheres, Bioresource Technology, 102 (2011) 5, pp. 4258 – 4264.

29. Guo X., Wang S., Wang Q., Guo Z., Luo Z., Properties of bio-oil from fast pyrolysis of rice husk, Chinese Journal of Chemical Engineering, 19 (2011) 1, pp. 116 – 121.

30. Zheng J-L., Pyrolysis oil from fast pyrolysis of maize stalk, Journal of Analytical and Applied Pyrolysis, 83 (2008) 2, pp. 205 – 212.

31. Bok J. P., Choi H. S., Choi Y. S., Park H. C., Kim S. J., Fast pyrolysis of coffee grounds: Characteristics of product yields and biocrude oil quality, Energy, 47 (2012) 1, pp. 17 – 24.

32. Park H. J., Heo H. S., Park Y-K., Yim J-H., Jeon J-K., Park J., Ryu C., Kim S-S., Clean bio-oil production from fast pyrolysis of sewage sludge: Effects of reaction conditions and metal oxide catalysts, Bioresource Technology, 101 (2010) 1 Supplement, S83 – S85.

33. Fonts I., Azuara M., Gea G., Murillo M. B., Study of the pyrolysis liquids obtained from different sewage sludge, Journal of Analytical and Applied Pyrolysis, 85 (2009), pp. 184 – 191.

34. Wang K., Brown R. C., Homsy S., Martinez L., Sidhu S. S., Fast pyrolysis of microalgae remnants in a fluidized bed reactor for bio-oil and biochar production, Bioresource Technology, in press.

35. Miao X., Wu Q., Yang C., Fast pyrolysis of microalgae to produce renewable fuels, Journal of Analytical and Applied Pyrolysis, 71 (2004) 2, pp. 855 – 863.

36. Mourant D., Lievens C., Gunawan R., Wang Y., Hu X., Wu L., Syed-Hassan S. S. A., Li C-Z., Effects of temperature on the yields and properties of bio-oil from the fast pyrolysis of mallee bark, Fuel, 108 (2013), pp. 400 – 408.

37. IEA Bioenergy, Task 34 – Pyrolysis, Country report for Finland, Available: http://www.pyne.co.uk/Resources/user/Country%20Update%2011%202011%20Finland.pdf.

38. Mante O. D., Agblevor F. A., Storage stability of biocrude oils from fast pyrolysis of poultry litter, Waste Management, 32 (2012) 1, pp. 67 – 76.

39. IEA Bioenergy, Task 34 – Pyrolysis, Pyrolysis oil combustion tests in an industrial boiler, Available: http://www.pyne.co.uk/?_id=4.

40. Diebold J. P., Czernik S., Additives to lower and stabilize the viscosity of pyrolysis oils during storage, Energy & Fuels, 11 (1997), pp. 1081 – 1091.

41. IEA Bioenergy, Task 34 – Pyrolysis, Hydrogen biomass by catalytic steam reforming of fast pyrolysis oil, Available: http://www.pyne.co.uk/?_id=6.

42. IEA Bioenergy, Task 34 – Pyrolysis, Fuels and chemicals from biomass, Available: http://www.pyne.co.uk/?_id=119.

43. Shah A., Darr M. J., Dalluge D., Medic D., Webster K., Brown R. C., Physicochemical properties of bio-oil and biochar produced by fast pyrolysis of stored single-pass corn stover and cobs, Bioresource Technology, 125 (2012), pp. 348 – 352.

44. Koutcheiko S., Monreal C. M., Kodama H., McCracken T., Kotlyar L., Preparation and characterization of activated carbon derived from the thermo-chemical conversion of chicken manure, Bioresource Technology, 98 (2007) pp. 2459 – 2464.

45. Heo H. S., Park H. J., Dong J-I., Park S-H., Kim S., Suh D. J., Suh Y-W., Kim S-S., Park Y-K., Fast pyrolysis of rice husk under different reaction conditions, Journal of Industrial and Engineering Chemistry, 16 (2010), pp. 27 – 31.

46. Scott D. S., Marjeski P., Piskorz J., Radlein D., A second look at fast pyrolysis of biomass-the RTI process, Journal of Analytical and Applied Pyrolysis, 51 (1999), 23 – 37.

47. Perry R. H., Green D. W., Perry's Chemical Engineers' Handbook, 8th edition, McGraw-Hill Professional, New York 2008, 2700 p.

48. Bedmutha R. J., Ferrante L., Briens C., Berruti F., Inculet I., Single and two-stage electrostatic demisters for biomass pyrolysis application, Chemical Engineering and Processing: Process Intensification, 48 (2009), 1112 – 1120.

49. Van de Velden M., Baeyens J., Boukis I., Operating parameters for circulating fluidized bed (CFB) pyrolysis of biomass, 2007 Proceedings of European Congress of Chemical Engineering (ECCE-6), Copenhagen.

50. Van de Velden M., Baeyens J., Brems A., Janssens B., Dewil R., Fundamentals, kinetics and endothermicity of the biomass pyrolysis reaction, Renewable Energy, 35 (2010) 1, pp. 232 – 242.

51. Di Blasi, C., Kinetics and modeling of biomass pyrolysis. In: Fast Pyrolysis of Biomass: a Handbook Volume 3, Bridgwater, A.V. (ed.), CPL Press, Newbury 121-146 (2005).

52. Luo Z., Wang S., Cen K., A model of wood flash pyrolysis in fluidized bed reactor, Renewable Energy, 30 (2005) 3, pp. 377 – 392.

53. Blondeau J., Jeanmart H., Biomass pyrolysis at high temperatures: Prediction of gaseous species yields from an acnisotropic particle, Biomass and Bioenergy, 41 (2012), pp. 107 – 121.

54. Lu H., Ip E., Scott J., Foster P., Vickers M., Baxter L. L., Effects of particle shape and size on devolatilization of biomass particle, Fuel, 89 (2010) 5, pp. 1156 – 1168.

55. French R., Czernik S., Catalytic pyrolysis of biomass for biofuel production, Fuel Processing Technology, 91 (2010), pp. 25 – 32.

56. Demirbas A., Sustainable cofiring of biomass with coal, Energy Conversion and Management, 44 (2003) 9, pp. 1465 – 1479.

57. Ahmarruzaman M., A review on the utilization of fly ash, Progress in Energy and Combustion Science, 36 (2010), 327 – 363.

58. An assessment of bio-oil toxicity for safe handling and transportation, Final Publishable Report, September 2005.

59. IEA Bioenergy, Task 34 – Pyrolysis, Experience with firing pyrolysis oil on industrial scale, Available: http://www.pyne.co.uk/Resources/user/PyNe%20July%202012%20-%20Issue%2031.pdf.

60. Bain R. L., Overend R. P., Craig K. R., Biomass-fired power generation, Fuel Processing Technology, 54 (1998), pp. 1 – 16.

61. Finnish national forest inventory, Available: http://www.metla.fi/ohjelma/vmi/vmi-mvarat-en.htm.

62. Sable I., Grinfelds U., Jansons A., Vikele L., Irbe I., Verovkins A., Treimanis A., Comparison of the properties of wood and pulp fibers from Lodgepole pine (Pinus contorta) and Scots pine (Pinus sylvestris), BioResources, 7 (2012) 2, pp. 1771 – 1783.

63. Blondeau J., Jeanmart H., Biomass pyrolysis in pulverized-fuel boilers: Derivation of apparent kinetic parameters for inclusion in CFD codes, Proceedings of the Combustion Institute, 33 (2011), pp. 1787 – 1794.

64. Haynes W. M., *CRC Handbook of Chemistry and Physics*, 93rd edition (Internet Version 2013), CRC Press/Taylor and Francis, Boca Raton, FL.

65. Summitt R., Sliker A., *Handbook of materials science Volume IV Wood*, CRC Press, USA 1980, 459 p.

66. Rath J., Wolfinger M. G., Steiner G., Krammer G., Barontini F., Cozzani V., Heat of wood pyrolysis, Fuel, 82 (2003), pp. 81 – 91.

67. Calonaci M., Grana R., Hemings E. B., Bozzano G., Dente M., Ranzi E., A comprehensive kinetic modelling study of bio-oil formation from fast pyrolysis of biomass, Energy Fuel, 24 (2010) 1, pp. 5727 – 5734.

68. Yaws C. L., *Yaws' Critical Property Data for Chemical Engineers and Chemists*, Knovel, 2012. Online version available at:

http://www.knovel.com/web/portal/browse/display?_EXT_KNOVEL_DISPLAY_bookid=5083&VerticalID=0.

69. Sinnott R., Towler G., Chemical engineering design, 5th edition, Butterworth-Heinemann, USA, 2009, 1255 p.

70. Geldart D, *Gas fluidization technology*, John Wiley & Sons Ltd, Great Britain, 1986,
468 p.

71. Anwar S., Caroll J. J., *Carbon Dioxide Thermodynamic Properties Handbook - Covering Temperatures from -20 Degrees to 250 Degrees Celsius and Pressures Up to 1000 Bar*, Wiley – Scrivener, 2011. Online version available at: http://www.knovel.com/web/portal/browse/display?_EXT_KNOVEL_DISPLAY_bookid=4105&VerticalID=0.

72. Kunii D., Levenspiel O., *Fluidization Engineering*, 2nd edition, Butterworth-Heinemann, USA 1991, 491 p.

73. Yaws C. L., *Yaws' Transport Properties of Chemicals and Hydrocarbons* (Electronic Edition), Knovel, 2010. Online version available at: http://www.knovel.com/web/portal/browse/display?_EXT_KNOVEL_DISPLAY_bookid=2905&VerticalID=0.

74. Gupta R. B., Demirbas A., *Gasoline, Diesel and Ethanol Biofuels from Grasses and Plants*, Cambridge University Press, 2010, 247 p. Online version available at: http://www.knovel.com/web/portal/browse/display?_EXT_KNOVEL_DISPLAY_bookid=3970&VerticalID=0.

75. Richard W., Sun X. S., *Bio-Based Polymers and Composites*, Elsevier, 2005, 685 p. Online version available at: http://www.knovel.com/web/portal/browse/display?_EXT_KNOVEL_DISPLAY_bookid=4772&VerticalID=0.

76. Huhtinen M., Wood biomass as a fuel, Material for 5EURES training sessions, 2006.

77. Filbakk T., Jirjis R., Nurmi J., Høibø O., The effect of bark content on quality parameters of Scots pine (Pinus sylvestris L.) pellets, Biomass and Bioenergy, 8 (2011) 35, pp. 3342 – 3349.

78. Francescato V., Antonini E., Bergomi L. Z., Wood fuels handbook, Italian Agriforestry Energy Association, 2008.

79. Values of wood fuel parameters, Available: http://www.woodenergy.ie/woodasafuel/listandvaluesofwoodfuelparameters-part2/.

80. Tolvanen H. M., Kokko L. I., Raiko R., The factors controlling combustion and gasification kinetics of solid fuels, Finnish-Swedish Flame Days 2011, The Swedish and Finnish National Committees of the International Flame Research Foundation.

81. ELA Verfahrenstechnik belt dryer specifications, Available: http://www.ela-vt.de/belt-dryer/belt-dryer.htm.

82. Pipe dimensions according European Standards, Available: http://www.engineeringtoolbox.com/pe-pipe-dimensions-d_321.html.

83. Absolute pipe roughness depending on pipe material, Available: http://www.efunda.com/formulae/fluids/roughness.cfm.

84. Process equipment cost estimates, Available: http://matche.com/toc.htm.

85. Economic Indicators, Chemical Engineering, 114 (2007) 7, pp. 84.

86. Economic Indicators, Chemical Engineering, 120 (2013) 5, pp. 76.

87. Currency exchange rates resource, Available: http://www.currency.me.uk/convert/eur/usd.

88. Hyvärinen R., senior process engineer, Pöyry, e-mail message, 30.07.2013.

89. Electricity prices for enterprises and public utilities, Available:

http://www.helen.fi/hinnasto/sahkohinnasto_helsinki_yritykset_englanti_1309.pdf.

90. European Union natural gas import price, Available: http://ycharts.com/indicators/europe_natural_gas_price.

91. Crude oil and commodity prices, Available: http://www.oil-price.net/.

APPENDIX I

BALANCE CALCULATOR DESCRIPTION

There was developed an Excel spreadsheet which calculates mass balances in all the equipment items so that values for all the inflow and outflow streams are displayed. Those cells where the input parameters required for calculations should be entered are highlighted with the yellow colour. The spreadsheet calculates mass balances by means of formulas contained in the module 5 of the current document and also formulas derived from them.

APPENDIX II

BALANCE CALCULATOR EXAMPLE

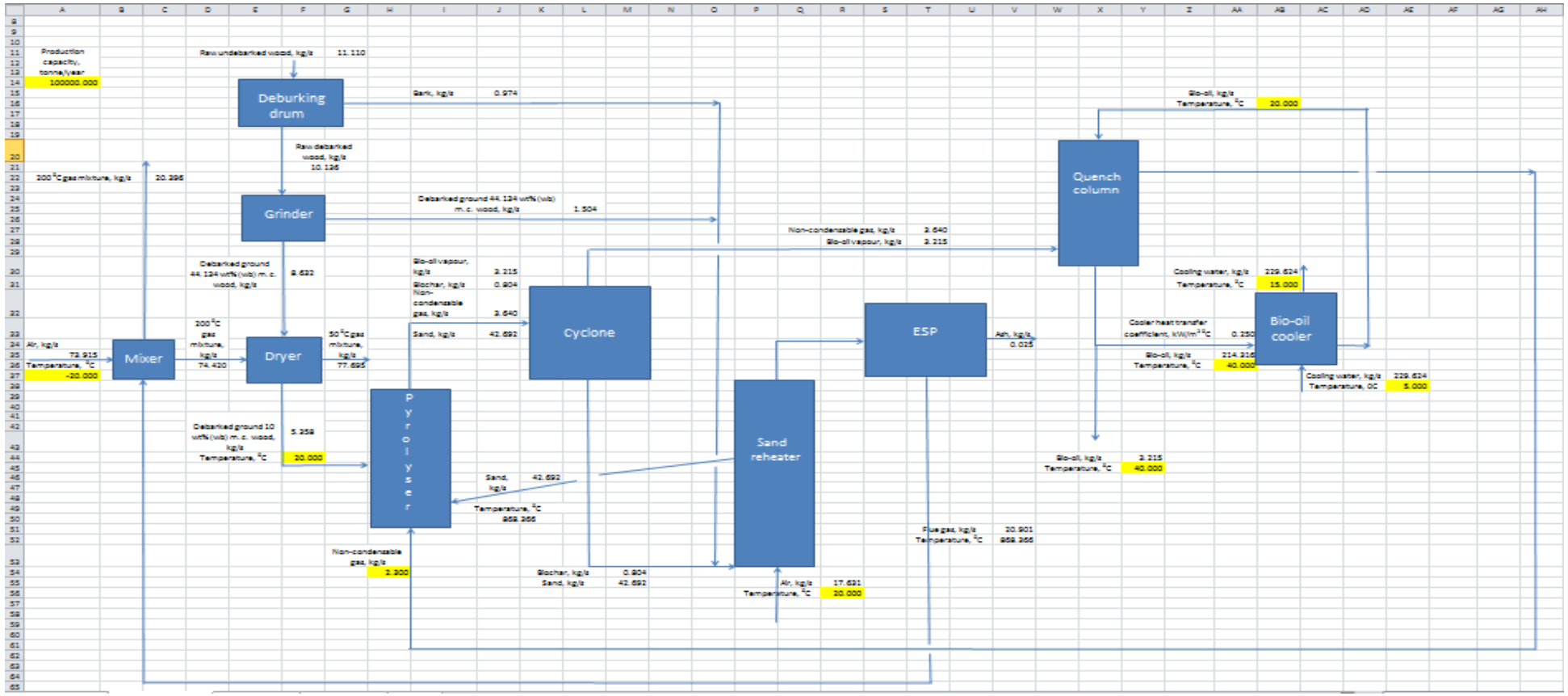

APPENDIX III

EQUIPMENT LIST

Name	Type	Technical parameters	Material
Debarker	Drum	Diameter 5 m, length 28 m	Stainless steel 316
Dryer	Belt	Length 3.98 m, width 4.3 m, height 3.1 m	Stainless steel 316
Pyrolyser	Horizon-tal column with round ends	Diameter 0.9 m, height 14.3 m	Stainless steel 316
Cyclone 1	Reverse-flow	Cylindrical part: diameter 1.35 m, height 2 m Conical part: bottom diameter 0.5 m, height 3.35 m Gas inlet: width 0.27 m, height 0.67 m Gas outlet: diameter 0.67 m, height 0.67 m	Carbon steel
Cyclone 2	Reverse-flow	Cylindrical part: diameter 1.35 m, height 2 m Conical part: bottom diameter 0.5 m, height 3.35 m Gas inlet: width 0.27 m, height 0.67 m Gas outlet: diameter 0.67 m, height 0.67 m	Carbon steel
Sand reheater	Riser reactor	Dense bed section: diameter 2.6 m, height 11 m	Inconel

	with a free-board and no internal cyclones	Conical section: bottom diameter 2.6 m, top diameter 5.7 m, height 1.5 m Freeboard section: diameter 5.7 m, height 3 m	
Electrosta-tic precipita-tor	Dry	Length 6.3 m, width 7.752, height 8.1 m, power 16.4 kW	Carbon steel
Quench tower	Horizon-tal column with round ends	Diameter 1.75 m, height 10 m	Stainless steel 316
Cooler 1	Shell and tube heat exchan-ger	Shell outer diameter 1.464 m, 1396 tubes of 32 mm outer diameter and 7.32 m height, approximate heat transfer area 1027 m^2	Stainless steel 316
Cooler 2	Shell and tube heat exchan-ger	Shell outer diameter 1.464 m, 1396 tubes of 32 mm outer diameter and 7.32 m height, approximate heat transfer area 1027 m^2	Stainless steel 316
Pump 1	Centri-fugal	Power 106.6 kW	Stainless steel 316
Pump 2	Centri-fugal	Power 66 kW	Stainless steel 316
Blower 1	Centri-fugal	Maximum capacity 92 m^3/min, power 99 kW	Carbon steel
Blower 2	Centri-fugal	Maximum capacity 1825 m^3/min, power 2983 kW	Carbon steel

Blower 3	Centri-fugal	Maximum capacity 4800 m^3/min, power 6711 kW	Carbon steel
Storage tank 1	Storage tank	Volume 3250 m^3	Stainless steel 316
Storage tank 2	Storage tank	Volume 3250 m^3	Stainless steel 316

APPENDIX IV

PROCESS FLOW DIAGRAMS

Flow no.		1	2	3	4	5	6	7	8	9	10	11	12	13	14	15 S	15 W	16 S	16 W	17 S	17 W	18 S	18 W	19 S	19 W	20 S	20 W
Raw bark*	kg/s								0.98																		
Raw debarked ground wood*	kg/s	8.64							1.58																		
Dried debarked ground wood*	kg/s		5.36																								
Sand	kg/s					42.7		42.7				42.7															
Bio-oil	kg/s					3.22	3.22																				
Non-condensable gas	kg/s			2.3	2.3	3.64	3.64																				
Biochar	kg/s					0.80		0.80																			
Air	kg/s									27.6	27.6					92.2	75.4	92.2	75.4								
Flue gas	kg/s												21.3		21.3												
Ash	kg/s												0.03	0.03													
Drying gas mixture	kg/s																			113.5	96.7	39	19.45	74.5	77.25	74.5	77.25
Water	kg/s																										
Temperature	°C	20	20	40	40	500	500	500	20	20	20	869	869	869	869	20	-20	20	-20	200	200	200	200	200	200	50	50
Pressure	bar			1	1.22	1.20	1.15			1	1.7		1.57		1.32	1	1	1.45	1.45	1.07	1.07	1	1	1.07	1.07	1	1
Outside pipe diameter	mm			200	200	500	500				560		560		560					800	800			800	800		
Inside pipe diameter	mm			190.2	190.2	475.4	475.4				532.6		532.6		532.6					760.8	760.8			760.8	760.8		

*Raw - 44 wt%(wb) moisture content
Dried - 10 wt%(wb) moisture content

	Diameter, m	Height, m
Pyrolyser	0.9	14.3
Sand reheater	5.7	15.5
Cyclone	1.35	5.35

	Length, m	Width, m	Height, m
ESP	6.3	7.75	8.1
Dryer	3.98	4.3	3.1

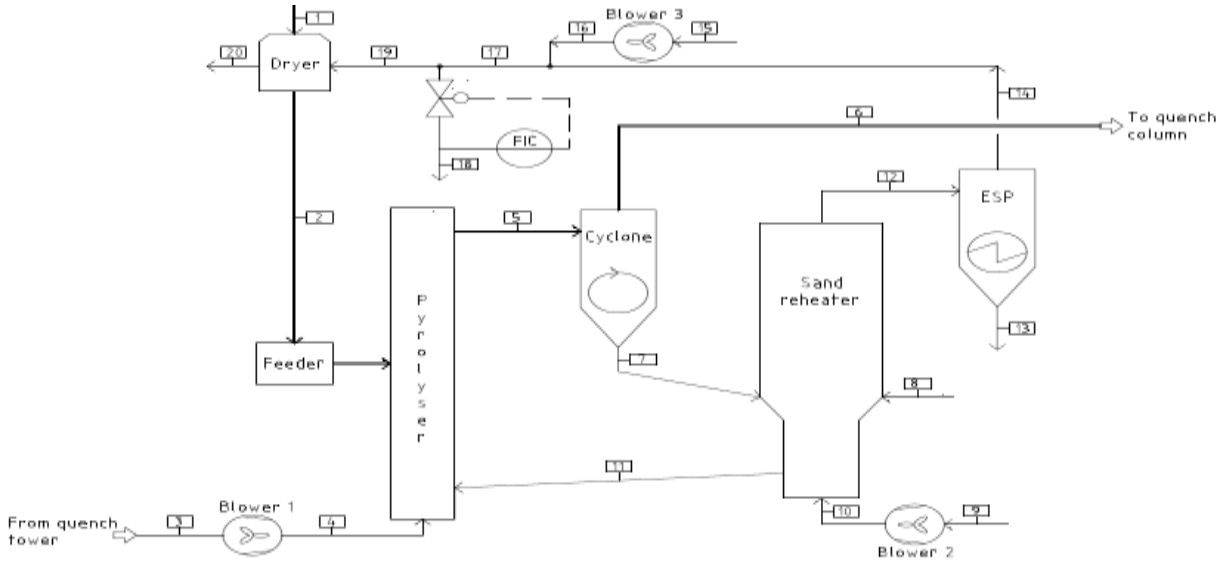

Flow no.		1	2	3	4	5	6	7	8	9	10	11	12	13	14
Raw bark	kg/s														
Raw debarked ground wood	kg/s														
Dried debarked ground wood	kg/s														
Sand	kg/s														
Bio-oil	kg/s	3.22	217.67	3.22	214.45	107.23	107.23	107.23	107.23	214.45					
Non-condensable gas	kg/s	3.64													2.3
Biochar	kg/s														
Air	kg/s														
Flue gas	kg/s														
Ash	kg/s														
Drying gas mixture	kg/s														
Water	kg/s										114.9	114.9	114.9	114.9	
Temperature	°C	500	40	40	40	40	20	40	20	20	5 (15)*	15 (25)*	5 (15)*	15 (25)*	40 (50)*
Pressure	bar		1	1	4.185	4.185	4.125	4.185	4.125	2.475	3.5		3.5		
Outside pipe diameter	mm	500	355	355	355	355	355	355	355	355	400	400	400	400	200
Inside pipe diameter	mm	475.4	314.8	314.8	314.8	314.8	314.8	314.8	314.8	314.8	369.4	369.4	369.4	369.4	190.2

	Diameter, m	Height, m
Quench tower	1.75	10
Cooler 1	1.464	~8.5
Cooler 2	1.464	~8.5

*The value in brackets is for the summer case